

University of Jordan
Faculty of Graduate Studies

Rainfall-Runoff Relationship for Representative
Watersheds in AL-Muwaqqar Basin

By
Mahmoud Khaleel Mahmoud Al-Akhras.

عصيدة كلية الدراسات العليا
جامعة الأردن


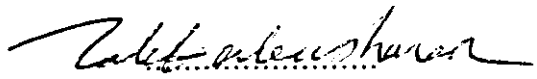

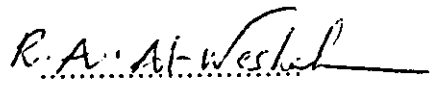
Supervised by
Dr. Muhammad Shatanawi

Submitted in Partial Fulfilment of the Requirements for
the Degree of Master of Science in Soils and Irrigation,
Faculty of Graduate Studies, University of Jordan.

5/5/96

January, 1996

This thesis was defended successfully on Jan. 6, 1996 and approved
by:

<u>Committee Members:</u>	<u>Signature</u>
1. Dr. Muhammad Shatanawi Assoc. Prof. of Irrigation and Hydraulic Engineering, Chairman of Committee	
2. Dr. Taleb Abu-Sharar Assoc. Prof. of Soil Chemistry, Member of Committee	
3. Dr. Ahmad Abu-Awwad Assoc. Prof. of Irrigation Engineering, Member of Committee	
4. Dr. Radwan Al-Weshah Asst. Prof. of Hydrology and Water Resource, Member of Committee	

DEDICATION

To

My Mother, Father

Sisters, Wife, and Daughter

ACKNOWLEDGEMENTS

Thank God for supporting me with power, patience, and determination throughout each step of the preparation of this thesis.

I should express my deep thanks and appreciations to Dr. Muhammad Shatanawi for his advice and guidance in the field work as well as in the preparation of this thesis in all its stages.

Thanks are extended to the committee members; Dr. Radwan Al-Weshah, Dr. Taleb Abu-Sharar, and Dr. Ahmad Abu-Awwad for their helpful advice in the field of their specialization, and for reading and criticizing drafts of various parts of this thesis.

Special thanks are extended for my friends especially Osama Hijazi.

Finally, special appreciation is extended to my Family for their encouragement during my presence at the university of Jordan.

This thesis is supported by the Water Harvesting Project funded by International Development Research Center (IDRC) of Canada. Their financial support is highly appreciated.

Table of contents

	<u>Page</u>
Committee Decision	ii
Dedication	iii
Aknowledgement	iv
Table of Contents	v
List of Tables	viii
List of Figures	xi
Abstract	xv
1. Introduction	1
2. Literature Review	3
2.1 Crust Formation and Infiltration Rate	3
2.2 Rainfall-Runoff Relationships	5
2.2.1 Rational Method	5
2.2.2 Unit Hydrograph	8
2.2.3 Regression Models	10
2.2.4 Computer Models	12
2.3 Flow Routing	13
2.3.1 Reservoir Routing	14
2.3.2 Channel Routing	15
3. Methodology	18
3.1 Study Location	18
3.2 Measurement of Soil Physical Properties	18
3.2.1 Infiltration Rate	18
3.2.2 Soil Moisture Content	19

3.3	Subbasin Selection	19
3.3.1	Weirs Construction	19
3.3.2	Water-Height Recorder	22
3.3.3	Rainfall Amounts and Intensities	24
3.3.4	Hydrograph development	24
3.4	Excess rainfall and Direct Runoff	24
3.5	Topographic Map	25
3.6	Runoff Coefficient	25
3.7	Modling	26
3.7.1	Basin Schematic	26
3.7.2	Model Components	29
3.7.3	Rainfall-Runoff Simulation	30
3.7.3.1	Precipitation Hyetograph	30
3.7.3.2	Interception and Infiltration	30
3.7.3.3	Unit Hydrograph	34
3.7.3.4	Flood Routing	35
3.7.4	Optimization Methodology	36
3.7.5	Verification Methodology	40
4.	Result and discussion	41
4.1	Infiltration Rate	41
4.2	Soil moisture Content	45
4.3	Relationship Between Rainfall and Runoff	47
4.4	Optimization Parameters	61
4.5	Verification	80
4.6	Stream Network Model	84
4.6.1	Channel Routing	84
4.6.2	Flow routing Through Dam	87
4.6.3	Simulated Runoff Hydrograph	88

5. Summary and Conclusions	95
6. References	97
7. Abstract in Arabic	101

List of Tables

No	Name of table	Page
1.	Channel configurations	16
2.	Dimensions of weirs at different sites	22
3.	Subbasins area for the Muwaqqar basin	26
4.	Classification of antecedent moisture classes (AMC) for the SCS method of rainfall abstractions	34
5.	The channel length, slope channel and roughness coefficient for all routing channel	36
6.	The weight average for all sites resulting optimization initial, and uniform loss rate	44
7.	The peak flow for the two selected sites	57
8.	Volume runoff and peak flow for three selected site	58
9.	Runoff coefficient for each storm for all sites during the period of 15 Nov. 1994 to 19 Dec. 1995	59
10.	Results of the optimization unit hydrograph and loss rate parameters for site 2	60
11.	Results of the optimization unit hydrograph and loss rate parameters for site 3	60
12.	Comparison between computed and observed runoff hydrographs for site 1 using method 1	64
13.	Comparison between computed and observed runoff hydrographs for site 1 using method 2	64
14.	Comparison between computed and observed runoff hydrographs for site 1 using method 3	65
15.	Comparison between computed and observed runoff	

hydrographs for site 1 using method 4	65
16. Comparison between computed and observed runoff hydrographs for site 2 using method 1	66
17. Comparison between computed and observed runoff hydrographs for site 2 using method 2	66
18. Comparison between computed and observed runoff hydrographs for site 2 using method 3	67
19. Comparison between computed and observed runoff hydrographs for site 2 using method 4	67
20. Comparison between computed and observed runoff hydrographs for site 3 using method 1	68
21. Comparison between computed and observed runoff hydrographs for site 3 using method 2	68
22. Comparison between computed and observed runoff hydrographs for site 3 using method 3	69
23. Comparison between computed and observed runoff hydrographs for site 3 using method 4	69
24. Error percentage for method 1 and site 1	70
25. Error percentage for method 2 and site 1	70
26. Error percentage for method 3 and site 1	71
27. Error percentage for method 4 and site 1	71
28. Error percentage for method 1 and site 2	72
29. Error percentage for method 2 and site 2	72
30. Error percentage for method 3 and site 2	73
31. Error percentage for method 4 and site 2	73
32. Error percentage for method 1 and site 3	74
33. Error percentage for method 2 and site 3	74
34. Error percentage for method 3 and site 3	75

35. Error percentage for method 4 and site 3	75
36. Average error percentage for all methods for site 1	76
37. Average error percentage for all methods for site 2	76
38. Average error percentage for all methods for site 3.....	76
39. The grand average percentage error for all methods for all sites	77
40. Results of the optimization unit hydrograph and loss rate parameters for site 1	77
41. Comparison between computed and observed runoff hydrographs for site 3 using method 4	81
42. Comparison between computed and observed runoff hydrographs for site 3 using method 1	81
43. Comparison between using method 4 and method 1 for site 3 .	81
44. Comparison between computed and observed runoff hydrographs for site 4 using method 4	82
45. Comparison between computed and observed runoff hydrographs for site 4 using method 1	82
46. Comparison between using method 4 and method 1 for site 4 .	82
47. The maximum stages of the dams during the 1994/1995 season	93
48. The lag time for all the subbasins	93
49. The surface runoff Volume and the peak flow during the 1994/1995 season	94

List of Figures

<u>No</u>	<u>Name of figure</u>	<u>Page</u>
1.	Muwaqqar watershed	20
2.	Typical shape of the sharp crested weir installed in Muwaqqar Basin	21
3.	The calibration curves for the three sharp crested weir installed at Muwaqqar Basin	23
4.	The subbasins area of the Al- Muwaqqar Basin	27
5.	HEC-1 basin schematic	28
6.	Solution of the SCS runoff equations	33
7.	Rating Curve of dams	37
8.	Elevation-storage-area relationship of existing dams	38
9.	Infiltration rate for site 1	43
10.	Infiltration rate for site 2	43
11.	Infiltration rate for site 3	43
12.	Soil water content as affected by rainfall amount with time for the surface layer 0-20 cm for site 1	46
13.	Soil water content as affected by rainfall amount with time for the surface layer 0-20 cm for site 2	46
14.	Soil water content as affected by rainfall amount with time for the surface layer 0-20 cm for site 2	46
15.	Surface runoff and excess rainfall incremental of the storm of Nov 23, 1994 on site 1	50
16.	Surface runoff and excess rainfall incremental of the storm of Nov 24, 1994 on site 1	50

17.	Surface runoff and excess rainfall incremental of the storm of Dec 2-3, 1994 on site 1	50
18.	Surface runoff and excess rainfall incremental of the storm of Dec 3, 1994 on site 1	51
19.	Surface runoff and excess rainfall incremental of the storm of Dec 3-4, 1994 on site 1	51
20.	Surface runoff and excess rainfall incremental of the storm of Nov 23, 1994 on site 2	52
21.	Surface runoff and excess rainfall incremental of the storm of Nov 24, 1994 on site 2	52
22.	Surface runoff and excess rainfall incremental of the storm of Nov 24, 1994 on site 2	52
23.	Surface runoff and excess rainfall incremental of the storm of Dec 2, 1994 on site 2	53
24.	Surface runoff and excess rainfall incremental of the storm of Dec 2-3, 1994 on site 2	53
25.	Surface runoff and excess rainfall incremental of the storm of Dec 19, 1994 on site 2	53
26.	Surface runoff and excess rainfall incremental of the storm of Nov 15, 1994 on site 3	54
27.	Surface runoff and excess rainfall incremental of the storm of Nov 23, 1994 on site 3	54
28.	Surface runoff and excess rainfall incremental of the storm of Nov 24, 1994 on site 3	54
29.	Surface runoff and excess rainfall incremental of the storm of Dec 2, 1994 on site 3	55
30.	Surface runoff and excess rainfall incremental of the storm of Dec 2-3, 1994 on site 3	55

31.	Surface runoff and excess rainfall incremental of the storm of Dec 3-4, 1994 on site 3	55
32.	Surface runoff and excess rainfall incremental of the storm of Dec 19, 1994 on site 3	56
33.	Surface runoff and excess rainfall incremental of the storm of Dec 19-20, 1994 on site 3	56
34.	Comparison between observed and computed runoff depth for site 2	78
35.	Comparison between observed and computed peak flow for site 2	78
36.	Comparison between observed and computed time to peak for. site 2	78
37.	Comparison of computed and observed hydrographs resulting from storm 2, using the four methods on site 1	79
38.	Comparison of computed and observed hydrographs resulting from storm 2, using the four methods on site 2	79
39.	Comparison of computed and observed hydrographs resulting from storm 2, using the four methods on site 3	79
40.	Comparison between observed hydrograph and calculated hydrograph for site 3	83
41.	Comparison between observed hydrograph and calculated hydrograph for site 4	83
42.	Variation of K with inflow for single reach routing	85
43.	Variation of X with inflow for single reach routing	85
44.	Routing results for channel caused by storm 2	86
45.	Routing results for channel caused by storm 7	86
46.	Inflow and storage relationship for Dam 1 caused by storm 1 ..	90
47.	Inflow and storage relationship for Dam 2 caused by storm 1 ..	90

48.	Inflow, outflow, and storage relationship for Dam 1 caused by storm 2	91
49.	Inflow, outflow, and storage relationship for Dam 2 caused by storm 2	91
50.	Inflow, outflow, and storage relationship for Dam 3 caused by storm 2	91
51.	Inflow, outflow, and storage relationship for Dam 1 caused by storm 3	92
52.	Inflow, outflow, and storage relationship for Dam 2 caused by storm 3	92
53.	Inflow, outflow, and storage relationship for Dam 3 caused by storm 3	92

ABSTRACT

Rainfall-Runoff Relationship for Representative Watersheds in AL-Muwaqqar Basin

By
Mahmoud Khaleel Mahmoud Al-Akhras.

Supervised by
Dr. Muhammad Shatanawi

Jordan, like most countries in the Middle East suffers from increasing water deficit. Over 85% of the country receives less than 200 mm of annual rainfall. In these areas where arid and semi-arid areas conditions prevails, rainfall fall is unpredictable, sporadic and intense storms resulting in high runoff and often causing floods. Three selected subbasins in Muwaqqar basin of area 7.3 , 0.5, and 5.8 km² for sites 1, 2, and 3, respectively are used to study the relationship between rainfall and runoff. This study determine the effect of rainfall characteristics and soil surface characteristics on runoff generation. The basic infiltration rates for all sites were low, and rainfall intensity is often greater than the rate of infiltration in the soil because of the thin crust layer at the soil surface. Therefore, a significant surface runoff occurs even with very low rainfall intensity. The runoff coefficient for the three selected subbasin were 0.25, 0.40, and 0.23 for sites 1, 2, and 3, respectively.

A hydrological Computational Model (HEC-1) which was developed by Hydrologic Engineering Center of the United States Army Corps of Engineers (1981) was used to simulate the surface runoff hydrograph for

the Muwaqqar basin, primarily the simulation of the transformation of a series of rainfall inputs to the resulting streamflow hydrographs for gauged and ungauged catchments. Three representative subbasins in Muwaqqar basin having measurements of streamflow and of the necessary meteorological variables were used in HEC-1 optimization technique. Verification of the HEC-1 model in the two subbasins were selected shows relatively good results. The derived parameters have been used to simulate streamflows for an ungauged catchment.

Among four input methods, the initial and uniform loss rate with soil conservation service (SCS) dimensionless unit hydrograph (method 4) was the most accurate simulating basin surface runoff. The difference between inflow and outflow runoff hydrograph ordinates for the channels was not significant which means that channel routing could be neglected. The total basin runoff volume caused by the storms during 1994/1995 season equal 0.79 million cubic meter (mcm) which means that only 5.8% from the total basin runoff volume would be stored in the existing dams which have a capacity of 0.05 mcm.

1. Introduction

Most countries of the Middle East, including Jordan, suffer from shortage of water. Such a shortage arises from many factors such as; low rainfall amount and uneven distribution, high losses of water due to evaporation and surface runoff, and high population growth⁽¹⁾.

Over 85% of the Jordan receives less than 200 mm of annual rainfall. In arid and semi-arid areas, rainfall is unpredictable, sporadic and intense storm of short duration cause large runoff and often causing floods⁽²⁾. The flood water then flows to flat saline and impermeable areas, and is mostly lost by evaporation. Very little amount of the rainfall is stored in the soil or percolates into the aquifer system. Therefore an imperative development would be the conversion of such wasteful runoff into a useful storage in the dams. It is estimated that the volume of water lost in this manner exceeds all the utilized sources of water in Jordan⁽²⁾.

To overcome this problem, building reservoirs to save surface runoff for irrigation is a matter of increasing interest. In addition, these reservoirs may reduce the risk of flash flooding during intense rain storms.

The development of a relationship between rainfall and surface runoff is very important in planning and managing water resource and flood control of any water resource system. This relationship depends on data available and modeling approach⁽³⁾.

A hydrological Computational model (HEC-1) model which developed by Hydrologic Engineering Center of the United State Army

Corps of Engineers, 1981 is designed to simulate the surface runoff response of a river basin to precipitation by representing the basin as an interconnected system of hydrologic and hydraulic components. Each component models an aspect of the precipitation-runoff entity, a stream channel, or a reservoir. Representation of a component requires a set of parameters which specify the particular characteristics of the component and mathematical relations which describe the physical processes. The result of the modeling process is the computation of stream flow hydrographs at desired locations in the river basin.

HEC-1 provide a powerful optimization technique for the estimation of some of the parameters when gauged precipitation and runoff data are available. By using this technique and regionalization the results, rainfall-runoff parameters for ungauged areas can also be estimated⁽⁴⁾.

A study was conducted at Al-Muwaqqar Basin to achieve the following objectives:

1. to estimate surface runoff hydrograph and runoff coefficient,
2. to develop the relationship between the basin characteristics and the runoff coefficient, and
3. to derive a regional rainfall-runoff forecasting model.

2. Literature Review

There is a clear need for improvement of the accuracy and generality of methods of flood estimation in large watersheds which can be done only through better understanding of the relationship between runoff hydrograph and rainfall and other physiographic factors⁽⁵⁾. It is important to study and evaluate the factors that affect the runoff production of a given watershed. Factors such as the infiltration rate, the slope and the length of the channel reach will be examined.

The relationship between runoff and rainfall can be expressed in a simple relation as the runoff is equal to a fraction of rainfall. This fraction is called effective rainfall.

2.1 Crust formation and infiltration rate:

Infiltration rate (IR) is defined as the volume flux of water flowing into the soil profile per unit surface area of soil. In general, soil infiltration capacity is initially high, particularly when the soil is initially dry, but it tends to decrease monotonically until it asymptotically approaches a constant rate known as the final or steady state IR⁽⁶⁾. It has been recognized that the driving force for the water entering the soil is the gradient of the water potential between the wetting front and the soil surface; thus the decrease in infiltration rate is an inevitable consequence of the decreasing water potential gradient during the infiltration process⁽⁷⁾. Hortan (1939) suggested that the reduction in infiltration rate with time, during the infiltration process, is controlled largely by factors operating at the soil

surface. A gradual deterioration of the soil structure and the consequent partial sealing of the profile by the formation of a surface crust may occur in some soils under certain conditions. The infiltration of water into a bare soil can be markedly reduced by a crust-seal formed on the soil surface by impact of raindrops⁽⁸⁾. The reduction, of course, depends upon the soil type, surface conditions, and the rainfall kinetic energy, intensity, and duration.

Crust formation is due to the combined effect of the raindrop impact energy and the dispersion of clay particles at the soil surface⁽⁹⁾. The formation of crusts at the soil surface, especially due to the action of raindrops is a common feature of cultivated soils in many regions of the world. Surface crusts are thin (<2 mm) and characterized by greater density, higher shear strength, finer pores, and lower saturated hydraulic conductivity than the underlying soil. Soil crusts have a prominent effect on many soil phenomena; for example, the reduction of infiltration and increase in runoff⁽¹⁰⁾. Researchers have shown the importance of cumulative rainfall or kinetic energy or levels of kinetic energy on seal formation and water infiltration⁽¹¹⁾. Rate and intensity of seal formation increase with increase in raindrop impact energy. Agassi et al.(1985) reported that no seal formation on either a loam-textured or clay textured under low-energy rain ($0.01 \text{ J mm}^{-1} \text{ m}^{-2}$). With high-energy rain ($23.0 \text{ J mm}^{-1} \text{ m}^{-2}$) both soils formed seals with very low hydraulic permeability. Difference in final infiltration rates between the two rainfall energies was 39 mm/h for the loam and 42 mm/h for the clay⁽⁹⁾. The higher the kinetic energy the steeper the drop in infiltration rate⁽¹¹⁾. The seal formation for soils with a high clay content has a greater effect on change in infiltration rate than on strength. For soils with silt contents of more than 70%, the reverse was true⁽¹⁰⁾. Soils with high clay content (approximately more than 40%) have the highest IR, soils with

medium clay content (approximately 10-40%) are the most susceptible to crust formation and have the lowest infiltration rate, and soils with very low clay content (<10%) have higher infiltration rate than soils with medium clay content but lower than the infiltration of soils with high clay content⁽⁶⁾.

Soil water deficit in the upper soil layer just before a rain storm is, perhaps, the most important factor involved in the rainfall-runoff relationship. It affects the infiltration capacity and the excess rainfall⁽¹²⁾. Soils have low aggregate stabilities for both air-dry and wetted aggregates, infiltration rate was less for wetted surface than for initially dry surface and the opposite for soils have high aggregate stability⁽⁶⁾.

2.2 Rainfall-Runoff Relationships:

2.2.1 Rational Formula:

The principles of the rational methods were explicit in the work of Mulvaney in 1951. As currently understood the formula was $Q = CiA$, where Q is the peak rate of runoff at the outlet point in cubic feet per second (cfs), C is the coefficient of runoff, A is the area of the watersheds in acres, and i is the main intensity of rainfall in inch per second during the period of time of concentration (T_c)⁽⁵⁾.

The basic assumptions associated with the rational method were:

1. The computed peak rate of runoff at the outlet point was a function of the average rainfall rate during the time of concentration. That could be explained as the peak discharge did not result from a more intense storm of

shorter duration, during which only a portion of the watershed was contributing to runoff at the outlet.

2. The duration is the time of concentration for the runoff to become established and flow from the most remote part of the drainage area to the inflow point at the outlet.

3. Rainfall intensity was constant throughout the storm duration⁽¹³⁾.

Runoff Coefficient:

Runoff coefficient (C) is the ratio of runoff volume to rainfall over a given time period. The runoff coefficient can be expressed

$$C = \frac{r_d}{\sum_{m=1}^M R_m} \dots\dots\dots (1)$$

Where C = runoff coefficient.

r_d = depth of runoff (mm), and

R_m = total rainfall depth (mm)⁽¹³⁾

The runoff coefficient of a catchments is difficult to generalize because it depends on many factors such as antecedent soil moisture, storm intensity, storm duration, land use, vegetation cover, and catchment size⁽¹⁴⁾.

Variation in surface runoff at different sites within the Muwaqqar basin can be attributed to variation in rainfall amounts, distribution, and intensities, and variation in watershed area⁽¹⁾. Under arid conditions the runoff coefficient also increases with the decrease size of the drainage basin⁽¹⁵⁾.

Vegetation cover is defined broadly to include the living plants as well as organic residues on the ground surface. This cover protects the soil against external factors (rain, wind) which mainly influence superficial rearrangement of soil particles⁽¹⁶⁾. The main effect of vegetation management is that it reduces the infiltration capacity⁽¹⁴⁾

Runoff threshold value (the required rainfall depth required before the soil becomes saturated) was found to be a function of the basin average soil texture. The lowest threshold value was 4.06 mm for clay soils and the maximum value was 9 mm for sandy texture. Although both sandy and clayey soils have approximately the same porosity (about 40% by volume), the volumetric soil water content at field capacity was about 0.10 for sandy soils and 0.30 for clayey soils. This means that the valuable porosity is much higher in the sandy soil and thus more rain depth is required before the soil becomes saturated, as indicated by the higher threshold level⁽¹²⁾.

Excess Rainfall and Direct Runoff:

The excess rainfall, or effective rainfall, is that rainfall which is neither retained on the land surface nor infiltrated into the soil. After flowing across the watershed surface, excess rainfall becomes direct runoff at the watershed outlet. The excess rainfall hyetograph (ERH), is a key component of the study of rainfall-runoff relationships. The excess rainfall hyetograph may be determined from the rainfall hyetograph depending on whether streamflow data .

The depths of direct runoff (excess rainfall) in mm are equal:

$$r_d = \sum_{m=1}^M (R_m - \phi \Delta t) \dots \dots \dots (2)$$

where ϕ -index is the constant rate of abstractions (in/hr or cm/hr),
and R_m is the observed rainfall (mm) in time interval m ⁽¹³⁾.

2.2.2 Unit Hydrograph:

The unit hydrograph defined as a direct runoff hydrograph (DRH) resulting from 1 inch or 1 cm of excess rainfall generated uniformly over the drainage area at a constant rate for an effective duration⁽¹³⁾. The excess rainfall hietograph is transformed to a subbasin outflow by utilizing the general equation:

$$Q(i) = \sum_{j=1}^i U(j) * X(i - j + 1) \dots \dots \dots (3)$$

Where $Q(i)$ is the subbasin outflow at the end of the computation interval i ,

$X(i)$ is the average rainfall excess for computation interval i . rain,

and $U(j)$ is the j th ordinate of the unit hydrograph

The equation is based in two important assumptions. First, the unit hydrograph is a characteristic for a subbasin and is not a storm dependent. Second, The runoff due to excess rainfall from different periods of rainfall can be linearly superposed⁽⁴⁾.

Observed Unit Hydrograph:

The observed unit hydrograph developed from rainfall and streamflow data on a watershed applies only for that watershed and for the point on the stream where the streamflow data were measured⁽¹³⁾.

Synthetic Unit Hydrograph:

Synthetic unit hydrograph procedures are used to develop unit hydrographs for other locations on the stream in the same watershed, or for nearby watersheds⁽¹³⁾. There are different methods for constructing unit hydrographs such as Snyder and SCS methods.

455829

Snyder Unit Hydrograph:

The Snyder method (1938) determines the unit hydrograph peak discharge, time to peak, and widths of the unit hydrograph at 50 and 75% of the peak discharge⁽⁴⁾.

The Snyder parameters are computed by the following equation

$$C_p = q_p * \frac{T_p - 0.5 * \Delta t}{C^2 * A} \dots\dots\dots (4)$$

Where C_p is a coefficient derived from gauged watersheds.

q_p is the maximum ordinate of the unit hydrograph.

T_p is the time when q_p occurs in hours.

Δt is the duration of excess rainfall, in hours

A is the subbasin area in square miles and,

C is a conversion factor.

$$t_p = 1.048 * (T_p - 0.75 * \Delta t) \dots\dots\dots (5)$$

Where t_p is Snyder's standard lag time for the computed unit hydrograph and T_p as defined before⁽¹³⁾.

SCS Dimensionless unit hydrograph:

Dimensionless unit hydrographs which give the ratio, q/q_p , of the discharge at any time to the maximum discharge in terms of ratio, t/T_p ,

where T_p is the time to peak, tend to eliminate the basin characteristics⁽⁵⁾. Input data for the soil conservation service, SCS, dimensionless unit hydrograph method (1972) consists of a single parameter, TLAG, which is equal to the lag time (hr) between the center of mass of excess rainfall and the peak of the unit hydrograph⁽⁴⁾.

A study of unit hydrograph of many large and small watersheds indicates that the basin lag time

$$t_p = 0.6 T_c \dots\dots\dots (6)$$

Where T_c is the time of concentration

$$t_p = T_p - \frac{t_r}{2} \dots\dots\dots (7)$$

Where the t_r is the excess rainfall duration⁽⁴⁾.

2.2.3 Regression Model:

Simple linear regression models for predicting total volume of runoff, peak rate of runoff, duration of runoff, and hydrograph lag-time were developed using three years of data from four small watersheds (e.g; 0.56 to 11.0 acres). The models developed indicated that runoff volume was most strongly correlated to total precipitation. The peak rate of runoff was most strongly correlated to the maximum 15-minute depth of precipitation. Also the flow duration was most strongly correlated to watershed length, and that lag time was most strongly correlated to watershed area⁽¹⁷⁾.

The study was conducted to clarify the hydrological process of runoff generation in some watersheds in Texas. A simple regression model which is of practical use for large catchment areas, to compute runoff using rainfall and watershed area variables. In the arid and semi-arid regions, it seems more adequate to use the total precipitation of the rainfall event than the

daily amount of rainfall as a variable when establishing predicting runoff equation⁽¹⁸⁾.

An empirical model to predict runoff yield in the Negev desert in Palestine has been developed. The equation assumes a linear relationship between annual rainfall and runoff for a given watershed taking into account the reduction in runoff efficiency with an increase in catchment size. It uses the statistical parameters (mean, σ) of rainfall in order to calculate the recurrence interval of runoff yields⁽¹⁵⁾.

Rainfall-Runoff relationships were described by an empirical quadratic regression equation which includes four parameters (threshold level (mm), recession factor, reduction factor, and curve factor (mm^{-1})). These parameters were estimated by an optimization subroutine which was used to determine the minimum difference between measured and modeled results. The optimized parameters enabled simulations of the continuous dynamic change of an index of the soil water content as well as predictions of runoff depths⁽¹²⁾.

Hydrological models were developed to estimate the rainfall-runoff relationship for Wadi Walah watershed in Jordan. In modeling rainfall-runoff, the linear time-invariant model was found to be less accurate in runoff prediction. Also the volterra functional series with first and second order functions was not satisfactory. The nonlinear time-invariant model in which the nonlinear terms were derived from the linear daily rainfall predicted the runoff quite well. The prediction of runoff was more accurate with respect to time of occurrence and to magnitude when there was continuous rainfall. The rainfall-runoff relationship was best estimated by considering cumulative rainfall during 4 days prior to the onset of runoff⁽³⁾.

2.2.4 Computer Models:

Plate (1988) developed the International Hydrological Decade (IHD) model for calculations of design floods for flood protection reservoirs. The model requires subdividing a catchment into small subcatchments which can be connected to form a basin model. The flood from each subbasin is calculated by means of a design rainfall pattern convoluted with a unit hydrograph. Runoff coefficients and unit hydrograph were calculated from a regionalization model which has been developed from a large number of measured hydrographs. Flood routing models were used to connect the subcatchments⁽¹⁹⁾.

The excess rainfall was modeled by using the two-parameter Green-Ampt infiltration approach. A six-parameter linear-discrete model was used to model the runoff hydrograph. The infiltration parameters were estimated by using the simplex method, and the runoff parameters by least squares. The model was calibrated on ten watersheds and verified on the seventh. The model-simulated runoff hydrographs were in close agreement with observed runoff hydrographs⁽²⁰⁾.

An existing, deterministic, physically based conceptual model has been modified and improved for the simulation of the hydrological events, primarily the simulation of the transformation of a series of rainfall inputs to the resulting streamflow hydrographs for gauged and ungauged catchments. Four representative catchments in the Central Highlands of Ethiopia having measurements of streamflow and of the necessary meteorological variables were used in the verification of the model. The derived parameters were used to simulate streamflows for an ungauged catchment in a subsequent application to design a reservoir⁽²¹⁾. Burn et. al. (1993) estimated

hydrological parameters at ungauged sites using classification of catchments into groups according to their flow regime, assignment of ungauged catchments to a group based on physical characteristics of the catchment and the use of similarity measures to transfer parameters from gauged to ungauged catchments⁽²²⁾.

Hydrologic Engineering center(HEC-1)

The hydrologic engineering center of the U. S. Army Corps of Engineers developed a model (HEC-1) to simulate the surface runoff response of a river basin to precipitation by representing the basin as an interconnected system of hydrologic and hydraulic components. Each component models an aspect of the precipitation-runoff entity, a stream channel, or a reservoir. Representation of a component requires a set of parameters which specify the particular characteristics of the component and mathematical relations which describe the physical processes. The result of the modeling process is the computation of stream flow hydrographs at desired locations in the river basin⁽⁴⁾.

2.3 Flow Routing:

Flow routing is a procedure to determine the time and magnitude of flow (the flow hydrograph) at a point on a watercourse from known or assumed hydrographs at one or more points upstream.

The flow in lumped system model is calculated as a function of time alone at a particular location, while in a distributed system routing the flow is calculated as a function of space and time throughout the system⁽⁴⁾.

The Muskingum routing and the Level pool routing are the lumped system methods.

Laureson (1964) developed a procedure to reproduce the surface runoff hydrograph of a catchment from the rainfall excess, knowing the lag time of the catchment and its variation with discharge. A computational model of the catchment storage is first developed, and the storage-discharge relations of the model storages are derived from an empirical relation between lag and mean outflow discharge for a particular catchment⁽²³⁾.

2.3.1 Reservoir Routing:

An invariable storage-outflow relationship applies to a reservoir with a horizontal water surface. Such reservoir have a pool that is wide and deep compared with its length in the direction of flow. The velocity of flow in the reservoir is very low. The invariable storage relationship requires that there be fixed discharge from the reservoir for a given water surface elevation. When a reservoir has a horizontal water surface, its storage is a function of its water surface elevation⁽¹³⁾.

Level Pool Routing:

Level pool routing is a procedure for calculating the outflow hydrograph from a reservoir with a horizontal water surface, given its inflow hydrograph and storage outflow characteristics⁽¹³⁾.

The change in reservoir storage, S , for a given time period, Δt , is equal to average inflow, I , minus average outflow, O ⁽⁴⁾.

$$\frac{S_2 - S_1}{\Delta t} = \frac{I_1 + I_2}{2} - \frac{O_1 + O_2}{2} \dots\dots\dots (8)$$

2.3.2 Channel Routing:

A variable storage-outflow relationship applies to long, narrow reservoirs, and to open channels or streams, where the water surface profile may be significantly curved due to the backwater effects. The amount of storage due to backwater depends on the time rate of change of flow through the system⁽¹³⁾.

Perumal (1992) used a rectangular channel with a width of 50 m for all test runs and the hydrograph was routed to a distance of 40 km from the inflow section. The method was tested on four different channel configuration as given in Table 1. The results indicated that as the channel type increased the magnitude of the reduced outflow was minimized. From the calibration curve between inflow discharge and weighting parameter (X), Perumal noted wide variation in X with reference to inflow discharge for channel types 1 and 2. An insignificant variation in X with reference to inflow discharge was observed while routing the inflow hydrograph in channel type 3 and 4. The higher values of X correspond to high channel slope and lower roughness coefficient. Also he notes a significant variation of the travel time K, with reference to inflow discharge during single reach routing in all four channel type was observed, with the range of its variation and its magnitude decreasing with increase in the bed slope and reduction in the channel roughness⁽²⁴⁾.

Table 1: Channel configurations used by Perumal (1992).

Channel type	Bed slope	n value
1	0.0002	0.04
2	0.0002	0.02
3	0.002	0.04
4	0.002	0.02

n value: manning roughness.

Muskingum Method:

The Muskingum method is a commonly used hydrologic routing method for handling a variable discharge-storage relationship. This method models the storage volume of flooding in a river channel by a combination of wedge and prism storages. The storage function for the Muskingum method is

$$S = K[XI + (1-X)Q] \dots\dots\dots (9)$$

Where S is the storage in m³

I is the inflow to the routing reach in m³/s

Q is the outflow from the routing reach in m³/s

K is the travel time through the reach in hours, and

X is the Muskingum weighting factor ($0 \leq X \leq 0.5$)⁽¹³⁾

$$K = \frac{\Delta x}{C_k} \dots\dots\dots (10)$$

Where the Δx is the reach length and

C_k is the wave celerity corresponding to the reference discharge considered (Q_0).

Using the method of matching difference schemes based on diffusion analogy principle (Cunge, 1969), X is expressed as

$$X = 0.5 - \frac{Q_o}{2 * S_o * B * C_k * \Delta x} \dots\dots\dots (11)$$

Where B is the width of channel in meter, and
S_o is the bed slope⁽²⁴⁾.

3. Methodology

3.1 Study Location:

The Muwaqqar watershed is a part of the Azraq basin. The watershed is located at the upstream end of the basin. The Muwaqqar basin has an area of 70.1 km² and is located in the 100-200 mm rainfall zone. In addition, the climate of the area is characterized by irregular, sporadic and unpredictable rainfall. Rainfall occurs during the winter season in form of intensive storms of short duration causing high rates of runoff. The intensity of rainfall is high and infiltration index is very low due to soil surface crust⁽¹⁾. The area is frequently subjected to flash floods.

The general topography of the area is gently undulating with some isolated hilly areas. Slopes are generally between 1% and 5% but not restricted to this range. Soils are highly calcareous with depth varies according to slope. Shallow soils are found at higher slopes but deep soils occur on slopes less than 2%. Soil texture is generally silty clay. Soil structure at the surface is very poor due to wind, rainfall impact, water erosion, and lack of vegetation cover. A crust is formed at the surface with very low water holding capacity and infiltration (less than 2 mm/hr). Storms amount as low as 5 mm could cause runoff⁽²⁷⁾.

3.2 Measurement of Soil Physical Properties:

3.2.1 Infiltration Rate:

Infiltration rate was measured using double ring infiltrometer as described by Bouwer⁽²⁸⁾. The internal diameters of the outer and the inner rings were 30 and 20 cm, respectively. The two rings were pushed 7 to 10

cm into the soil surface . During infiltration the depth of water in the inner ring was allowed to vary from 4 to 10 cm. Infiltration rate was measured three times at the three selected sites.

3.2.2 Soil moisture content:

Soil moisture content was measured for surface layer by gravimetric method. Three samples were taken from the surface layer every week for each subbasin. Measurements were taken from 8 Nov, 1994 to 12 April, 1995 during the rainy season.

3.3 subbasin Selection:

Three subbasin with areas; 7.3, 0.5, and 5.7 km² for the sites 1, 2, and 3, respectively, were selected within the major basin of Muwaqqar (Figure 1). They represent different slopes and soil characteristics for the major basin.

3.3.1 Weirs Construction:

Three rectangular sharp-crested contracted weirs were constructed across the wadis ends (natural channel). The size of each weir reflected the wadi shape and size. The general shape of these weirs is shown on Figure 2. The dimensions for different sites are shown in Table 2⁽²⁷⁾.

The general form of rectangular weir equation is

$$Q = \frac{2}{3} C_d W (2g)^{\frac{1}{2}} H_w^{\frac{3}{2}} \dots\dots\dots (12)$$

In which

C_d = Discharge coefficient.

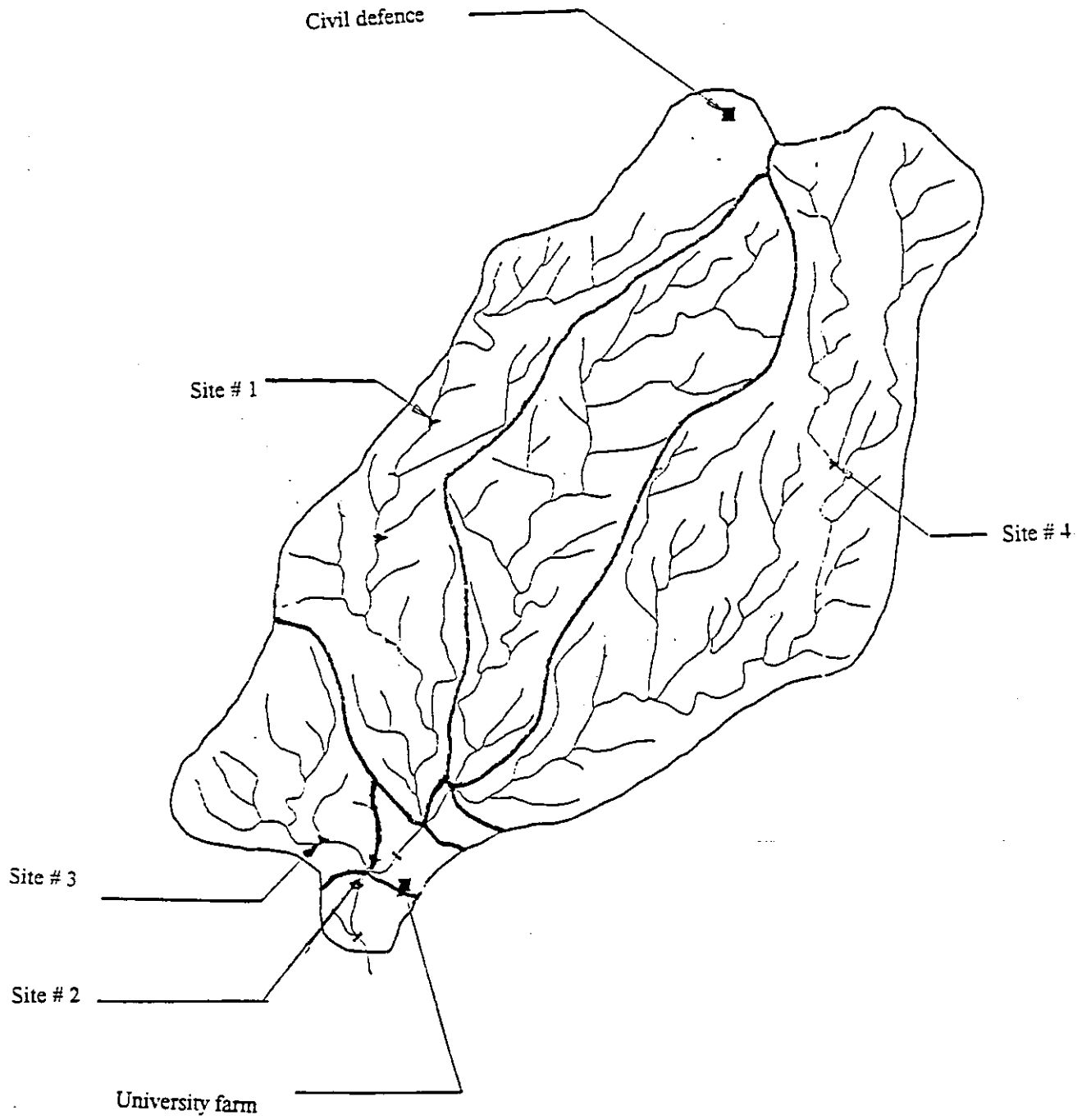


Fig. 1: Muwaqqar watershed

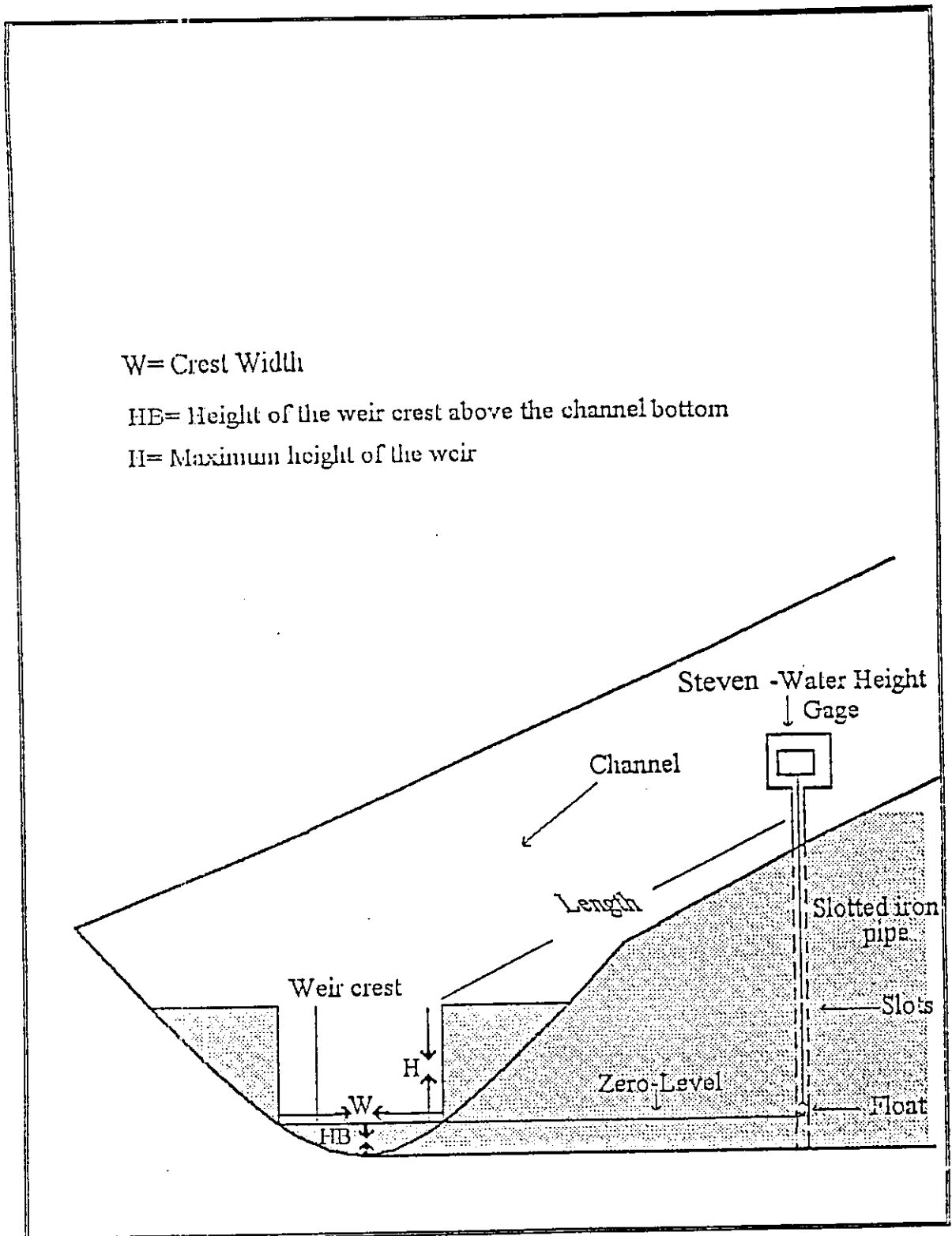


Fig. 2: Typical shape of the sharp crested weir installed in Muwaqqar Basin.

H_B = Crest height

H_w = Height of water above the weir crest.

W = Width of the crest.

H = Maximum height of the weir⁽²⁸⁾.

The discharge coefficient (C_d) depends on the flow conditions, type and dimension of the weir. To simplify the calculation of the discharge, three calibration curves were developed for three weirs⁽²⁷⁾. These calibration curves are presented in Figure 3. In constructing the calibration curves the approaching velocities and the effective the flood wave were considered.

Table 2: Dimensions of weirs at different sites.

Weir Site No	W(m)	H_B (m)	H(m)
1	2.50	0.09	1.14
2	2.00	0.10	1.14
3	2.00	0.30	0.90

3.3.2 Water-Height Recorder:

For each weir, a Steven-Water height recorder to measure the height of water above the crest of the weir was installed. The recorder measures the distance from the weir crest to the water height measurement point. The measurement was done via a float installed inside a cylindrical 6 inches steel pipe. The height of water was recorded with time on a graph. These graphs along with the calibration curves were used to construct the flood hydrograph⁽²⁷⁾.

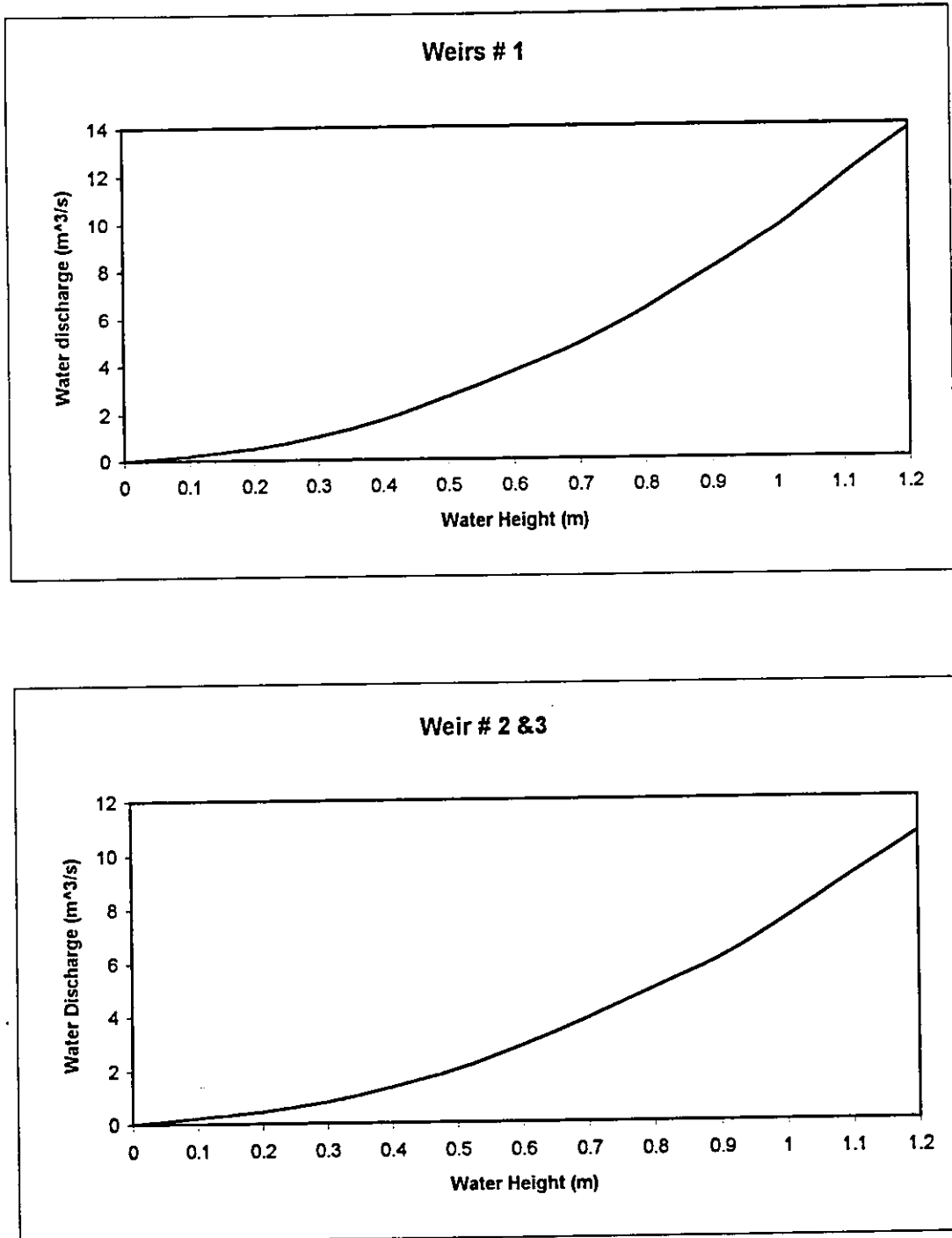


Figure 3: The Calibration curves for the three sharp crested weir installed at Muwaqqar Basin.

3.3.3 Rainfall Amounts and Intensities:

To measure rainfall amounts and intensities, two float recording type raingauges were installed in the eastern and western part of the basin. The first rain gauge was installed at the Civil Defense station at the upstream end of the catchment while the second was installed at the University Experimental Station. Rainfall charts were used to calculate rainfall amounts, accumulated rainfall and rainfall intensities⁽²⁷⁾.

3.3.4 Hydrograph development:

For each site and for each storm the height of water above the crest of weir was determined for each 5 minutes from the graphs, then using the H-Q rating curves established before to establish a flood hydrograph.

3.4 Excess rainfall and direct runoff:

The excess rainfall hyetograph may be determined from the rainfall hyetograph depending on weather streamflow data. The ϕ -index is that constant rate of abstractions (mm/hr) that will yield an excess rainfall hyetograph with a total depth equal to the depth of direct runoff r_d over the watershed⁽¹³⁾.

The depths of direct runoff or excess rainfall in mm were calculated using the following equation

$$r_d = \sum_{m=1}^M (R_m - \phi \Delta t) \dots\dots\dots (2)$$

where ϕ -index is the constant rate of abstractions (in/hr or cm/hr),
and R_m is the observed rainfall (mm) in time interval m ⁽¹³⁾.

3.5 Topographic Map:

A topographic map was used for the following purposes:

- 1- determining the exact area and defining the boundary of each subbasin.
- 2- determining the length and the slope of main channel for each subbasin.

The topographic map was prepared by the Royal Jordanian Geographic Center with a scale of 1:20000.

Length of main channel and area of each subbasin was determined using the plannometer.

3.6 Runoff coefficient:

Runoff coefficient was calculated for each storm and for each subbasin using the following equation

$$C = \frac{r_d}{\sum_{m=1}^M R_m} \dots\dots\dots (1)$$

Where C = runoff coefficient.

r_d = depth of runoff (mm), and

R_m = total rainfall depth (mm)⁽¹³⁾

3.7 Modeling:

The hydrological model (HEC-1) which developed by the hydrological Engineering Center of the U. S. Army Corps of Engineers is an event simulation model and is used for modeling a single rainfall-runoff event. The HEC-1 model is probably the most widely used hydrologic event simulation model⁽¹³⁾.

3.7.1 Basin Schematic:

The basin is subdivided into an interconnected system of wadi or stream network components (Figure 4) using topographic map and other geographic information. A basin schematic diagram (Figure 5) of these components was developed using the following steps

1. The boundary of the study area watershed boundary is delineate from topographic map.
2. The basin is divided into a number of subbasins (table 3). Then the number and types of stream network components to be used in the model are determined.

Table 3: The areas of subbasins in the Muwaqqar basin.

Subbasin	S10	S20	S30	S40	S50	S60	S70
Area (k m ²)	27.60	15.70	17.60	0.25	0.90	6.90	1.12

3. Each subbasin will be represented by a combination of model components: subbasin runoff, channel routing, and reservoir components.



Fig. 4: The subbasins area of the Al-Muwaqqar Basin.

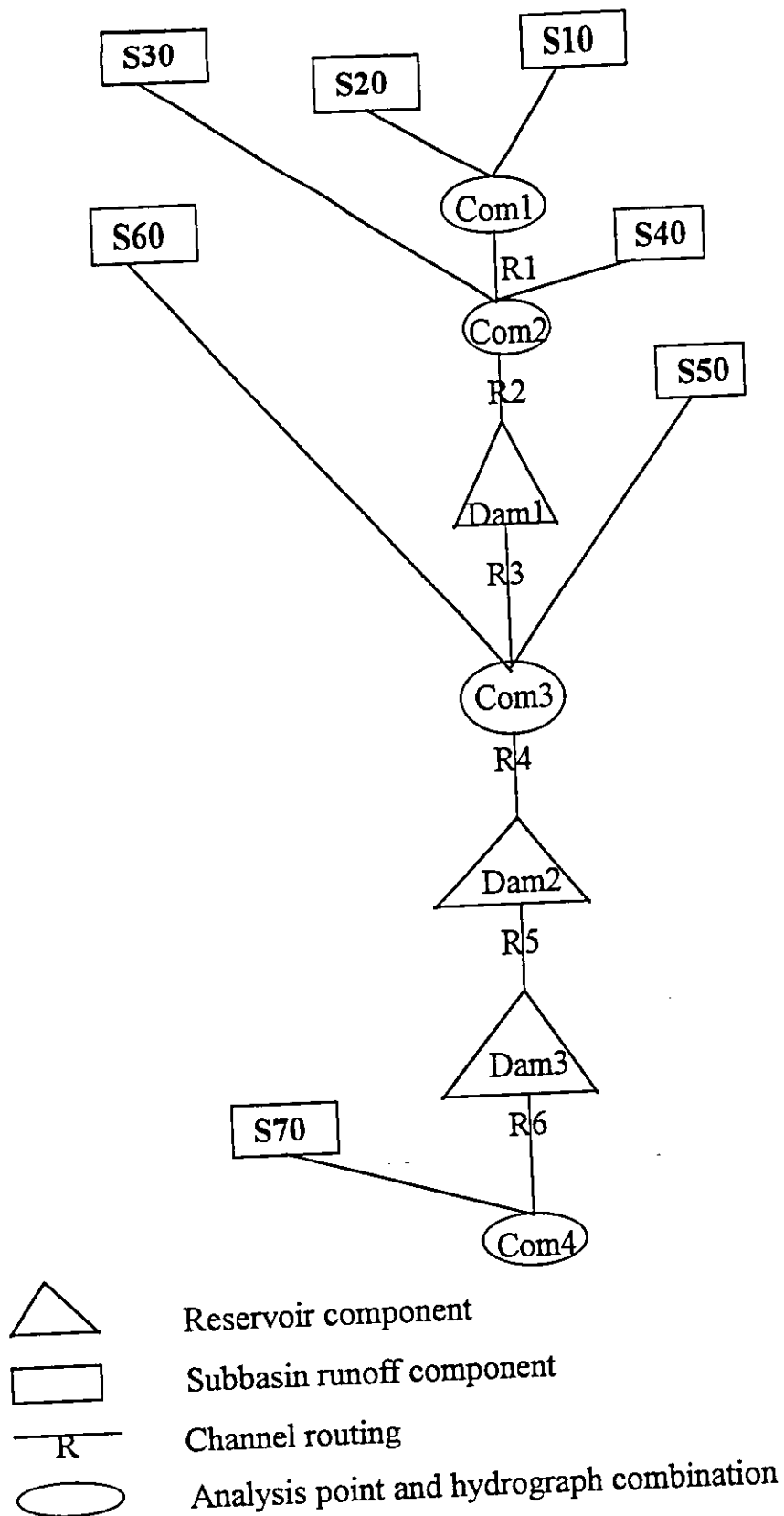


Figure 5: HEC-1 Basin Schematic.

4. Subbasins and their components are linked together to represent the connectivity of the river basin. HEC-1 has available number of methods for combining or linking together outflow from different components. This step finalizes the basin schematic⁽⁴⁾.

3.7.2 Model Components:

1. Land Surface Runoff Component:

The subbasin land surface runoff component, namely subbasin S10, S20, S30, S40, S50, S60, and S70 are used to represent the movement of water over the land surface and in stream channels. The input to this component is a precipitation hyetograph. Precipitation excess is computed by subtracting infiltration losses based on a soil water infiltration rate function. The resulting rainfall excesses are then routed by the unit hydrograph to the outlet of the subbasin producing a runoff hydrograph.

2. Channel Routing Component:

A channel routing component (element R 1, Fig. 5) is used to represent flood wave movement in a channel. The input to this component is an upstream hydrograph resulting from individual or combined contributions of subbasin runoff. The hydrograph is routed to a downstream point based on the characteristics of the channel.

3. Combined Use of Channel Routing and Subbasin Runoff Components:

The model consider the use of subbasin runoff components S10, S20, S30, S40 are considered, and the analysis point Com 1 in Fig. 5 and

the corresponding subbasins S10, S20, S30, and S40 in Fig. 4. The runoff from components S10 and S20 are calculated and combined at analysis point Com 1. The runoff from analysis point Com 1 is routed to analysis point Com 2. Runoff from subbasins S30, and S40 are calculated and combined with the outflow hydrograph from R 1 at analysis point Com 2.

4. Reservoir Component:

The use of the reservoir component is similar to that of the channel routing component. The reservoir component can be used to represent the storage-outflow characteristics of a reservoir. The reservoir component functions by receiving upstream inflows and routing these inflows through a reservoir using storage routing methods. Reservoir outflow is a function of storage (or water surface elevation)⁽⁴⁾.

3.7.3 Rainfall-Runoff Simulation:

3.7.3.1 Precipitation Hyetograph:

A precipitation hyetograph is used as an input for all runoff calculations. The specified precipitation is assumed to be the basin average (i.e., uniformly distributed over the subbasin). The Hyetograph represents the average precipitation depths over the computation interval. The precipitation is calculated by Thiessen polygons method⁽¹³⁾.

3.7.3.2 Interception and Infiltration:

Land surface interception, depression storage and infiltration are referred to in the HEC-1 model as precipitation losses. Interception and depression storage are intended to represent the surface storage of water by trees or

grass, local depressions in the ground surface, in cracks and crevices in parking lots or roofs, or in surface area where water is not free to move as overland flow. Infiltration represents the movement of water to areas beneath the land surface.

In the case of the unit hydrograph component, the precipitation loss is considered to be a subbasin average (uniformly distributed over an entire subbasin).

Two methods used to calculate the precipitation loss. An average precipitation loss is determined for a computation interval and subtracted from the rainfall/snowmelt hyetograph. The resulting precipitation excess is used to compute an outflow hydrograph for a subbasin.

1. Initial and Uniform Loss Rate:

An initial loss (mm), and a constant loss rate (mm/hr) are specified for this method. All rainfall is lost until the volume of initial loss is satisfied. After the initial loss is satisfied, rainfall is lost at the constant rate.

2. SCS Curve Number:

The basic equation for computing the depth of excess rainfall or direct runoff from a storm by the SCS method is

$$P_e = \frac{(P - I_a)^2}{P - I_a + S} \dots\dots\dots (13)$$

Where P_e is the depth of excess precipitation in inches

P is the depth of rainfall in inches

I_a is the initial abstraction before ponding in inches

S is the potential maximum retention in inches.

By evaluating the results from many small experimental watersheds, an empirical relation between I_a and S was developed for experimental watersheds in USA, as

$$I_a = 0.2S \dots\dots\dots (14)$$

On this basis

$$P_e = \frac{(P - 0.2S)^2}{P + 0.8S} \dots\dots\dots (15)$$

Plotting the data for P and P_e from many watersheds, the SCS developed curves shown in Figure 6⁽¹³⁾ To standardize these curves, a dimensionless curve number (CN) is defined such that $0 \leq CN \leq 100$. As an illustration.

The curve number and S are related by

$$S = \frac{1000}{CN} - 10 \dots\dots\dots (16)$$

Where S is in inches.

The curve numbers shown in Fig. 6 apply for normal antecedent moisture conditions (CN II). For dry conditions (CN I) or wet conditions (CN III), equivalent curve numbers can be computed by

$$CN(I) = \frac{4.2CN(II)}{10 - 0.058CN(II)} \dots\dots\dots (17) \text{ and}$$

$$CN(III) = \frac{23CN(II)}{10 + 0.13CN(II)} \dots\dots\dots (18) \text{ respectively}$$

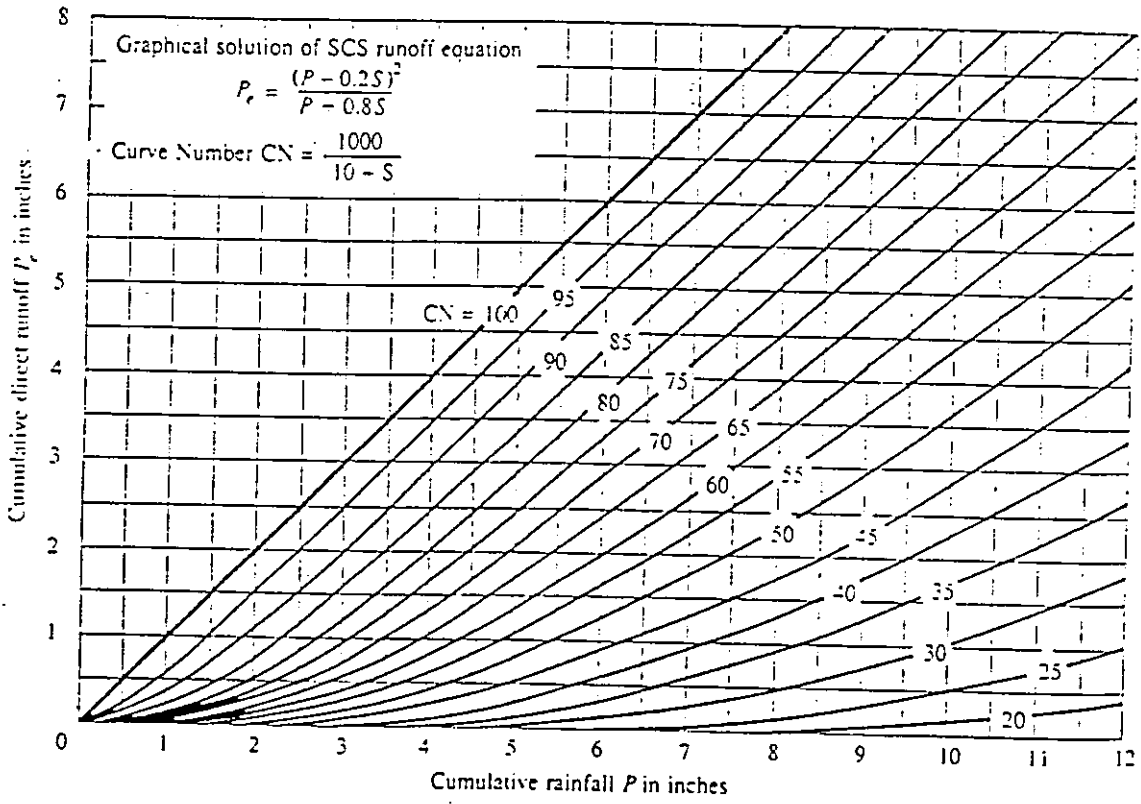


Figure 6: Solution of the SCS runoff equations.

The range of antecedent moisture conditions for each class is shown in Table 4⁽¹³⁾.

The SCS provides information on relating soil group type to the curve number as a function of soil cover, land use type and antecedent moisture conditions⁽⁴⁾.

Table 4: Classification of antecedent moisture classes (AMC) for the SCS method of rainfall abstractions⁽¹³⁾.

AMC group	Total 5-day antecedent rainfall (in)	
	Dormant season	Growing season
I	Less than 0.5	less than 1.4
II	0.5 to 1.1	1.4 to 2.1
III	Over 1.1	Over 2.1

(source: Soil Conservation Service, 1972, Table 4.2, p. 4.12.)

Since the SCS method gives total excess for a storm, the incremental excess (the difference between rainfall and precipitation loss) for a time period is computed as the difference between the accumulated excess at the end of the previous period⁽⁴⁾.

3.7.3.3 Unit Hydrograph:

The unit hydrograph technique is used in the subbasin runoff component to transform rainfall excess to subbasin outflow. A unit hydrograph can be directly input to the program or a synthetic unit hydrograph can be computed from user supplied parameters, or optimization.

Basic Methodology:

A 1-hour unit hydrograph is defined as the subbasin surface outflow due to a unit (1 inch or mm) rainfall excess applied uniformly over a subbasin in a period of one hour. Unit hydrograph duration's other than an hour are common.

Synthetic Unit Hydrographs:

The parameters for the synthetic unit hydrograph can be determined from gauge data by employing the parameter optimization option. Two synthetic unit hydrograph methods are available in the model; they are:

1. Snyder Unit Hydrograph:
2. SCS Dimensionless Unit Hydrograph:

3.7.3.4 Flood Routing:

Flood routing is used to simulate flood wave movement through river reaches and reservoirs. Most of the flood-routing methods available in HEC-1 are based on the continuity equation and some relationship between flow and storage or stage.

1. Muskingum Method:

The Muskingum method is used for channel routing computes outflow from a reach.

Table 5 shows the length of channel, the channel slopes, and the roughness coefficient.

Table 5: The channel length, slope channel and roughness coefficient for all routing channel.

Routing	Channel length (km)	Slope	Manning Roughness ²⁹
R 1	0.650	0.010	0.030
R 2	0.576	0.008	0.030
R 3	0.504	0.008	0.030
R 4	0.400	0.003	0.030
R 5	0.522	0.003	0.030
R 6	0.386	0.003	0.030

2. Level-Pool Reservoir Routing:

Level-Pool reservoir routing assumes a level water surface behind the reservoir. A reservoir storage volume versus elevation relationship is required for level-pool reservoir routing.

Instruments installed to measure the discharge of water through the spillway of the first dam, rating curves were prepared for dam 1 and dam 2 (Figure 7)⁽³⁰⁾. The same calibration curve for dam 3 is used because its spillway has the same characteristics of dam 1. The elevation-Storage-Area Curves of the three dams were used (Figure 8)⁽³⁰⁾.

3.7.4 Optimization Methodology:

HEC-1 provides a powerful optimization technique for the estimation of some of the hydrologic parameters when gauged precipitation and runoff data are available. By using this technique and regionalizing the results, rainfall-runoff parameters for ungauged areas can also be estimated.

The parameters calibration option has the capability to automatically determine a set of unit hydrographs and loss rate parameters that "best"

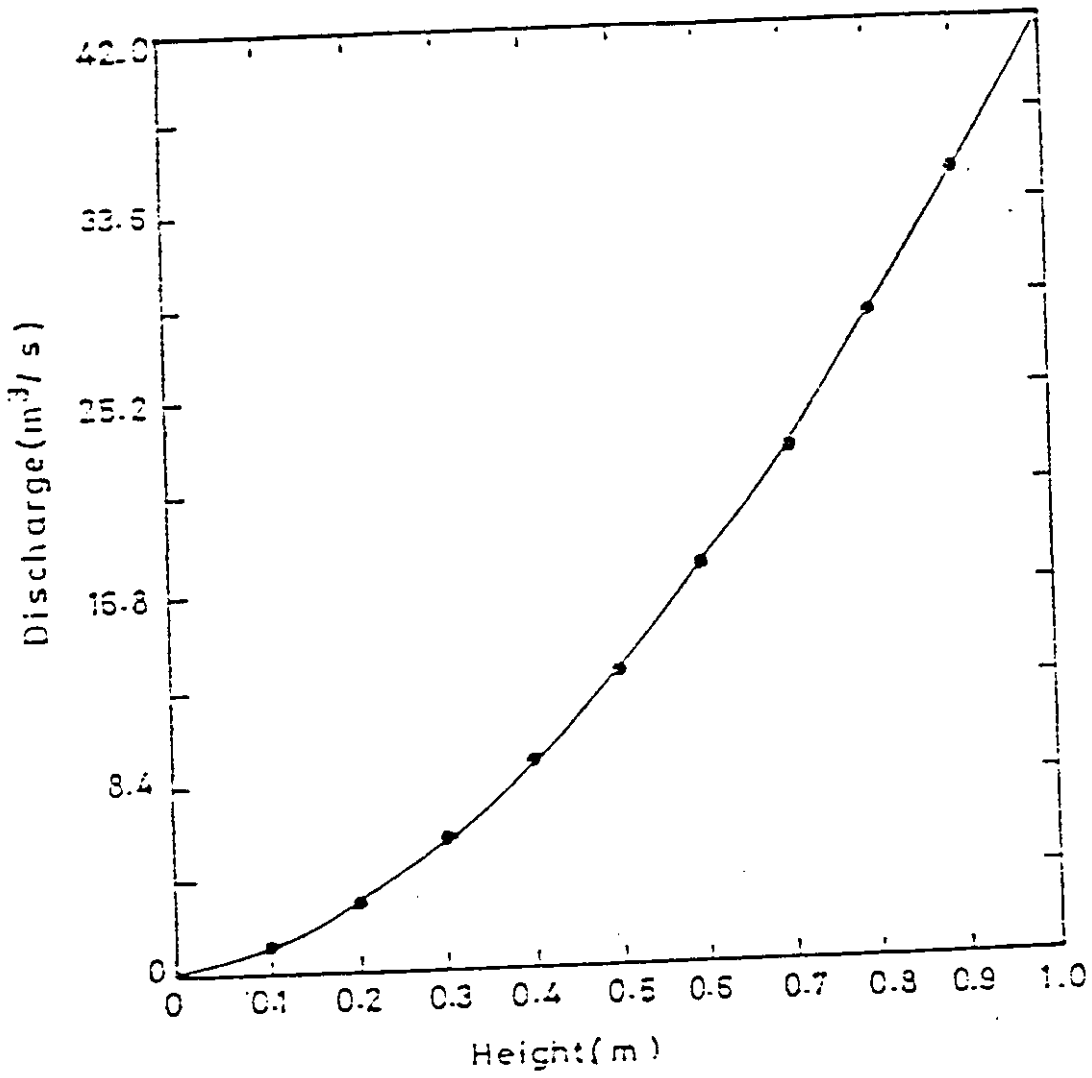


Figure 7: Rating curve of dams.

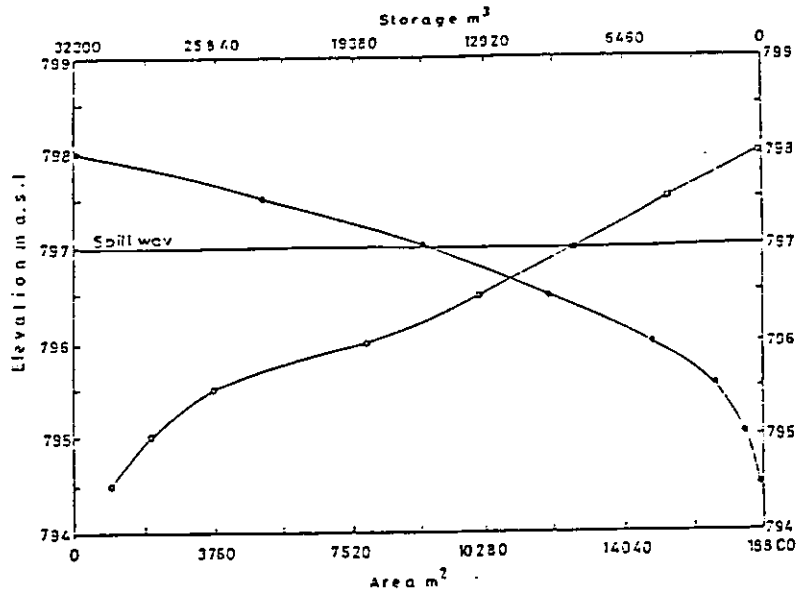
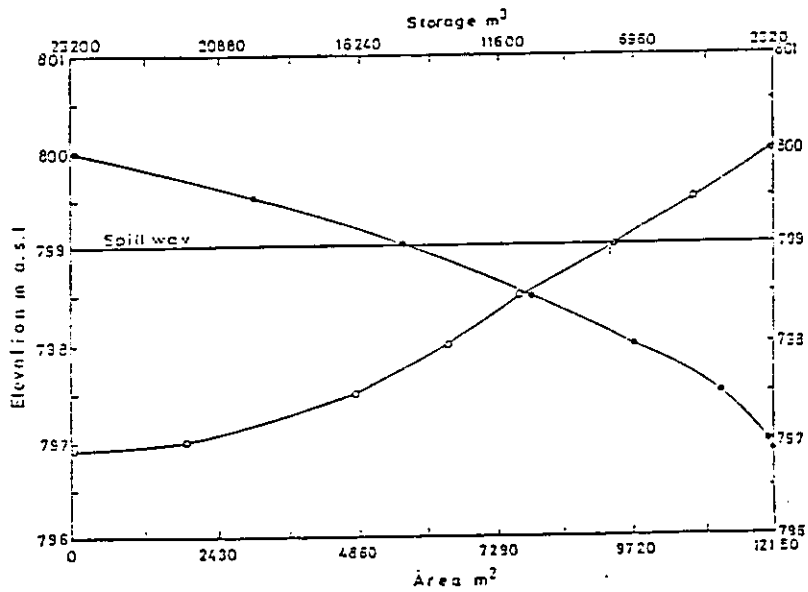
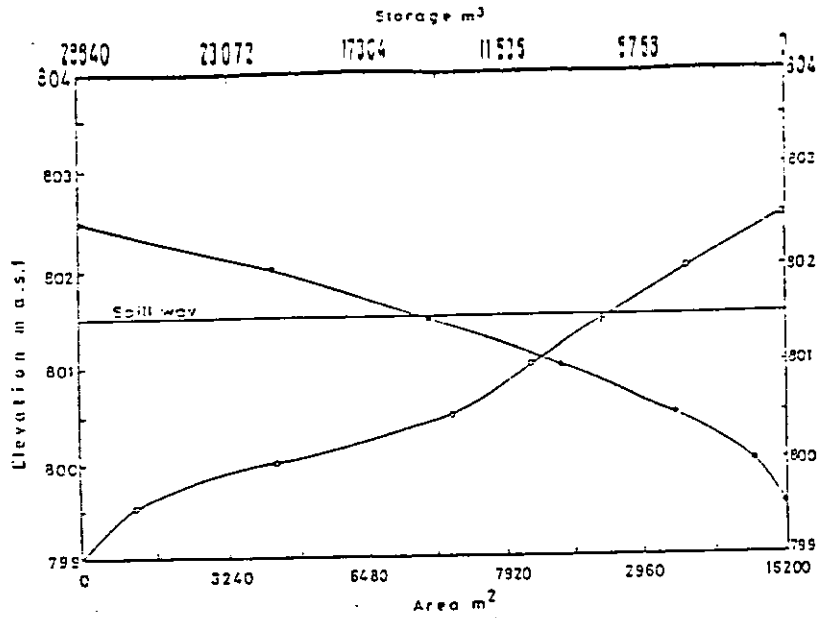


Fig. 8: Elevation-storage-area relationship of existing dams.

reconstitute an observed runoff hydrograph for a subbasin. The data which must be provided to the model are: basin average precipitation; basin area; and the outflow hydrograph. Unit hydrograph and loss rate parameters can be determined individually or in combination. Parameters that are not to be determined from the optimization process must be estimated and input to the model.

The runoff parameters that can be determined in the calibration are the unit hydrograph parameters of the Snyder and SCS methods and the loss rate parameters of the SCS and initial/constant methods. If the Snyder method is employed, the Clark parameters (time of concentration, and Clark storage coefficient) will be determined and converted to the Snyder parameters.

The objective function is the square root of the weighted squared difference between the observed and computed hydrograph. This difference will be a minimum for the optimal parameters estimates.

The objective function computed as follows.

$$OF = \left[\sum (QO_i - QC_i)^2 * WT_i / n \right]^{1/2} \dots\dots\dots (19)$$

Where QO_i is the observed runoff hydrograph ordinate i

QC_i is the runoff hydrograph ordinate for time period i computed by HEC-1

n is the total number of hydrograph ordinates

WT_i is the weight for the hydrograph ordinate i computed from the following equation.

$$WT_i = \frac{(QO_i - QA)}{2 * QA} \dots\dots\dots (20)$$

Where the QA is the 'average observed discharge.

Three subbasin were selected with different areas 7.3, 0.5, and 5.8 km² for site 1, site 2, and site 3 (Figure 1) respectively in order to make the optimization unit graph and loss rate parameters. The gauged rainfall and runoff data must be provided to the model. The estimate of the hydrological parameter for the ungauged catchment is then calculated as the weighted average of the hydrological parameters values for the three selected sites.

3.7.5 Verification methodology:

The HEC-1 model has different verification criteria to compare the observed and calculated discharges. It is possible to compare the observed and the calculated discharges graphically. This graphical representation visually helps verify the differences between observed and simulated discharges. The correlation coefficient (R^2) was calculated for selected storms.

For the comparison between observed and calculated hydrograph sites 3 and 4 were selected, using data from the previous year (1993/1994). The parameters derived from the HEC-1 optimization technique for site 3 was used. For Site 4, the weighted average of the infiltration rate parameters derived from the HEC-1 optimization technique for the three sites were used. The lag time was calculated from the time of concentration.

4. Results and discussions

4.1 Infiltration Rate:

The relationships between surface runoff, rainfall depth and intensity, soil water content, and infiltration rate are the basis for any hydrological study.

Infiltration rates for the three selected sites are illustrated in Figures 9, 10, and 11. Results indicated that the basic (long term) infiltration rates measured using the double ring infiltrometer for all sites were high and the value was 12, 5, and 11 mm/h for sites 1, 2, and 3 respectively. According to these results, surface runoff should be minimum and almost zero. However, measured surface runoff indicates that a significant surface runoff occurs even with very low rainfall intensity (e.g. storm 4 in table 6). This means that the infiltration measured by the double ring infiltrometers in soils with crust is not accurate for two reasons.

1. Crust formation in soils exposed to the beating action of falling drops (structural crust) is due to breakdown of the soil aggregates crusted by the impact action of the rain drops reduces the average size of the pores of the surface layer. Also the impact of raindrops causes compaction of the uppermost layer of the soil. These factors produce a thin skin seal at the soil surface.

2. When the double ring infiltrometer was driven into the soil, the crust was crashed especially around the wall, so the pores of the soil surface increased, which in turn increases the infiltration rates.

Actual basic infiltration rates for all storms were determined during 15 Nov. 1994 - 19 Dec. 1994 depending on observed rainfall and surface runoff data by using the HEC-1 optimization techniques. The results indicated that the basic (long term) infiltration rate varied according to storms and soil surface characteristics from 0.4 mm/h - 6.7 mm/h with an average of 1.7 mm/hr as show in table 6.

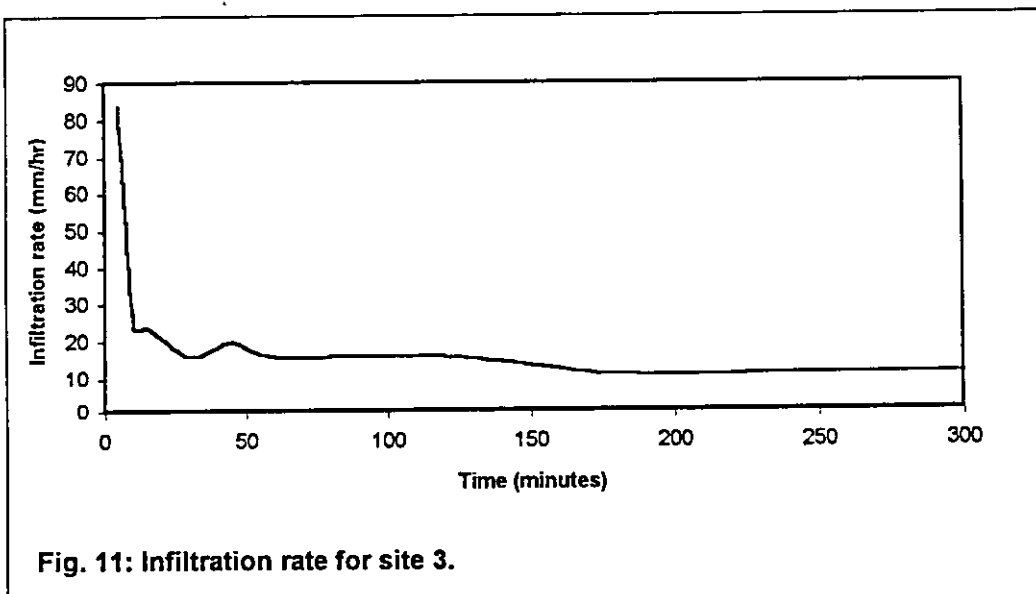
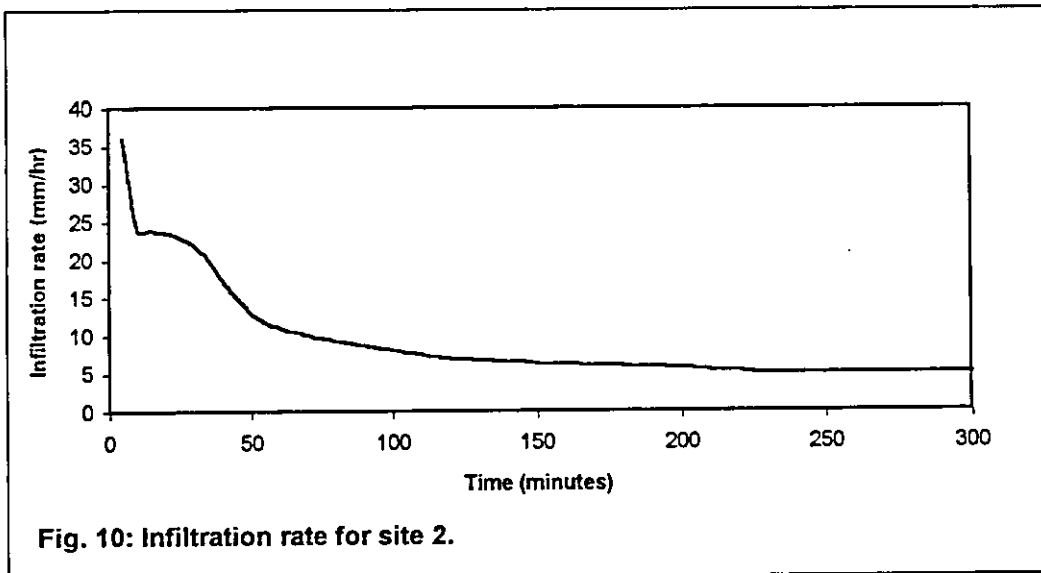
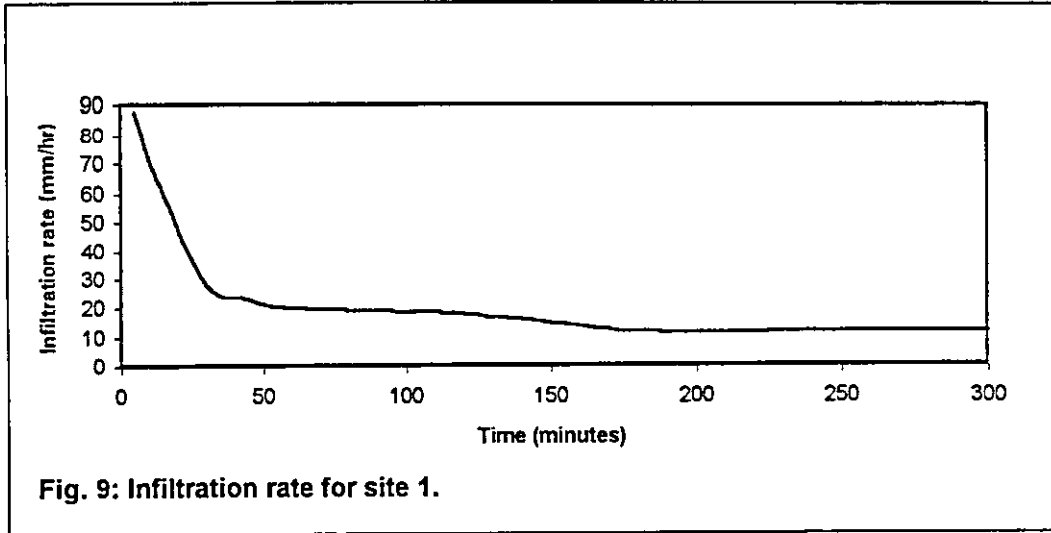


Table 6: The weight average of all sites resulting optimization initial, and uniform loss rate.

Storm	Date	I. l.	U. l. rate
1	15/11/94	2.01	0.34
2	23/11/94	4.19	6.7
3	23/11/94	3.22	1.96
4	24/11/94	1.55	1.25
5	2/12/94	3	0.62
6	3/12/94	0.12	0.4
7	3/12/94	1.04	1.2
8	19/12/94	3.82	1.27
Average		2.4	1.7

I. l.: Initial loss (mm)

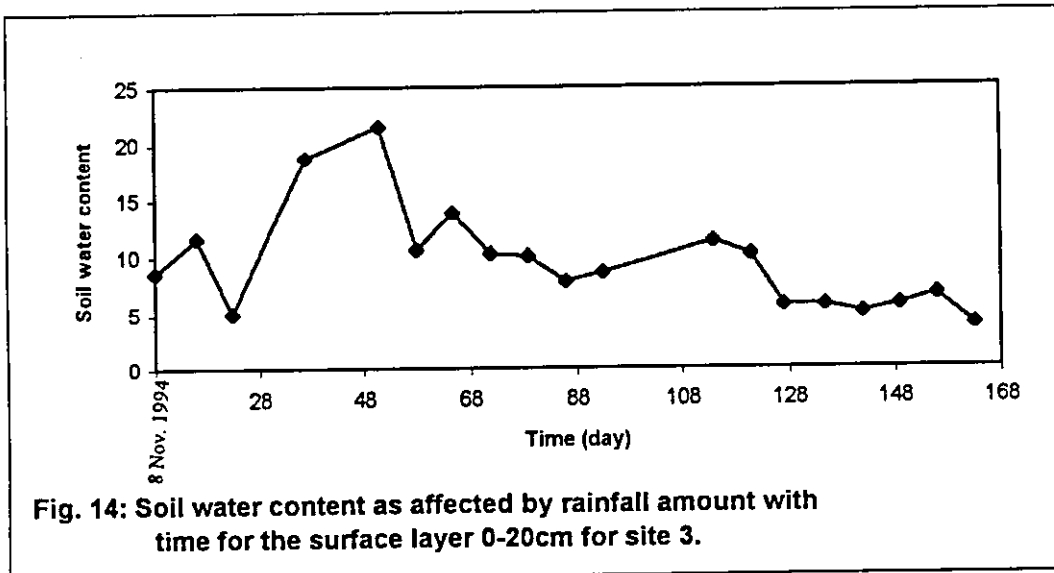
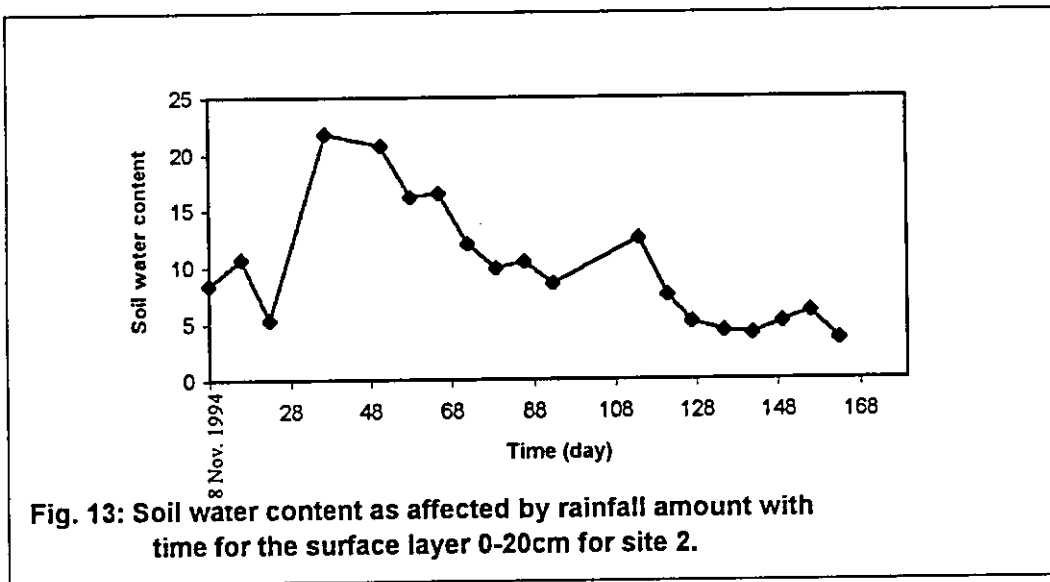
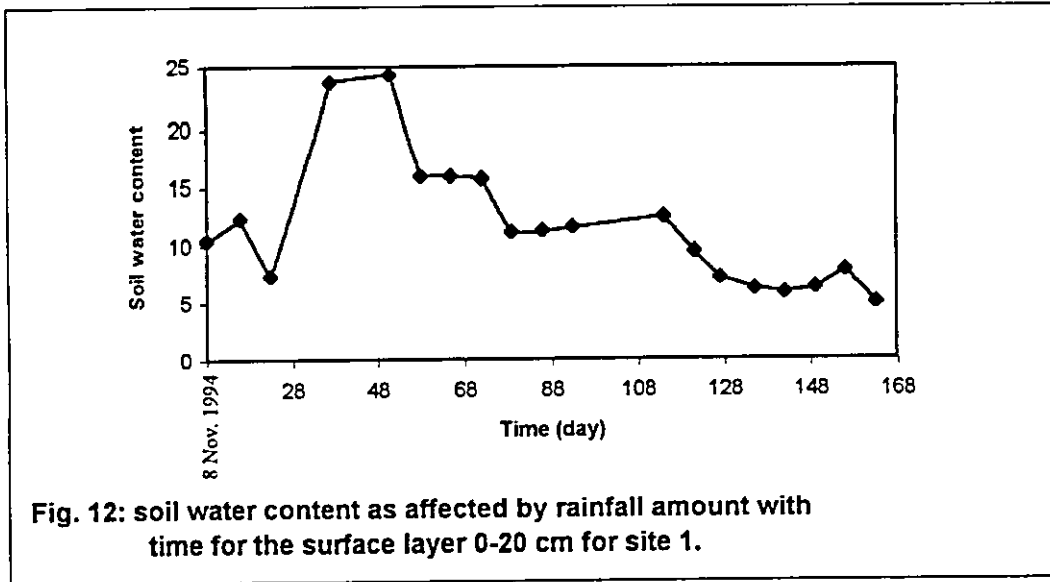
U. l. rate: Uniform loss rate (mm/hr)

5.2 Soil Moisture Content:

Soil moisture content for the surface layer for the three selected site are shown in Figures 12 through 14. Results indicated that soil water content had changed with time according to rainfall amounts and the interval between the rainfall storms. The maximum weighted average of soil water content was 23% and the minimum weighted average was 4.5%. Maximum change in soil water content was found to be 18.5% during the period between Nov. 8,1994 to Apr. 12,1995.

No runoff occurs at the outlet of the basin as long as the total amounts of rainfall during the rainfall event were less than initial abstraction. If the initial soil moisture contents were high, the amount of rainfall to satisfy the initial abstraction would be low. This is due to two reasons.

1. When the soil is wet, the capacity of the soil to absorb water decrease until it becomes less than the rainfall intensity. At this point the water ponding become on the soil surface. As rainfall continues, the surface ponding exceeds the surface retention capacity and the runoff begins.
2. Surface seal formation due to rain drop impact generally begins after the soil has been wetted to a certain degree and the breakdowns of soil aggregates occurs sooner when the initial soil water content is high and the internal aggregate resistance or cohesion is low. The breakdown under rainfall is mainly due to slaking, which is caused by rapid aggregate breakdown. The inter-aggregate pore space becomes quickly filled with the smaller aggregate produced. At this stage infiltration is reduced and runoff begin to develop quickly.



4.3 Relationship Between Rainfall and Runoff:

Figures 15 to 33 illustrate the excess rainfall related to the surface runoff hydrograph for each storm for the selected sites.

From Fig. 30 through 32, the excess rainfall intensity was constant and the discharge of the subbasin was also constant. After the time of concentration (T_c) every part of the catchment contributed to the surface runoff.

From Figure 15 the peak flow was high due to high rainfall intensity. The duration of surface runoff for site 2 was small (Figure 20 to 25) as compared to site 1 or site 3.

If runoff was expressed as discharge per unit area ($m^3/s/km^2$), the observed peak flows for site 2 is higher than that for site 3 (Table 7). This was due to the time taken by the water to flow through stream channels to the control section (the time of concentration).

In calculating the surface runoff volume and determining the peak flow, it was clear that the volume of runoff and the peak flow varied from storm to another according to rainfall amount, intensity and distribution, and the soil surface characteristics (Table 8).

At site 1 the maximum surface runoff volume was $41104 m^3$ caused by storm 3, while the total observed surface runoff volume during 1994/1995 season was $84751 m^3$. On the other hand the maximum peak flow caused by storm 2 is the highest because it has higher maximum and average intensity than the other storms.

At site 2, the maximum surface runoff volume is $5000 m^3$ caused by storm 3 which has the maximum peak flow. The total runoff volume during the 1994/1995 season equals $13020 m^3$.

At site 3 the maximum surface runoff volume is 37369 m³ caused by storm 3 which has the maximum peak flow with a total runoff volume during 1994/1995 season of 99056 m³.

Table 9 shows that the runoff coefficient varied according to rainfall intensity, duration, and distribution, and soil surface characteristics. At site 1, the runoff coefficient varied from a minimum of 0.06 to a maximum of 0.38 with an average value of 0.25 with storms of total rainfall of 2.78 mm and 3.57 mm, respectively. Same results concerning runoff coefficient were found by Shatanawi, and Abu-Awwad⁽¹⁾. Storm 4 has the lowest runoff coefficient because the rainfall is very low and most of it is used to satisfy the initial abstraction.

At site 2, the runoff coefficient varied from a minimum 0.1 to a maximum 0.68 with an average value of 0.40 with storms of total rainfall of 4.75 mm and 4.13 mm, respectively. The runoff coefficient is high due to the following:

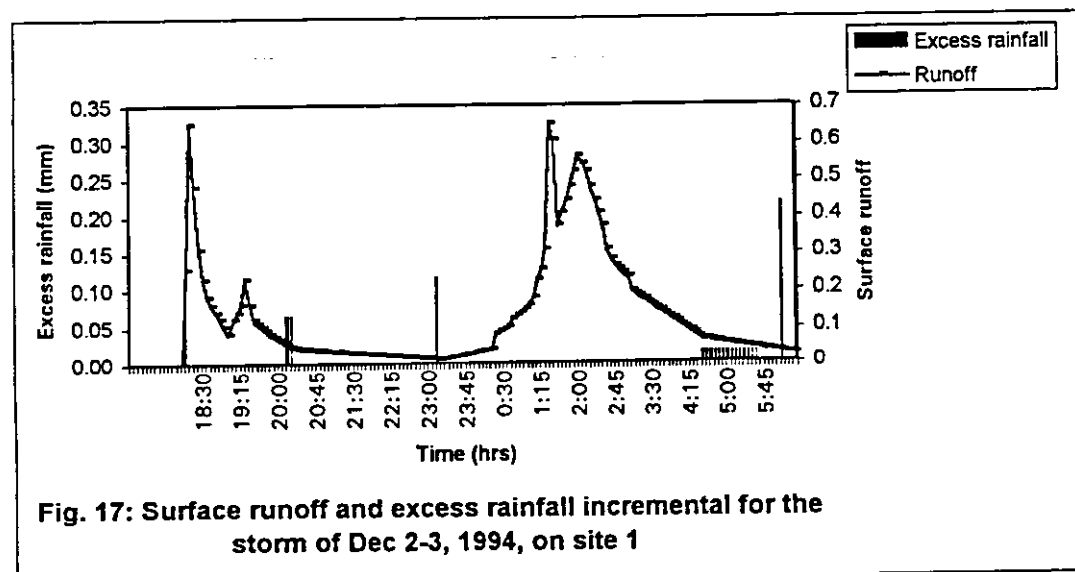
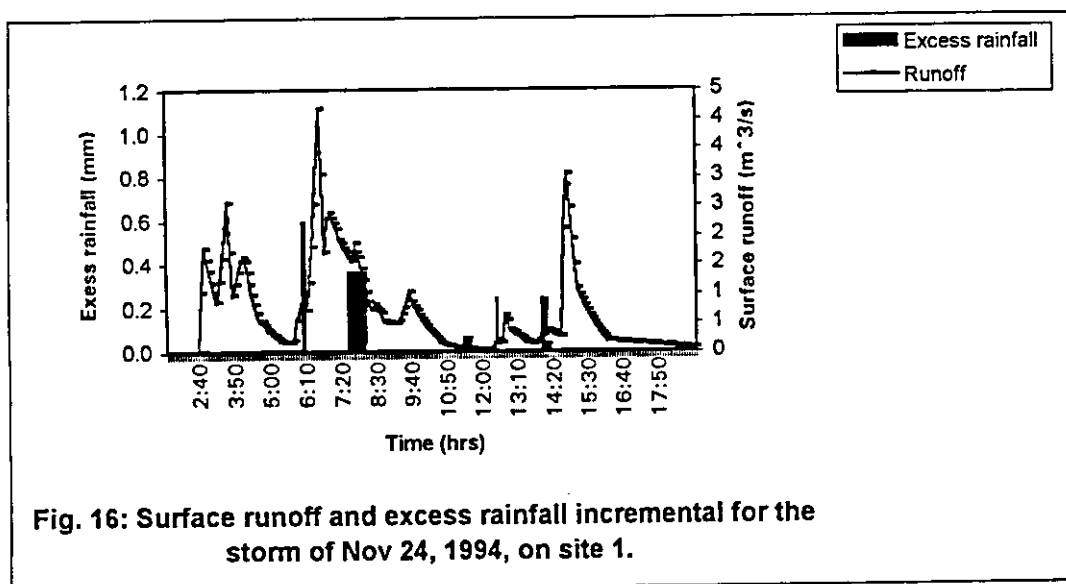
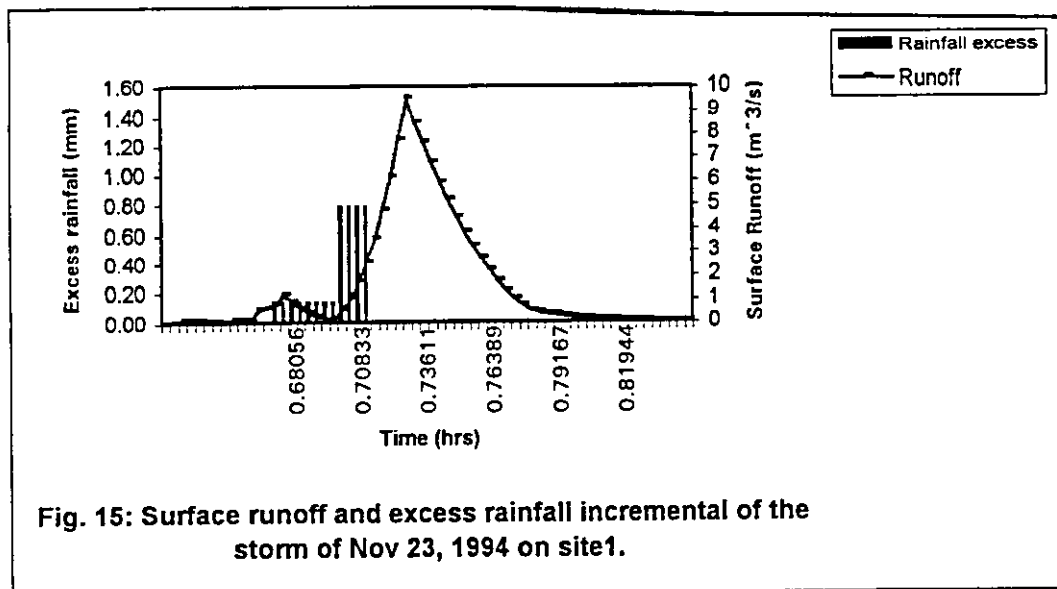
1. The basic infiltration rate is very low (Table 10) caused by crust formation due to the combined effect of the raindrop impact energy and the dispersion of clay particles at the soil surface. Same results were found by Ben Her et al.⁽⁸⁾ and Bardford et al⁽¹⁰⁾.
2. The subbasin area was small, so the runoff coefficient was high. Same result were found by Karniel et al⁽¹⁵⁾.
3. The slope of subbasin was high, so the infiltration capacities tend to be lower as slopes get steeper and vegetation gets less dense, thus the runoff was high.

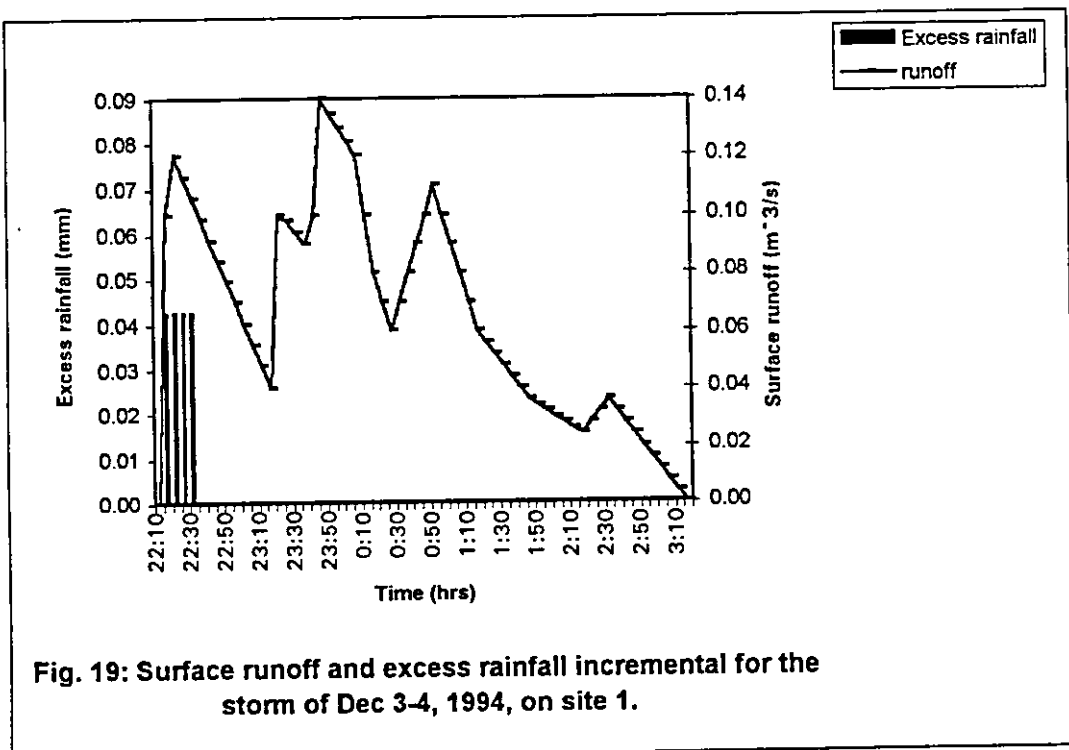
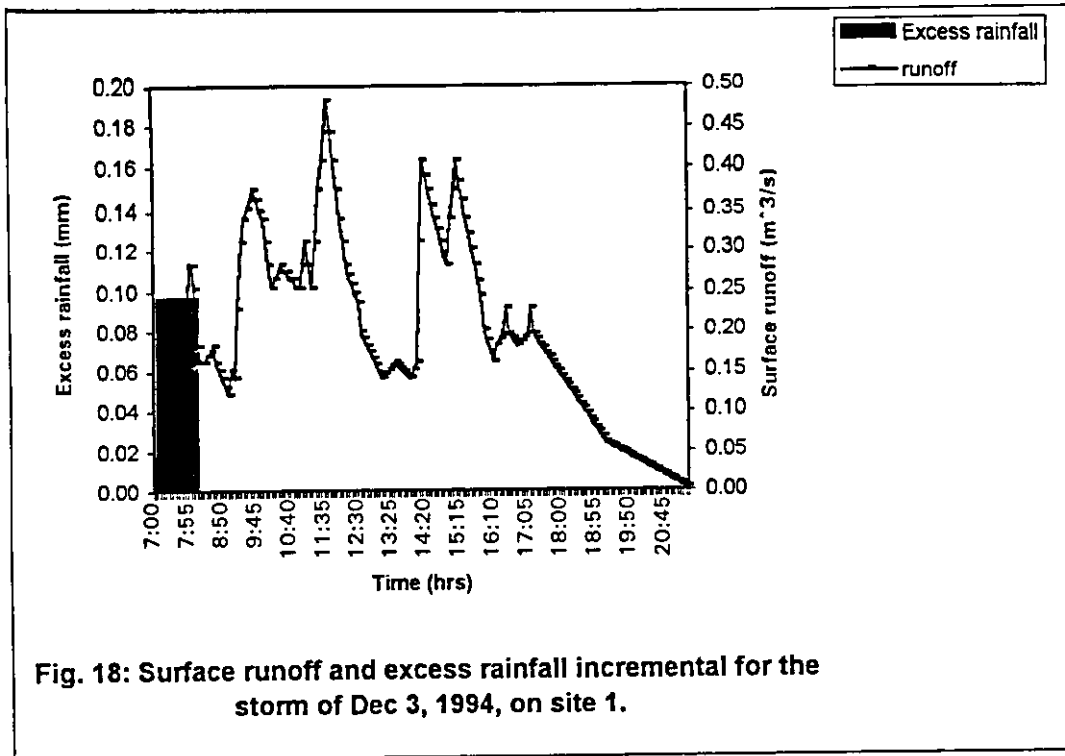
The moisture content of the soil increase gradually from storm 1 and 2, for the same storms, so the initial infiltration rate will decrease (Table 10),

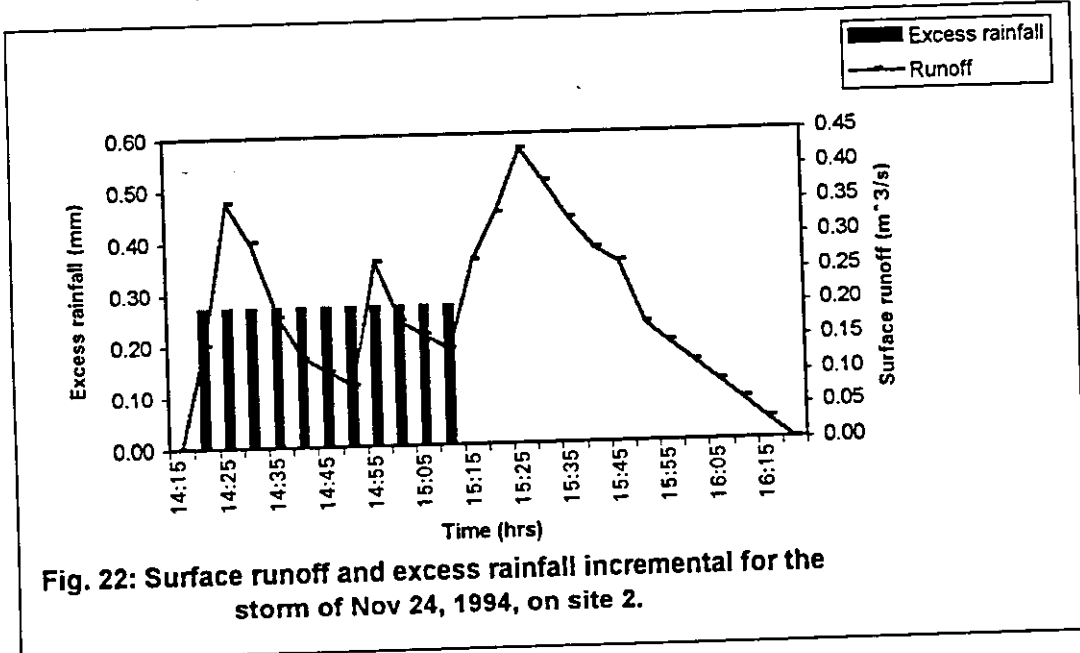
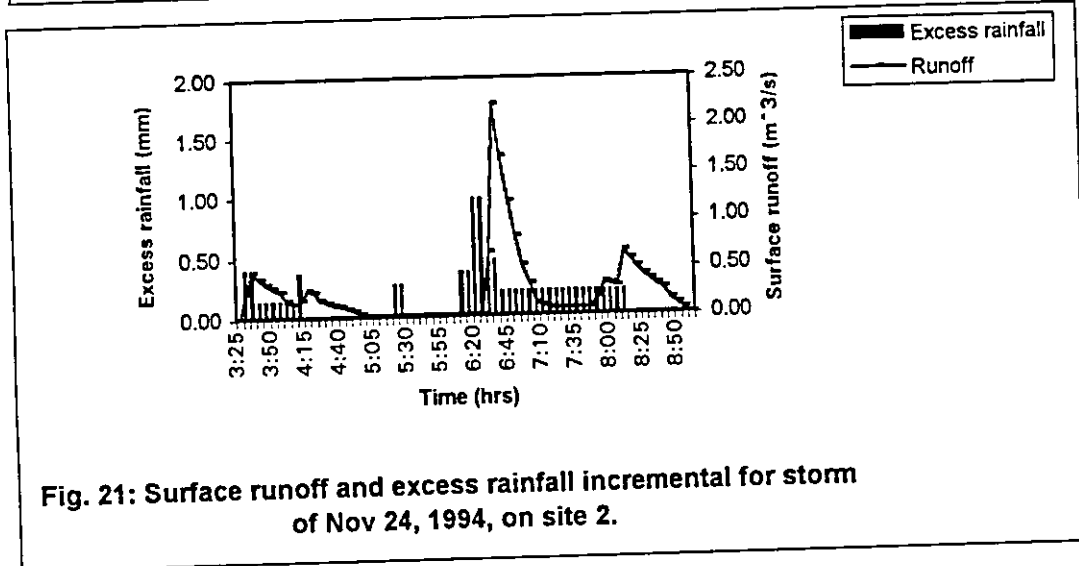
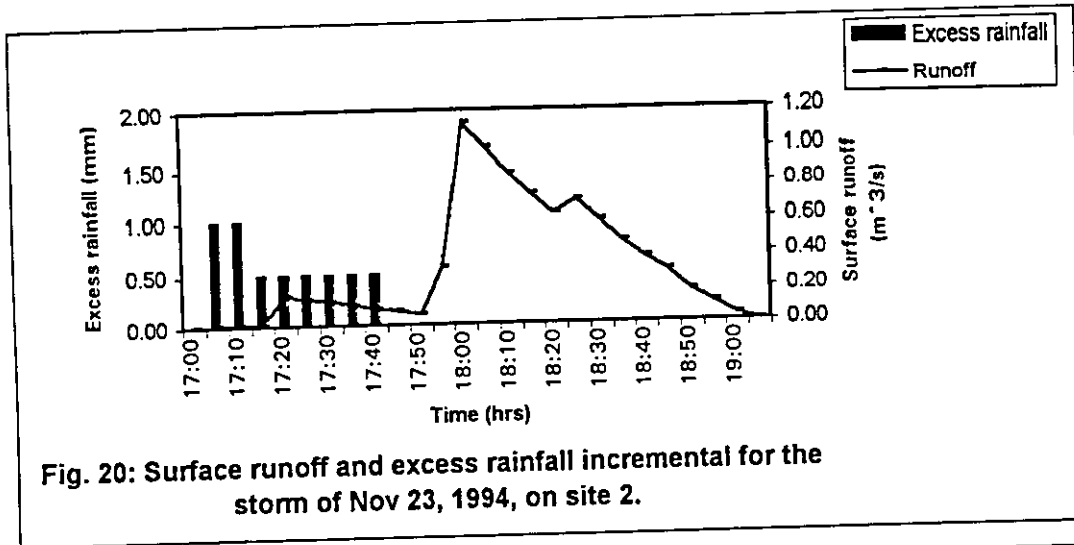
then the runoff coefficient increases (Table 9). Same results were found by Karniel et al.⁽¹²⁾.

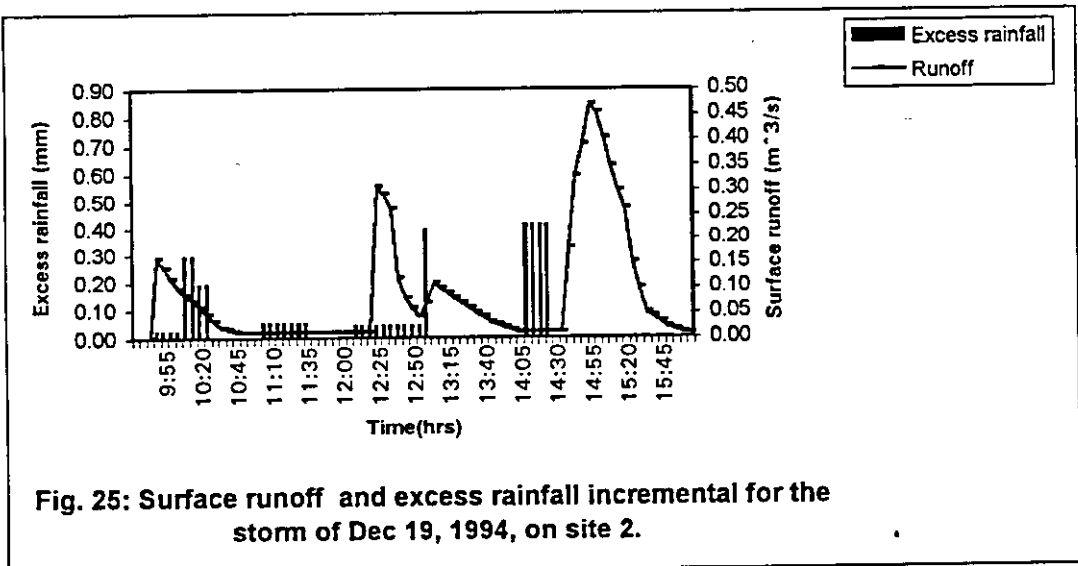
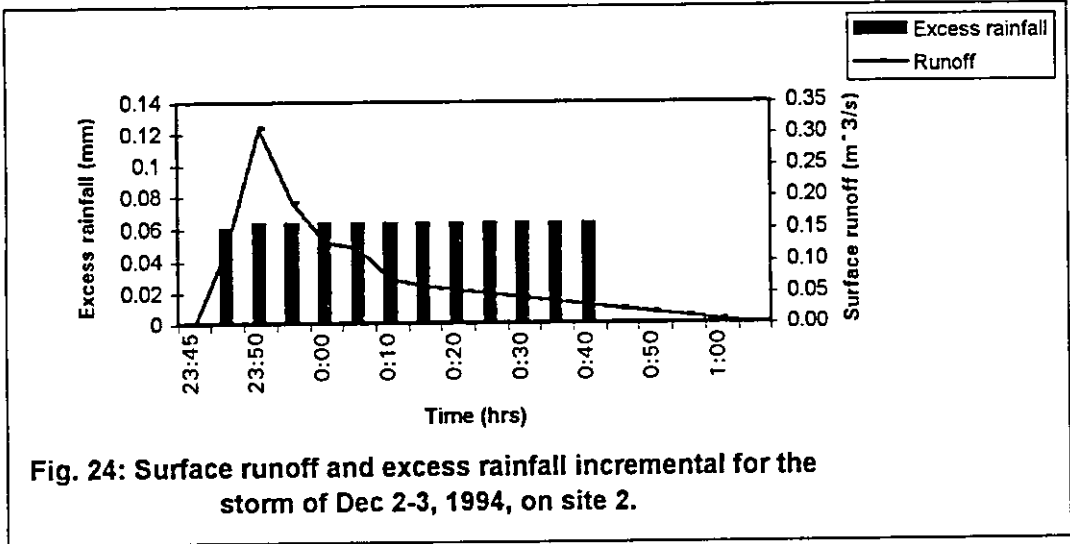
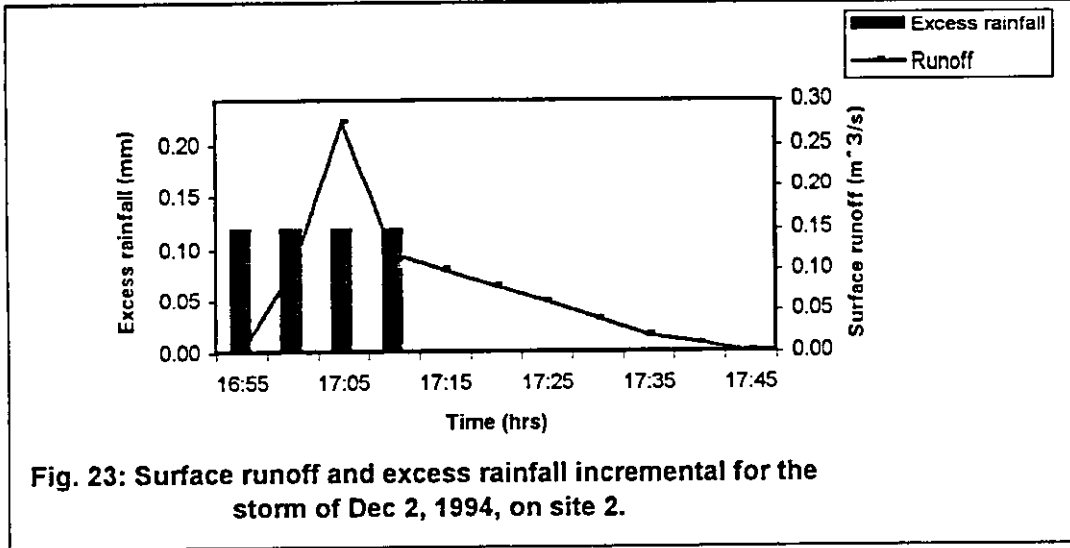
At site 3, the runoff coefficient varied from a minimum of 0.07 to a maximum of 0.4 with an average value of 0.23 with storms of total rainfall of 2.61 mm and 16.06 mm, respectively. The runoff coefficient of site 3 was less than that of site 1 because site 3 has higher initial and basic infiltration rate (Table 11). The runoff coefficient of site 1 and 3 is less than that of site 2 because non uniform distribution of the rainfall occurs sometime, so the area actually contributing to runoff is smaller than the total area of the basin, and therefore the volume of the runoff when related to the whole basin size, would be also small. Therefore the larger the catchment the smaller the runoff percentage. Same results were found by Karniel et al.⁽¹⁵⁾.

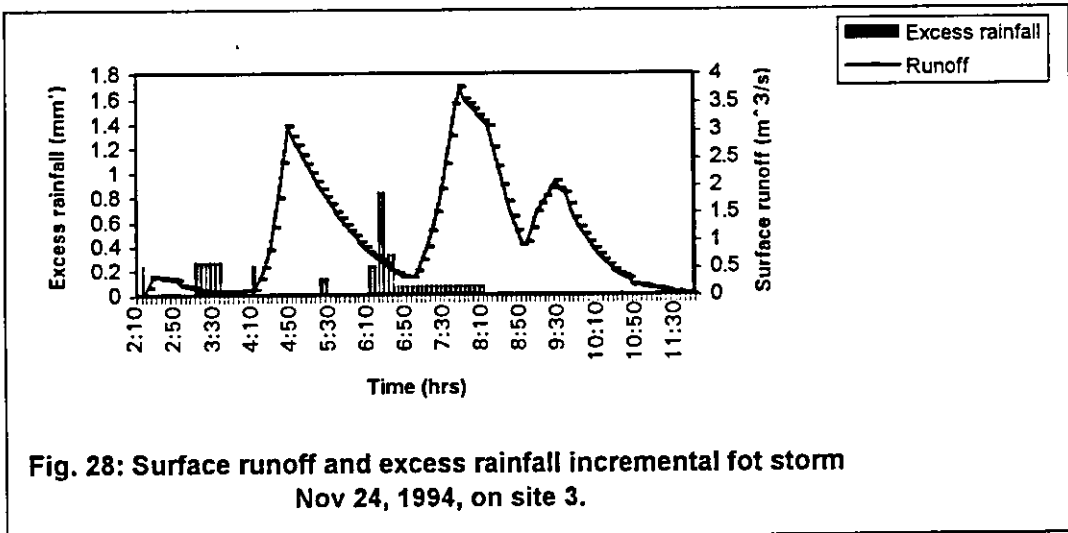
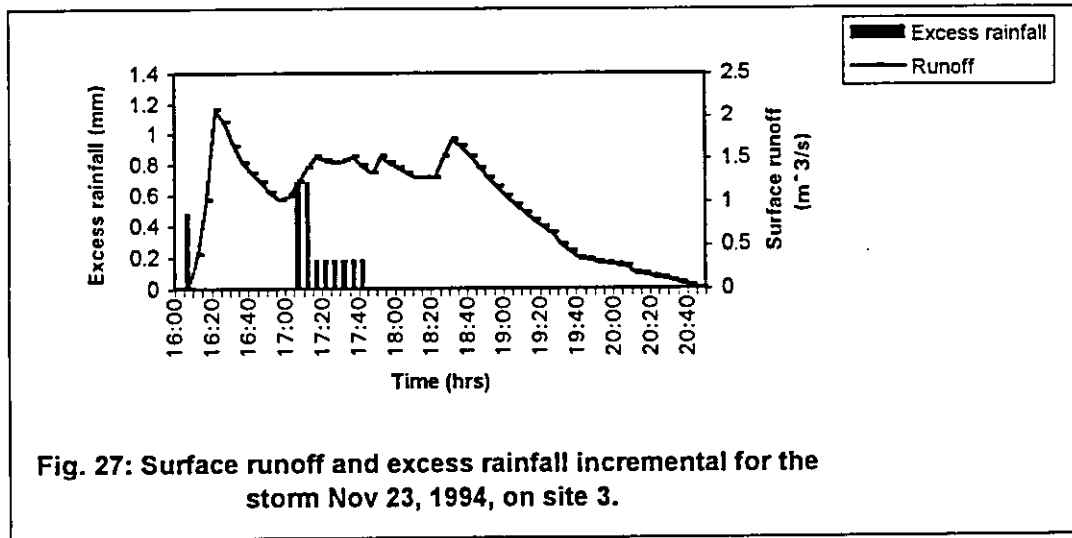
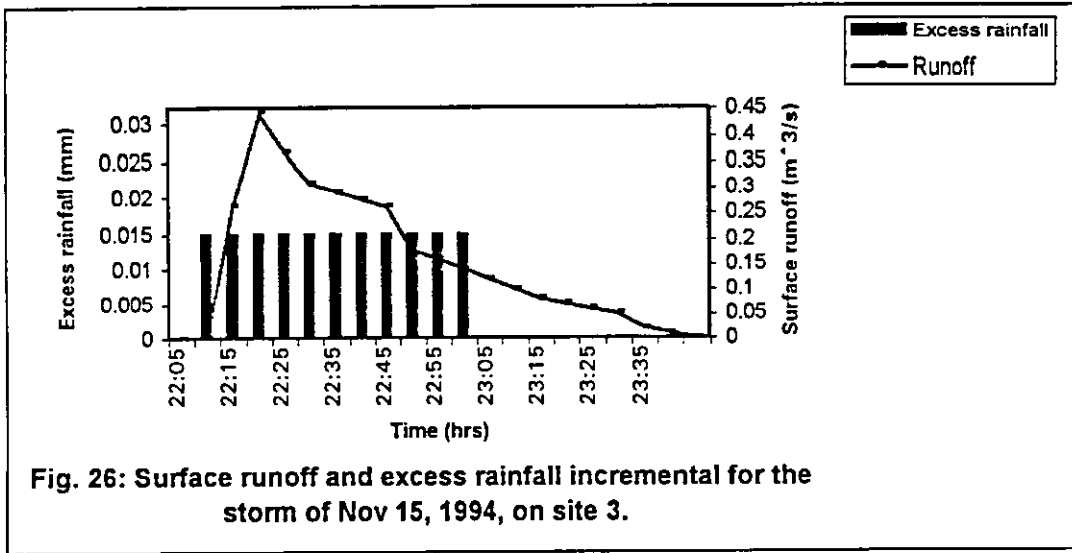
From the table 9, the small amounts of rainfall (e.g 2.5 mm) produce runoff because the rainfall intensity is often greater than the rate of infiltration in the soil because of the thin crust layer at the soil surface.

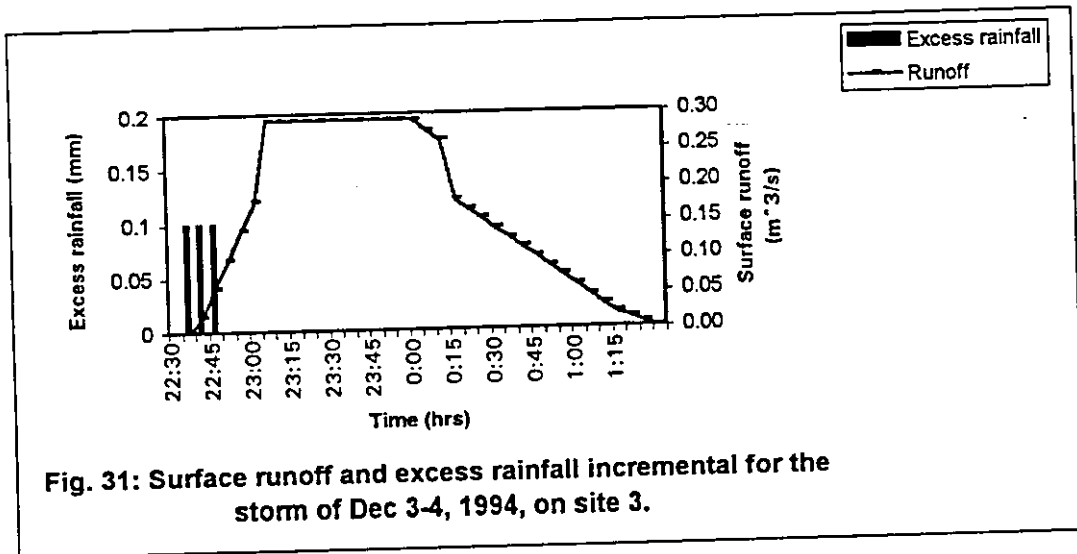
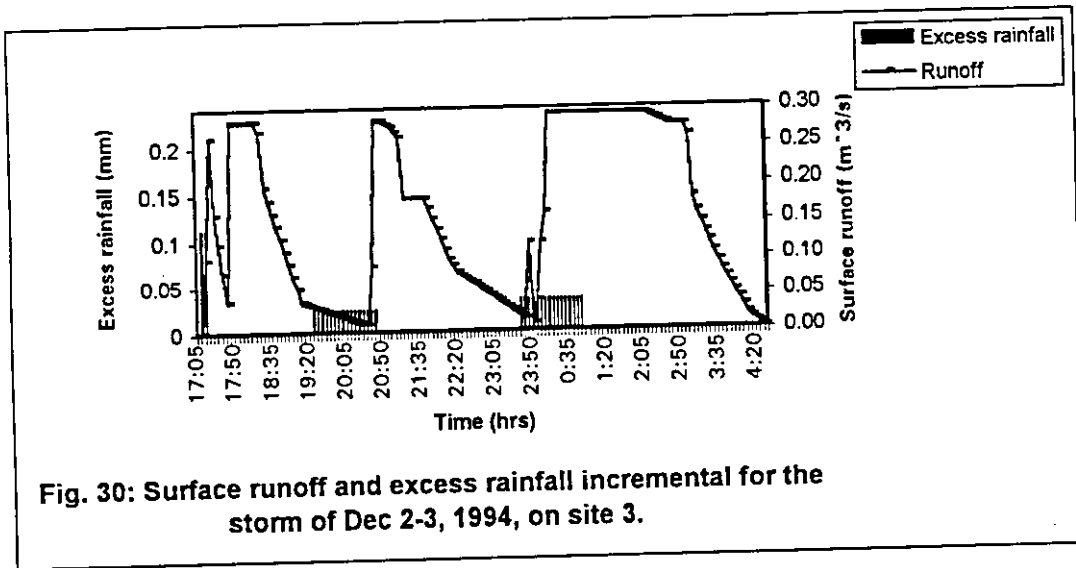
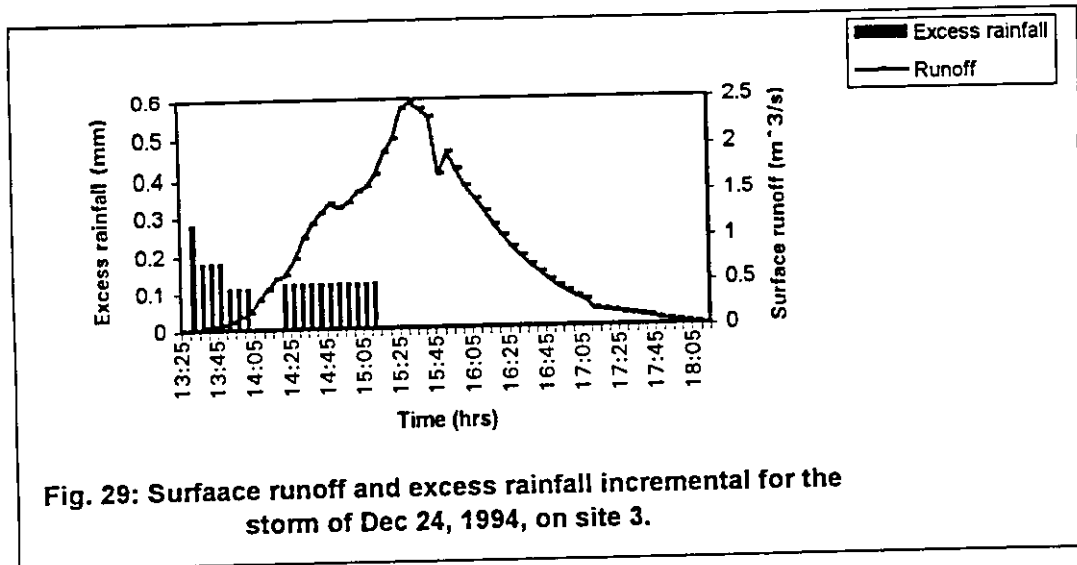












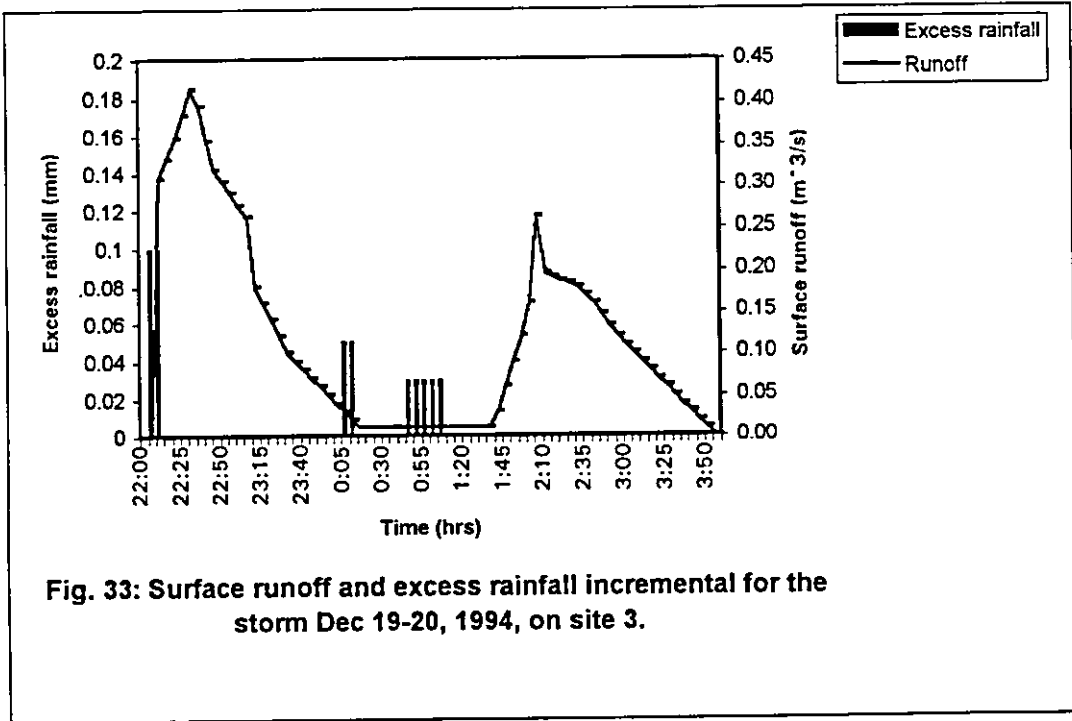
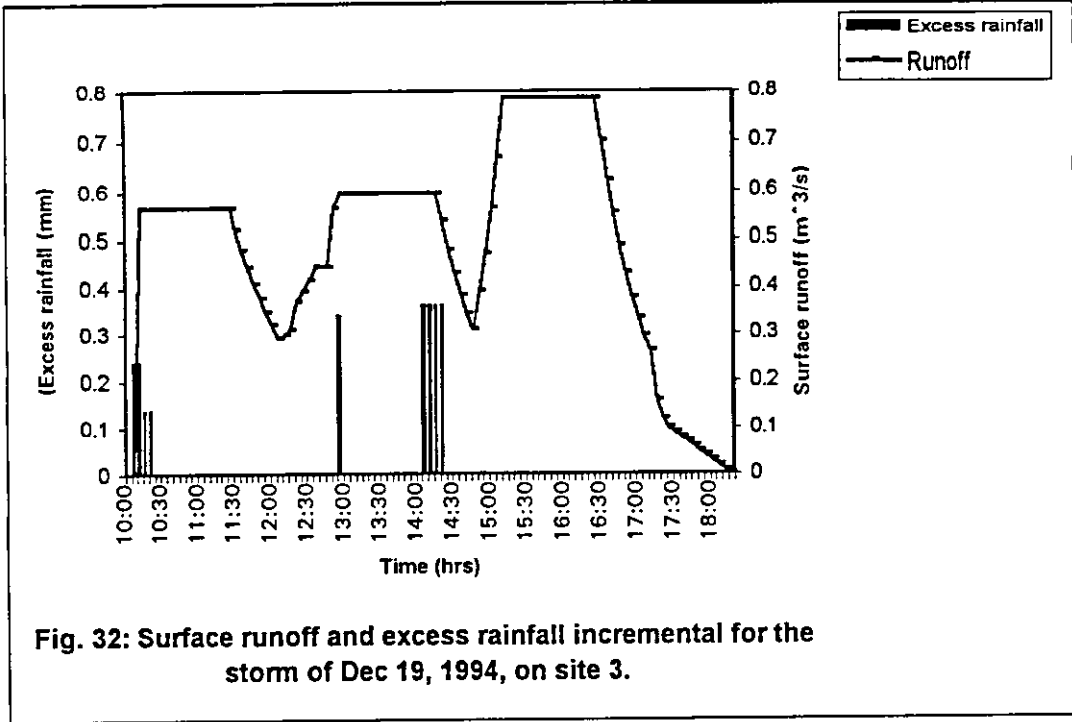


Table 7: The peake flow for the two selected site.

Rainfall	Site2	Site3
	Peak flow ($\text{m}^3/\text{s}/\text{km}^2$)	Peak flow ($\text{m}^3/\text{s}/\text{km}^2$)
1	2.28	0.35
2	4.4	0.65
3	0.86	0.42

Table 8: Runoff volume runoff and peak flow for three selected site

Storm	Date	Site 1		Site 2		Site 3	
		Volume (m ³)	Peak flow (m ³ /s)	Volume (m ³)	Peak flow (m ³ /s)	Volume (m ³)	Peak flow (m ³ /s)
1	15/11/94					977	0.44
2	23/11/94	30770	9.4	2500	1.14	16672	2.04
3	23/11/94	41104	4.15	5000	2.2	37369	3.75
4	24/11/94	1164	0.18	1500	0.43	14085	2.44
5	2/12/94	582	0.65	240	0.28	6323	0.29
6	2/12/94			380	0.308		
7	3/12/94	9894	0.48	1400	0.61	5002	0.29
8	3/12/94	1237	0.14			1725	0.29
9	19/12/94			2000	0.47	14373	0.82
10	19/12/94					2530	0.56
Total		84751		13020		99056	

Table 9: Runoff coefficient for each storm for all site during the period of 15 Nov. 1994 to 19 Dec. 1995.

Storms	Site 1			Site 2			Site 3		
	Rainfall (mm)	Runoff (mm)	Runoff coefficient	Rainfall (mm)	Runoff (mm)	Runoff coefficient	Rainfall (mm)	Runoff (mm)	Runoff coefficient
1							2.61	0.17	0.07
2	13.48	4.24	0.31	17.68	5	0.28	17.68	2.9	0.16
3	20.56	5.65	0.27	16.06	10	0.62	16.06	6.5	0.40
4	2.78	0.16	0.06	6.84	3	0.44	6.84	2.45	0.36
5	7.29	0.8	0.11	4.75	0.48	0.10	7.97	1.1	0.14
6				3.22	0.76	0.24			
7	3.57	1.36	0.38	4.13	2.8	0.68	4.14	0.87	0.21
8	2.5	0.17	0.07				2.7	0.3	0.11
9				12.71	4	0.31	12.7	2.5	0.20
10							2.91	0.44	0.15
Total	50.18	12.38		65.39	26.04		73.61	17.06	
Average			0.25			0.4			0.23

Table 10: Results of the optimization unit hydrograph and loss rate parameters for site 2.

Storm	Method 1			Method 4		
	tp (hr.)	In. loss (mm)	CN	tp (hr.)	In. loss (mm)	U. l. rate (mm/hr)
1	0.62	2.9	90.44	0.68	5.97	5.25
2	0.09	1.46	94.01	0.09	4.48	0.31
3	0.52	0.19	92.72	0.51	2.98	0.66
4	0.64	1.95	90.8	0.09	3.74	0.47
5	1.06	0.9	93.23	0.09	2.1	0.11
6	1.38	0.1	100	1.39	0.1	0.01
7	0.56	1.19	90.68	0.53	1.56	1.57
Average	0.12	1.2	93	0.48	3	1.2

tp: Lag time.

I. loss:Initial loss.

U. l. rate:Uniform loss rate.

Table 11: Results of the optimization unit hydrograph and loss rate parameters for site 3.

Storm	Method 1			Method 4		
	tp (hr.)	In. loss (mm)	CN	tp (hr.)	In. loss (mm)	U. l. rate (mm/hr)
1	1.13	0.37	90.16	1.94	2.3	0
2	0.52	7.15	89.76	0.86	3.28	9.98
3	1.07	0.32	90.57	1.26	1.15	2.08
4	0.52	1.05	92.41	0.88	0.2	2.65
5	0.97	1.85	90.02	0.95	4.04	0.45
6	0.68	0.6	90.74	0.93	1.56	1.09
7	1.41	0.13	83.56	1.53	4.04	1.9
8	0.93	0.11	90.72	0.34	1.4	0.57
Average	0.9	1.4	90	1.1	2.2	2.3

5.4 Optimization of Parameters

The surface runoff volume, peak flow, and time to peak were predicted from the optimization unit graph and loss rate parameters and were compared to the observed parameters. This comparison is shown in tables 12 to 23. The percentage error was calculated for the equivalent depth, peak flow, and time to peak for each storm and for the four methods for all sites. The results showed in tables 24 to 35. The equivalent depth, peak flow, and time to peak varied from one method to another and from one storm to another according to rainfall and soil characteristics. The calculated average percentage errors for all storms are shown in table 36, 37 and 38. From these tables the result indicates the following:

1. The Soil Conservation Service (SCS) curve number with SCS dimensionless unit hydrograph referred to as Method 1, the equivalent depth is smaller than the actual equivalent depth with an average difference of 24%, 33%, and 22% for sites 1, 2, and 3, respectively. The predicted peak flow is lower than the actual peak flow with an average of 44%, 66%, and 34% for site 1, 2, and 3, respectively. The predicted time to peak flow is almost higher than the actual time to peak flow with an average of 54%, 14%, and 30% for site 1, 2, and 3, respectively.

2. For the SCS curve number with Snyder unit hydrograph, referred to as Method 2, the equivalent depth is smaller than the actual equivalent depth with an average of 26%, 49%, and 23% for sites 1, 2, and 3, respectively. The predicted peak flow is lower than the actual peak flow with an average of 55%, 58%, and 40% for site 1, 2, and 3, respectively. The predicted time to peak flow is almost higher than the actual time to peak flow with an average of 47%, 14%, and 36% for site 1, 2, and 3, respectively.

3. For initial and uniform loss rate method with Snyder unit hydrograph, referred to as Method 3, the predicted equivalent depth is almost equal to the actual equivalent depth for sites 1, 2, and 3. The predicted peak flow is lower than the actual peak flow with an average variation of 46%, 52%, and 32% for site 1, 2, and 3, respectively. The predicted time to peak flow is almost higher than the actual time to peak flow with an average deviation of 42%, 15%, and 29% for site 1, 2, and 3, respectively.

4. The prediction of initial and uniform loss rate with dimensionless unit hydrograph, referred to as Method 4 shows that, the predicted equivalent depth is almost equal to the actual equivalent depth for sites 1, 2, and 3. The predicted peak flow is lower than the actual peak flow with an average deviation of 33%, 45%, and 39% for site 1, 2, and 3, respectively. The predicted time to peak flow is almost higher than the actual time to peak flow with an average deviation of 45%, 10%, and 19% for site 1, 2, and 3, respectively.

The predicted runoff and the peak flow for site 2 is less accurate than that for site 1 and 3. The time to peak for site 2 is more accurate than that of site 1 and 3.

The grand average percent error for the four methods were calculated and presented in table 39. The results indicates that method 4 is the most accurate. A closer results were obtained when the curve number method was used with Snyder unit hydrograph or with dimensionless unit hydrograph, but when the SCS dimensionless unit hydrograph was used with SCS curve number or Initial and uniform loss rate method, different results were obtained.

The results of the optimization unit hydrograph and the loss rate parameters for the method 1 and 4 for the three sites are presented in tables 40, 10, and 11. For site 1 (Table 40), the average initial loss and the average uniform loss are 1.9 and 1.5, respectively for the initial and uniform loss rate method with SCS dimensionless unit hydrograph.

For site 2 (Table 10), the average initial loss and the average uniform loss are 3 and 1.2, respectively for the initial and uniform loss rate method with SCS dimensionless unit hydrograph.

For site 3 (Table 11), the average initial loss and the average uniform loss are 2.24 and 2.43, respectively for the initial and uniform loss rate method with SCS dimensionless unit hydrograph.

Site 2 was selected to make a comparison between observed and calculated runoff depth, peak flow, and time to peak (Figure 34-36).

Also storm 2 was selected to make a comparison between predicted and observed runoff hydrograph for all sites; the results are graphically presented in figures 37-39.

Table 12: Comparison between computed and observed runoff hydrographs for site 1 using method 1.

Storm	Rainfall (mm)	Equivalent Depth		Peak flow(m ³ /s)		Time to peak	
		O. (mm)	C. (mm)	O.	C.	O. (hr)	C. (hr)
1	13.48	4.24	2.80	9.40	2.80	5.00	4.92
2	20.56	5.65	4.43	4.15	3.05	8.25	10.25
3	2.78	0.16	0.13	0.18	0.09	3.00	3.08
4	7.29	0.80	0.80	0.65	0.47	7.50	22.00
5	3.57	1.36	0.49	0.48	0.13	5.57	9.75
6	2.50	0.17	0.17	0.14	0.16	4.75	3.58

Method 1: SCS curve number with SCS dimensionless unit hydrograph.

O. : Observed

C. : Calculated by the HEC-1 optimization technique.

Table 13: Comparison between computed and observed runoff hydrographs for site 1 using method 2.

Storm	Rainfall (mm)	Equivalent Depth		Peak flow(m ³ /s)		Time to peak	
		O. (mm)	C. (mm)	O.	C.	O. (hr)	C. (hr)
1	13.48	4.24	3.04	9.4	2.4	5	5
2	20.56	5.65	5.61	4.15	2.25	8.25	10.58
3	2.78	0.16	0.156	0.18	0.11	3	3.17
4	7.29	0.8	0.376	0.65	0.15	7.5	21.17
5	3.57	1.36	0.49	0.48	0.13	5.57	9.75
6	2.5	0.17	0.16	0.14	0.17	4.75	3.67

Method 2: SCS curve number with Snyder unit hydrograph.

Table 14: Comparison between computed and observed runoff hydrographs for site 1 using method 3.

Storm	Rainfall	Equivalent Depth		Peak flow(m ³ /s)		Time to peak	
	(mm)	O. (mm)	C. (mm)	O.	C.	O. (hr)	C. (hr)
1	13.48	4.24	4.24	9.4	4.4	5	5
2	20.56	5.65	5.65	4.15	8	8.25	10.42
3	2.78	0.16	0.16	0.18	0.11	3	3.17
4	7.29	0.8	0.8	0.65	0.22	7.5	22.27
5	3.57	1.36	1.36	0.48	0.36	5.57	4.42
6	2.5	0.17	0.17	0.14	0.14	4.75	4.92

Method 3: Initial and uniform loss rate with Snyder unit hydrograph.

Table 15: Comparison between computed and observed runoff hydrographs for site 1 using method 4.

Storm	Rainfall	Equivalent Depth		Peak flow(m ³ /s)		Time to peak	
	(mm)	O. (mm)	C. (mm)	O.	C.	O. (hr)	C. (hr)
1	13.48	4.24	4.24	9.4	4	5	5
2	20.56	5.65	5.65	4.15	4.25	8.25	10.5
3	2.78	0.16	0.16	0.18	0.11	3	3.17
4	7.29	0.8	0.8	0.65	0.22	7.5	24.08
5	3.57	1.36	1.36	0.48	0.4	5.57	6.33
6	2.5	0.17	0.17	0.14	0.16	4.75	5

Method 4: Initial and uniform loss rate with SCS dimensionless unit hydrograph.

Table 16: Comparison between computed and observed runoff hydrographs for site 2 using method 1.

Storm	Rainfall	Equivalent Depth		Peak flow(m ³ /s)		Time to peak	
	(mm)	O. (mm)	C. (mm)	O.	C.	O. (hr)	C. (hr)
1	17.68	5.5	5	1.14	0.48	4	4.08
2	16.06	10.2	6.9	2.2	0.78	7.5	7.58
3	6.48	3	1.56	0.43	0.17	2.42	2.5
4	4.75	0.48	0.258	0.28	0.03	6.08	6.75
5	3.22	0.88	0.22	0.308	0.016	4.58	6.25
6	4.13	3.5	3.6	0.61	0.13	4.83	7.17
7	12.71	4	3.3	0.47	0.4	7.83	7.83

Table 17: Comparison between computed and observed runoff hydrographs for site 2 using method 2.

Storm	Rainfall	Equivalent Depth		Peak flow(m ³ /s)		Time to peak	
	(mm)	O. (mm)	C. (mm)	O.	C.	O. (hr)	C. (hr)
1	17.68	5.5	4.83	1.14	0.5	4	4.17
2	16.06	10.2	7	2.2	0.76	7.5	7.67
3	6.48	3	1.34	0.43	0.135	2.42	2.58
4	4.75	0.48	0.16	0.28	0.28	6.08	7.17
5	3.22	0.88	0.25	0.308	0.03	4.58	5.58
6	4.13	3.5	0.36	0.61	0.15	4.83	7
7	12.71	4	3.3	0.47	0.22	7.83	7.92

Table 18: Comparison between computed and observed runoff hydrographs for site 2 using method 3.

Storm	Rainfall	Equivalent Depth		Peak flow(m ³ /s)		Time to peak	
	(mm)	O. (mm)	C. (mm)	O.	C.	O. (hr)	C. (hr)
1	17.68	5.5	5.5	1.14	0.64	4	4.08
2	16.06	10.2	10.2	2.2	1.22	7.5	7.67
3	6.48	3	2.8	0.43	0.335	2.42	2.5
4	4.75	0.48	0.48	0.28	0.175	6.08	6.42
5	3.22	0.88	0.24	0.308	0.03	4.58	7.42
6	4.13	3.5	3.5	0.61	0.14	4.83	6.2
7	12.71	4	3.8	0.47	0.26	7.83	8

Table 19: Comparison between computed and observed runoff hydrographs for site 2 using method 4.

Storm	Rainfall	Equivalent Depth		Peak flow(m ³ /s)		Time to peak	
	(mm)	O. (mm)	C. (mm)	O.	C.	O. (hr)	C. (hr)
1	17.68	5.5	5.5	1.14	0.68	4	4.08
2	16.06	10.2	10.2	2.2	1.28	7.5	7.58
3	6.48	3	3	0.43	0.4	2.42	2.42
4	4.75	0.48	0.48	0.28	0.176	6.08	6.42
5	3.22	0.88	0.82	0.308	0.1	4.58	5.33
6	4.13	3.5	3.5	0.61	0.13	4.83	7.17
7	12.71	4	3.8	0.47	0.27	7.83	7.83

Table 20: Comparison between computed and observed runoff hydrographs for site 3 using method 1.

Storm	Rainfall	Equivalent Depth		Peak flow(m ³ /s)		Time to peak	
	(mm)	O. (mm)	C. (mm)	O.	C.	O. (hr)	C. (hr)
1	2.61	0.17	0.136	0.44	0.12	1.58	1.58
2	17.68	2.8	2.8	2.04	2.72	2.25	4.08
3	16.06	6.5	5.88	3.75	2.75	8.67	9
4	6.84	2.45	1.26	2.44	1.54	2.42	2.5
5	7.97	1.1	1.1	0.29	0.33	13.08	14.42
6	2.7	0.32	0.162	0.288	0.172	6	6.58
7	12.7	2.5	2.48	0.82	1.02	8.08	8.42
8	2.91	0.47	0.27	0.56	0.7	3	6.75

Table 21: Comparison between computed and observed runoff hydrographs for site 3 using method 2.

Storm	Rainfall	Equivalent Depth		Peak flow(m ³ /s)		Time to peak	
	(mm)	O. (mm)	C. (mm)	O.	C.	O. (hr)	C. (hr)
1	2.61	0.17	0.137	0.44	0.135	1.58	1.5
2	17.68	2.8	2.8	2.04	1.8	2.25	4.33
3	16.06	6.5	5.8	3.75	2.55	8.67	9.33
4	6.84	2.45	1.4	2.44	1.36	2.42	2.5
5	7.97	1.1	1.1	0.29	0.316	13.08	14.32
6	2.7	0.32	0.21	0.288	0.168	6	6.5
7	12.7	2.5	2.47	0.82	1	8.08	8.33
8	2.91	0.47	0.1	0.56	0.04	3	7.83

Table 22: Comparison between computed and observed runoff hydrographs for site 3 using method 3.

Storm	Rainfall	Equivalent Depth		Peak flow(m ³ /s)		Time to peak	
	(mm)	O. (mm)	C. (mm)	O.	C.	O. (hr)	C. (hr)
1	2.61	0.17	0.17	0.44	0.2	1.58	3.17
2	17.68	2.8	2.8	2.04	2.42	2.25	4.25
3	16.06	6.5	6.5	3.75	2.9	8.67	8.75
4	6.84	2.45	2.45	2.44	1.8	2.42	2.5
5	7.97	1.1	1.1	0.29	0.385	13.08	14.25
6	2.7	0.32	0.32	0.288	0.344	6	6.5
7	12.7	2.5	2.5	0.82	1.08	8.08	8.75
8	2.91	0.47	0.47	0.56	0.39	3	3.33

Table 23: Comparison between computed and observed runoff hydrographs for site 3 using method 4.

Storm	Rainfall	Equivalent Depth		Peak flow(m ³ /s)		Time to peak	
	(mm)	O. (mm)	C. (mm)	O.	C.	O. (hr)	C. (hr)
1	2.61	0.17	0.06	0.44	0.2	1.58	3.25
2	17.68	2.8	2.8	2.04	2.96	2.25	4.17
3	16.06	6.5	6.5	3.75	3	8.67	8.83
4	6.84	2.45	2.45	2.44	1.8	2.42	2.58
5	7.97	1.1	1.1	0.29	0.49	13.08	11.42
6	2.7	0.32	0.32	0.288	0.4	6	6.58
7	12.7	2.5	2.5	0.82	1.2	8.08	8.67
8	2.91	0.47	0.47	0.56	0.61	3	3.08

Table 26: Error percentage for method 3and site 1.

Storm	Rainfall	Eq.d. Error%	Pf Error%	Tp Error%
1	13.48	0.00	53.00	0.00
2	20.56	0.00	93.00	26.00
3	2.78	0.00	39.00	5.60
4	7.29	0.00	66.00	197.00
5	3.57	0.00	25.00	21.00
6	2.5	0.00	0.00	4.00
Average		0.00	46.00	42.00

Table 27: Error percentage for method 4and site 1.

Storm	Rainfall	Eq.d. Error%	Pf Error%	Tp Error%
1	13.48	0.00	57.00	0.00
2	20.56	0.00	2.40	27.00
3	2.78	0.00	39.00	5.60
4	7.29	0.00	66.00	221.00
5	3.57	0.00	17.00	13.60
6	2.5	0.00	14.00	5.30
Average		0.00	33.00	45.00

Table 28: Error percentage for method 1, and site 2.

Storm	Rainfall	Eq.d. Error%	Pf Error%	Tp Error%
1	17.68	9.00	58.00	2.00
2	16.06	32.00	65.00	1.00
3	6.48	48.00	60.00	3.30
4	4.75	46.00	89.00	11.00
5	3.22	75.00	94.00	36.00
6	4.13	3.00	78.00	48.00
7	12.71	18.00	15.00	0.00
Average		33.00	66.00	14.00

Table 29: Error percentage for method 2, and site 2.

Storm	Rainfall	Eq.d. Error%	Pf Error%	Tp Error%
1	17.68	12.00	56.00	4.00
2	16.06	31.00	65.00	2.00
3	6.48	55.00	69.00	7.00
4	4.75	67.00	0.00	18.00
5	3.22	72.00	90.00	22.00
6	4.13	90.00	75.00	45.00
7	12.71	18.00	53.00	1.00
Average		49.00	58.00	14.00

Table 30: Error percentage for method 3 and site 2.

Storm	Rainfall	Eq.d. Error%	Pf Error%	Tp Error%
1	17.68	0.00	44.00	2.00
2	16.06	0.00	45.00	2.00
3	6.48	7.00	22.00	3.30
4	4.75	0.00	38.00	5.60
5	3.22	73.00	90.00	62.00
6	4.13	0.00	77.00	28.00
7	12.71	5.00	45.00	2.10
Average		12.00	52.00	15.00

Table 31: Error percentage for method 4, and site 2.

Storm	Rainfall	Eq.d. Error%	Pf Error%	Tp Error%
1	17.68	0.00	40.00	2.00
2	16.06	0.00	42.00	1.00
3	6.48	0.00	7.00	0.00
4	4.75	0.00	37.00	5.60
5	3.22	7.00	68.00	16.00
6	4.13	0.00	79.00	48.00
7	12.71	5.00	43.00	0.00
Average		1.70	45.00	10.00

Table 32: Error percentage for method 1, and site 3.

Storm	Rainfall	Eq.d. Error%	Pf Error%	Tp Error%
1	2.61	20.00	73.00	0.00
2	17.68	0.00	33.00	81.00
3	16.06	10.00	27.00	3.80
4	6.84	49.00	37.00	3.30
5	7.97	0.00	14.00	10.00
6	2.7	49.00	10.00	9.70
7	12.7	1.00	24.00	4.20
8	2.91	43.00	25.00	125.00
Average		22.00	30.00	30.00

Table 33: Error percentage for method 2, and site 3.

Storm	Rainfall	Eq.d. Error%	Pf Error%	Tp Error%
1	2.61	19.00	69.00	5.10
2	17.68	0.00	12.00	92.00
3	16.06	11.00	32.00	7.60
4	6.84	43.00	44.00	3.30
5	7.97	0.00	9.00	9.30
6	2.70	34.00	42.00	8.30
7	12.70	1.00	22.00	3.10
8	2.91	79.00	93.00	161.00
Average		23.00	40.00	36.00

Table 34: Error percentage for method 3, and site 3.

Storm	Rainfall	Eq.d. Error%	Pf Error%	Tp Error%
1	2.61	0.00	54.00	100.00
2	17.68	0.00	38.00	88.00
3	16.06	0.00	23.00	1.00
4	6.84	0.00	26.00	3.30
5	7.97	0.00	32.00	8.90
6	2.70	0.00	19.00	8.30
7	12.70	0.00	32.00	8.30
8	2.91	0.00	30.00	11.00
Average		0.00	32.00	29.00

Table 35: Error percentage for method 4, and site 3.

Storm	Rainfall	Eq.d. Error%	Pf Error%	Tp Error%
1	2.61	65.00	55.00	10.60
2	17.68	0.00	45.00	85.00
3	16.06	0.00	20.00	13.40
4	6.84	0.00	26.00	6.60
5	7.97	0.00	69.00	12.70
6	2.7	0.00	39.00	9.70
7	12.7	0.00	46.00	9.30
8	2.91	0.00	9.00	2.70
Average		8.00	39.00	19.00

Table 36: Average error percentage for all methods for site 1.

Method	Eq. d. Error%	Pf Error%	Tp Error%
1	24.00	44.00	54.00
2	26.00	55.00	47.00
3	0.00	46.00	42.00
4	0.00	33.00	45.00

Table 37: Average error percentage for all methods for site 2.

Method	Eq. d. Error%	Pf Error%	Tp Error%
1	33	66	14
2	49	58	14
3	12	52	15
4	1.7	45	10

Table 38: Average error percentage for all methods for site 3.

Method	Eq. d. Error%	Pf Error%	Tp Error%
1	22	34	30
2	23	40	36
3	0	32	29
4	8	39	19

Table 39: The grand average percentage error for all methods for the all sites.

Method	Eq. d. Error%	Pf Error%	Tp Error%
1	26	47	33
2	33	51	32
3	4	43	29
4	3	39	25

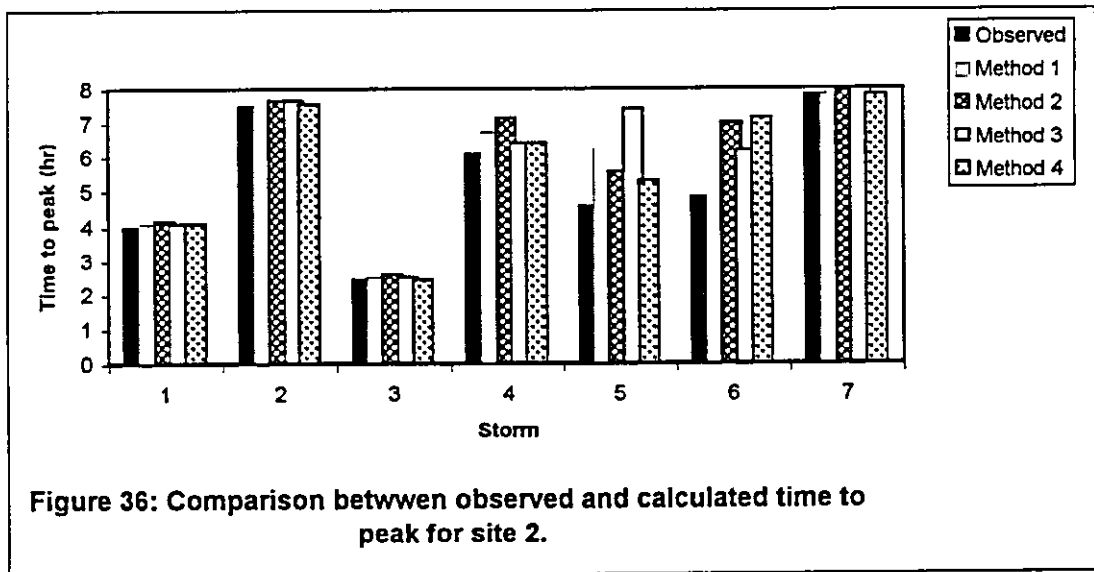
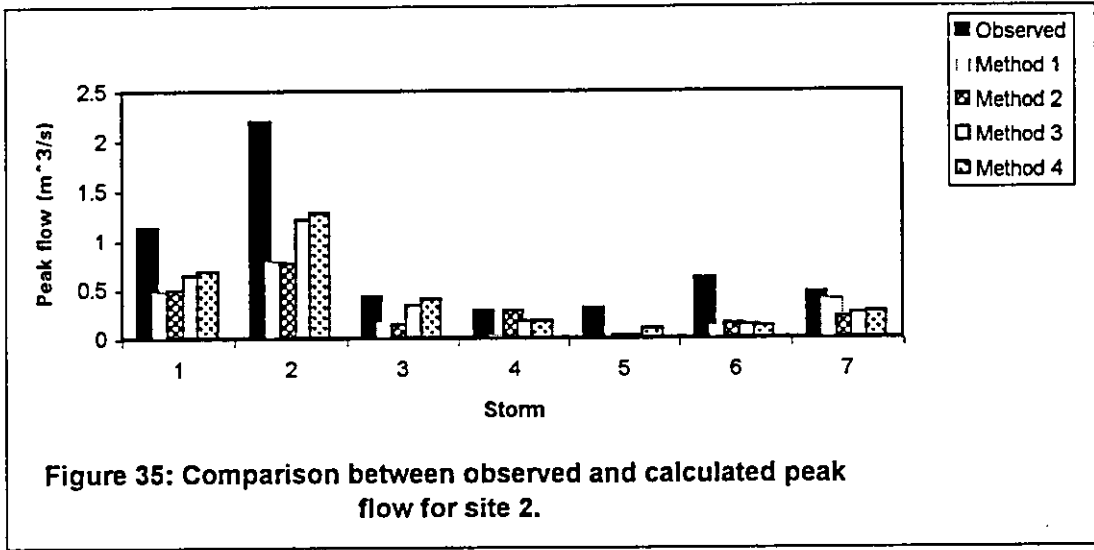
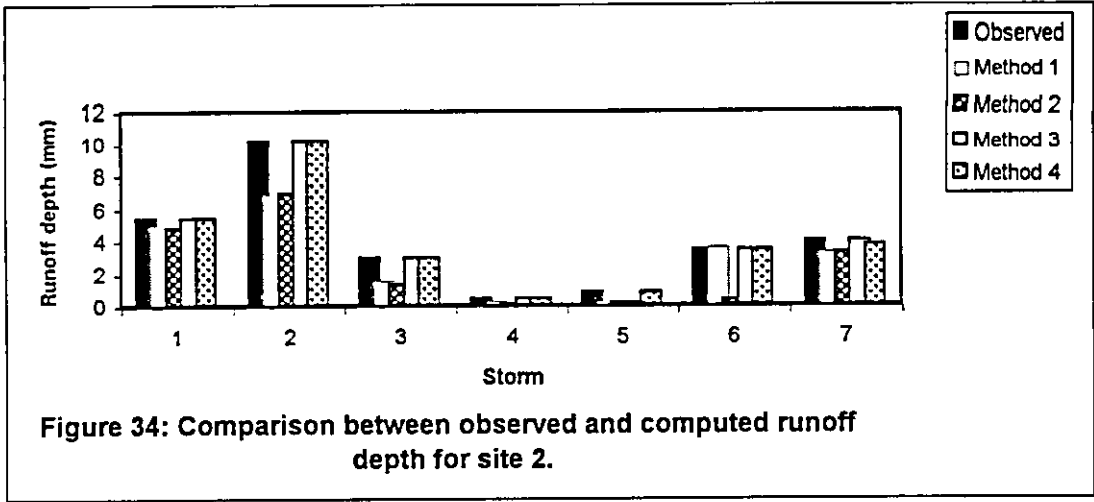
Table 40: Results of the optimization unit hydrograph and loss rate parameters for site 1.

Storm	Method 1			Method 4		
	tp (hr.)	In. loss (mm)	CN	tp (hr.)	In. loss (mm)	U. l. rate (mm/hr)
1	1.4	4.01	91.96	1.5	4.76	4.28
2	0.57	7.74	91.26	0.93	4.73	1.99
3	2.26	0.82	90.16	2.12	2.49	0.21
4	3.03	6.32	100	5.49	2.13	0.77
5	1.63	0.2	92.8	4.64	0.12	0.42
6	0.11	0.26	90.01	1.59	0.63	1.29
Average	1.5	3.22	92.7	2.7	2.5	1.5

tp: Lag time.

I. loss:Initial loss.

U. l. rate:Uniform loss rate.



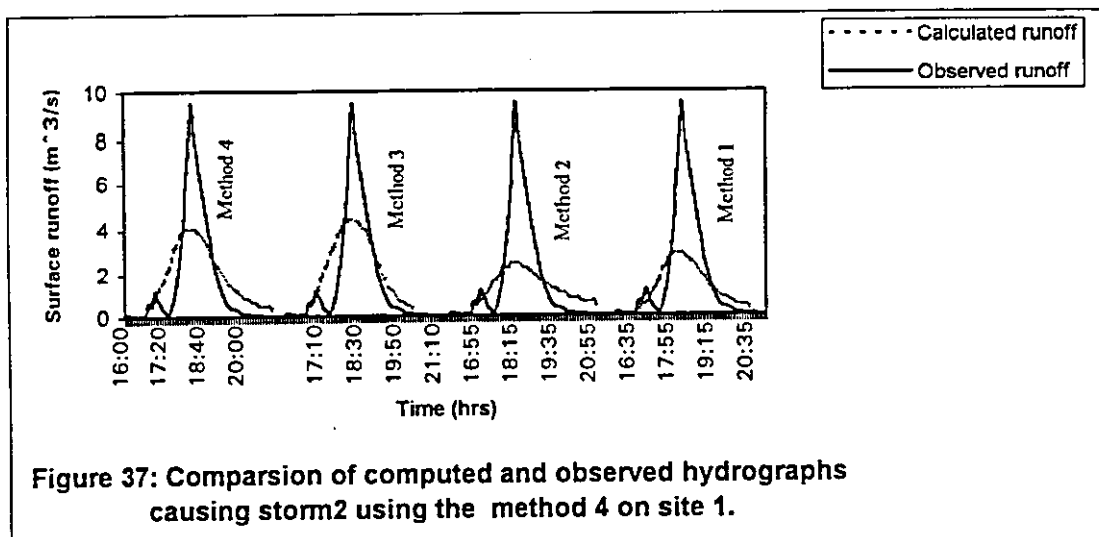


Figure 37: Comparison of computed and observed hydrographs causing storm2 using the method 4 on site 1.

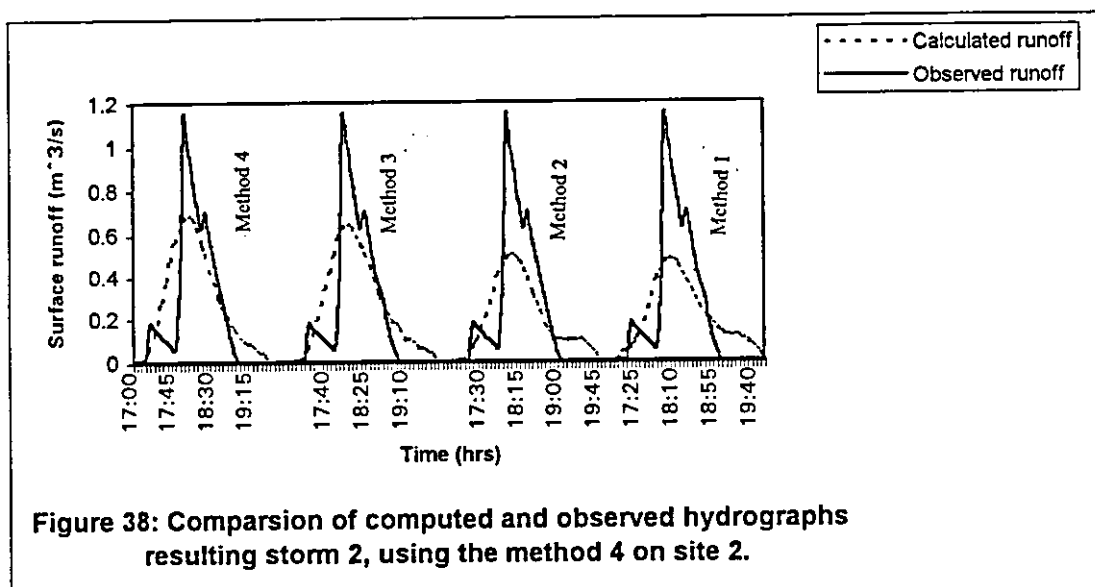


Figure 38: Comparison of computed and observed hydrographs resulting storm 2, using the method 4 on site 2.

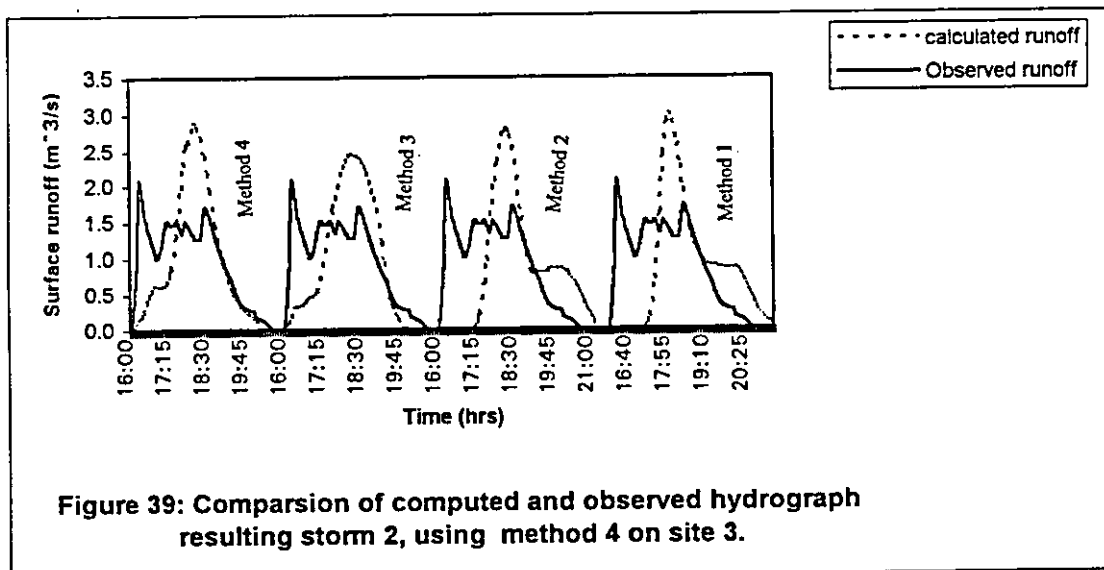


Figure 39: Comparison of computed and observed hydrograph resulting storm 2, using method 4 on site 3.

4.5 Verification:

This section is used to compare the simulated and observed runoff hydrograph on Muwaqqar watershed using HEC-1 model.

Tables 43 and 44 show the comparison between observed and calculated hydrograph using method 1 method 4. The simulated discharge caused by storm 4 are zero for method 4 (Table 43) and significant for method 1 (Table 44), because the total rainfall is less than the initial abstraction parameters for method 4 and large than the initial abstraction parameter for method 1.

The calculated discharge from the measured rainfall for storm 2 is higher than the measured discharge.

The HEC-1 model was also developed to represent graphically the results of the simulation. Figure 40 and 41 shows the comparison between observed and calculated hydrograph caused by storm 2 and storm 4 for sites 3 and 4 respectively. The correlation coefficient between observed and calculated discharge for site 3 were 0.89 and .81 for the methods 4, and 3, respectively. The correlation coefficient between observed and calculated discharge for site 4 were 0.9 and .81 for the methods 4, and 3, respectively.

The results obtained from the comparison between observed and calculated hydrograph for the two sites (table 43 and 46) are relatively good for method 4 and less accurate for method 1. Therefore method 4 was used to simulate the runoff hydrograph for the total basin.

Table 41: Comparison between computed and observed runoff hydrographs for site 3 using method 4.

Storm	Rainfall	Equivalent Depth		Peak flow(m ³ /s)		Time to peak	
	(mm)	O. (mm)	C. (mm)	O.	C.	O. (hr)	C. (hr)
1.00	9.61	3.75	2.65	3.90	2.00	2.42	2.75
2.00	11.44	3.87	3.20	3.80	1.90	1.92	2.08
3.00	13.27	3.65	2.55	2.20	1.80	1.92	8.22
4.00	2.30	0.52	0.00	1.00	0.00	2.75	0.00

Table 42: Comparison between computed and observed runoff hydrographs for site 3 using method 1.

Storm	Rainfall	Equivalent Depth		Peak flow(m ³ /s)		Time to peak	
	(mm)	O. (mm)	C. (mm)	O.	C.	O. (hr)	C. (hr)
1.00	9.61	3.75	1.85	3.90	1.00	2.42	2.75
2.00	11.44	3.87	2.63	3.80	1.40	1.92	5.33
3.00	13.27	3.65	3.48	2.20	1.30	1.92	8.08
4.00	2.30	0.52	0.03	1.00	0.10	2.75	4.13

Table 43: Comparison between using method 4 and method 1 for site 3.

Storm	Eq. d. error% for Method		Pf error% for Method		Tp Error% for Method	
	4	1	4	1	4	1
1	29	50.00	49.00	74.00	14.00	14.00
2	17	32.00	50.00	63.00	8.00	18.00
3	30	5.00	18.00	40.00	328.00	320.00
4	100	94.00	100.00	90.00	!	50.00

Table 44: Comparison between computed and observed runoff hydrographs for site 4 using method 4.

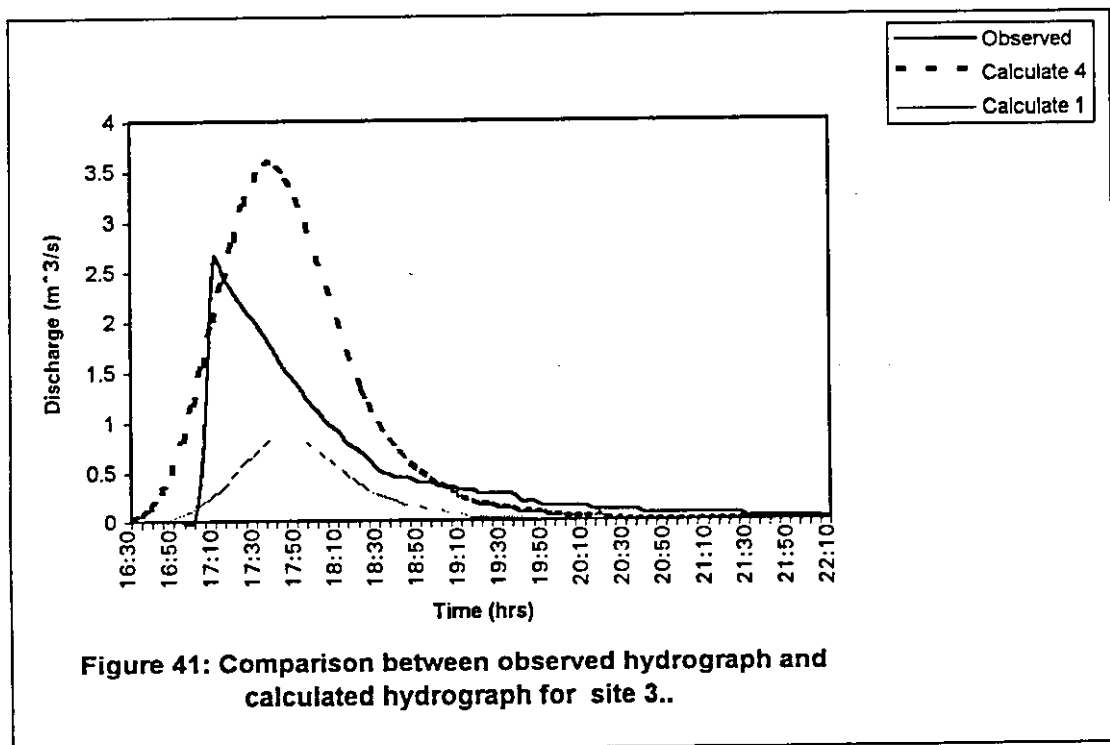
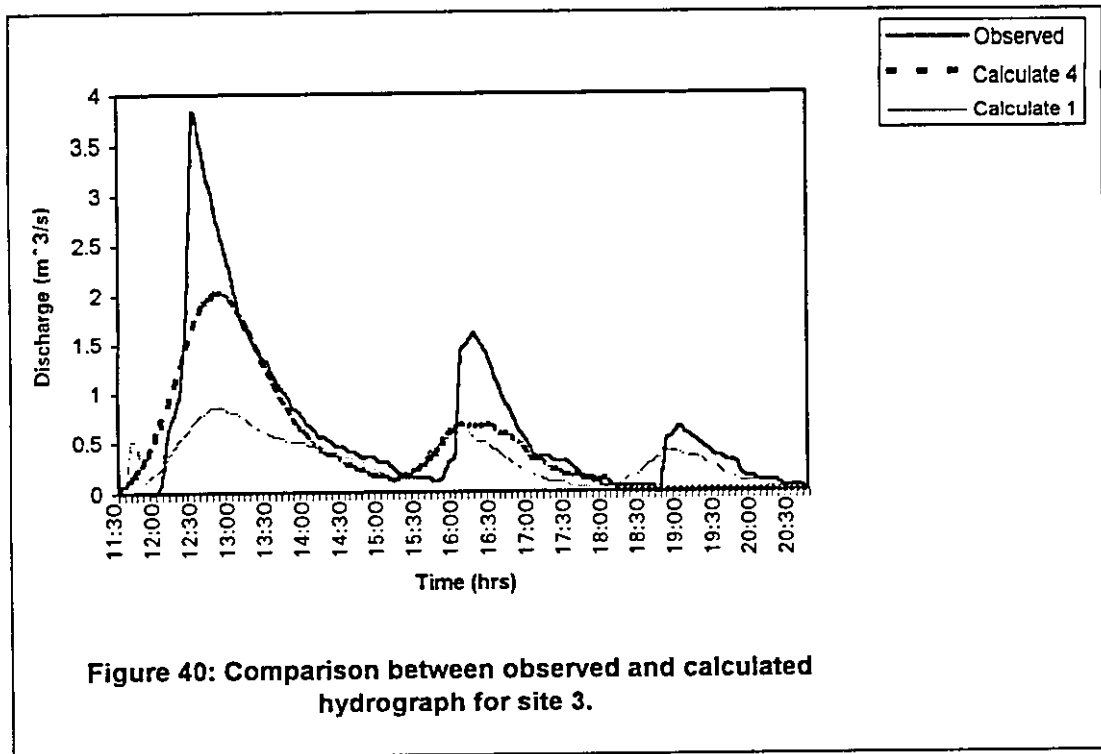
Storm	Rainfall	Equivalent Depth		Peak flow(m ³ /s)		Time to peak	
	(mm)	O. (mm)	C. (mm)	O.	C.	O. (hr)	C. (hr)
1.00	11.07	2.74	3.33	2.10	2.10	9.00	2.42
2.00	13.08	0.21	2.34	0.10	3.00	6.00	8.00
3.00	5.28	0.55	0.16	0.38	0.25	8.42	9.50
4.00	6.43	1.82	2.64	2.80	3.60	1.17	1.67

Table 45: Comparison between computed and observed runoff hydrographs for site 4 using method 1.

Storm	Rainfall	Equivalent Depth		Peak flow(m ³ /s)		Time to peak	
	(mm)	O. (mm)	C. (mm)	O.	C.	O. (hr)	C. (hr)
1.00	11.07	2.74	2.35	2.10	1.40	9.00	2.42
2.00	13.08	0.21	3.36	0.10	1.00	6.00	8.00
3.00	5.28	0.55	0.34	0.38	0.25	8.42	9.67
4.00	6.43	1.82	0.59	2.80	0.85	1.17	1.75

Table 46: Comparison between using method 4 and method 1 for site 4.

Storm	Eq. d. error% for Method		Pf error% for Method		Tp Error% for Method	
	4	1	4	1	4	1
1	22	14.00	0.00	33.00	73.00	73.00
2	1000	1500.00	2900.00	2900.00	33.00	33.00
3	70	39.00	21.00	21.00	11.00	15.00
4	45	68.00	29.00	70.00	43.00	50.00



Calculated 1: Calculated using method 1.

Calculated 4: Calculated using method 4.

4.6 Stream Network Model:

4.6.1 Channel Routing:

Figure 42 shows the variation of the travel time (K) with reference to inflow discharge during single reach routing. The high variation in k occur at the low inflow discharge and at the high inflow discharge with low variation.

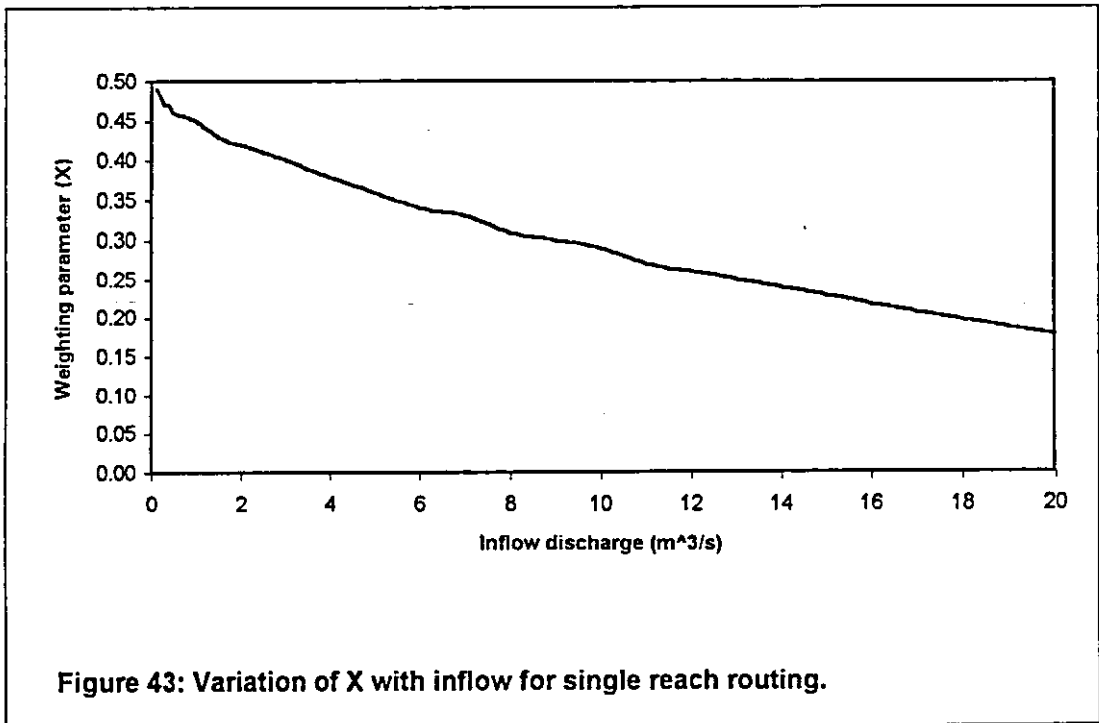
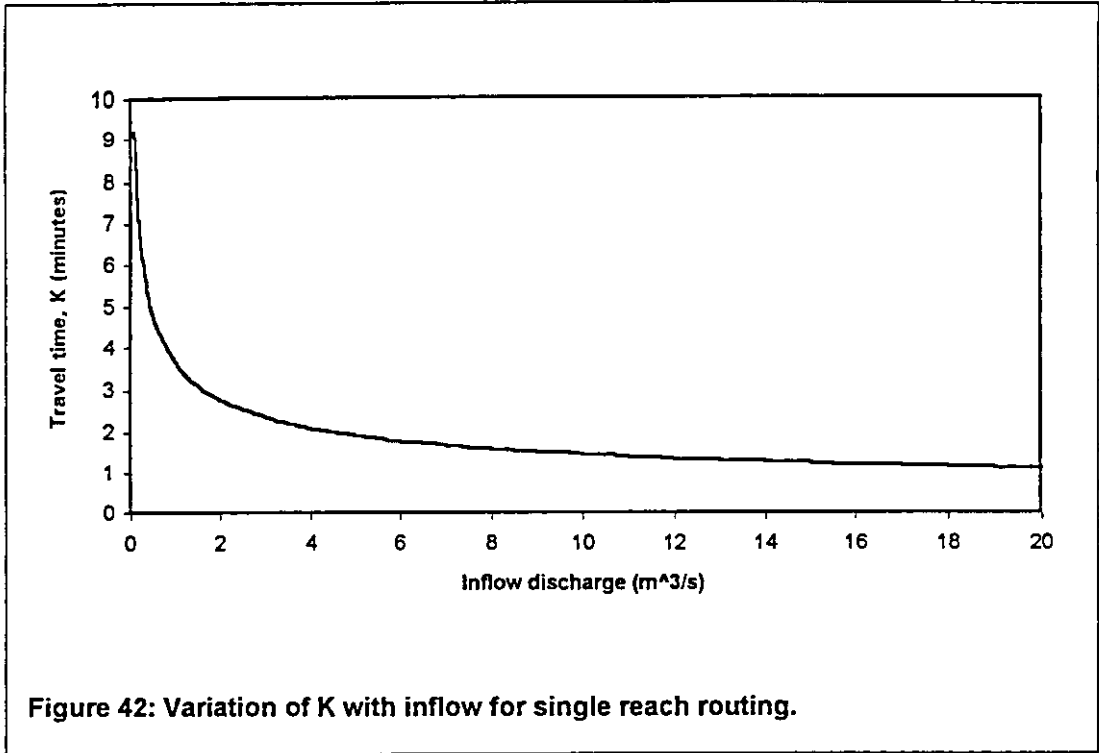
Figure 43 shows the variation of Muskingum parameter, the weighting parameters (X), with reference to inflow discharge during single reach routing. The value of X varied from 0.2 - 0.49; the high value of X indicated that most of the storage channel is wedge storage, Knowing that a value of 0.5 for X is for a full wedge.

Figure 44 - 45, refer to the routing result of the channel (522 m long). They show the inflow and outflow hydrograph. During the advance of flood wave, inflow exceeds outflow, producing a wedge of storage. During the recession, outflow exceeds inflow, resulting in a negative wedge. From figure 45, the time between peaks is approximately equal the travel time which is equal to 5 minutes. In comparison between two storms we find the difference between two peaks (inflow and outflow) was determined. For storm 7, the difference is higher than that of storm 2, because the inflow discharge caused by storm 7 is low, because wave celerity is low, then the travel time is high.

The reduction in outflow discharge was very low because:

1. the high channel slope.
2. low infiltration rate.
3. small interval time, due to small channel length.

In general the difference between two peaks was low because the small channel length, causing the travel time to be low.



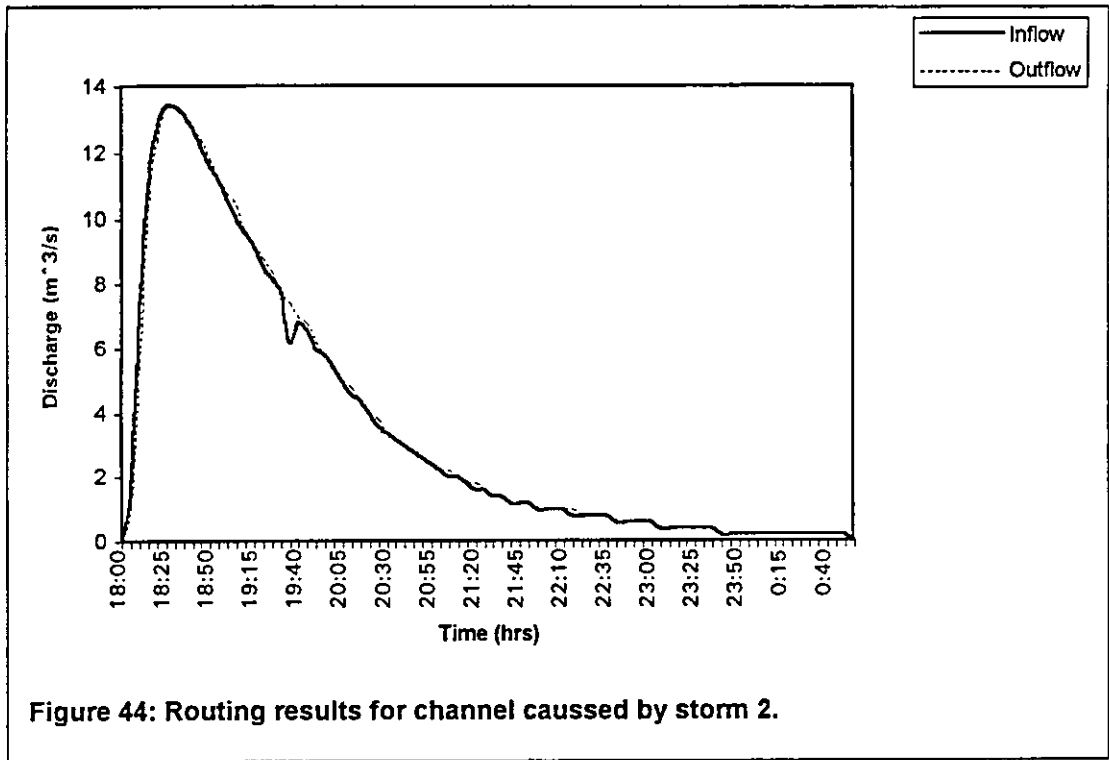


Figure 44: Routing results for channel caused by storm 2.

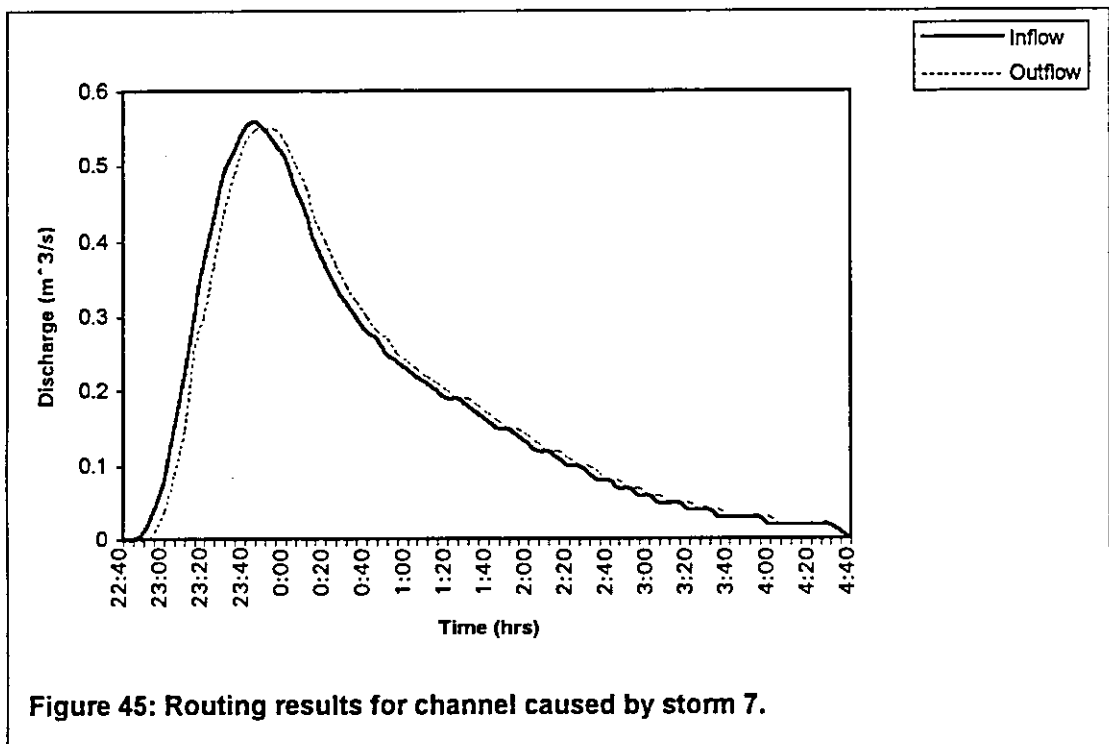


Figure 45: Routing results for channel caused by storm 7.

4.6.2 Routing Flow Through Dam:

Figure 46 to 53, show the inflow, outflow, and storage relationship. From these figures, the peak outflow occurs when the outflow hydrograph intersects the inflow hydrograph, because the maximum storage occurs when $ds/dt = I - Q = 0$ and the storage and outflow are related by $s = f(Q)$ or steady state condition.

The inflow of dam 1 resulting from 61.17 km² surface area, inflow to dam 2 is a result of dam 1 outflow combined with 7.8 km² surface area, while the inflow of dam 3 is a result of dam 2 outflow.

The storage 6800 m³ and 1440 m³ occur in dam 1 and dam 2 respectively, the storage is built as a result of the average inflow discharge of 0.28 m³/s during 400 minutes, and .15 during 160 minutes for dam 1 and dam 2 respectively. No storage in dam 3 because the outflow from dam 2 equal zero figure 46 and 47.

The total losses of storage from Dam 1 between the storm 2 and the storm 1 is 1300 m³, where most the losses caused by the infiltration rate. Storm 2 occurred when storage in dam 1 was 3500 m³. The storage of 11000 m³ occurred in dam 1 as a result of the average inflow 1.74 m³/s during 105 minutes. After that the outflow started when dam 1 reached its full capacity of 14800 m³ (Figure 48).

The total losses of 1440 m³ from Dam 2 storage occurred between the storm 2 and the storm 1. Most of these were losses caused by the infiltration rate. Storm 2 occurred when the dam 2 was empty. The storage of 13500 m³ occurred in dam 2 with an average inflow was 2.16 m³/s during 100 minutes. After that the outflow from dam 1 combined to the outflow from the 7.8 km² watershed, and inflow to dam 2. The total amount after the combination was 1500 m³ stored in dam 2 with an average flow 5 m³/s during 5 minutes.

After that outflow began because the dam reached to the full capacity of 15000 m³ (Figure 49).

Dam 3 reached its full capacity of 16000 m³ resulting from an average inflow of 13.3m³/s in 20 minutes (Figure 50).

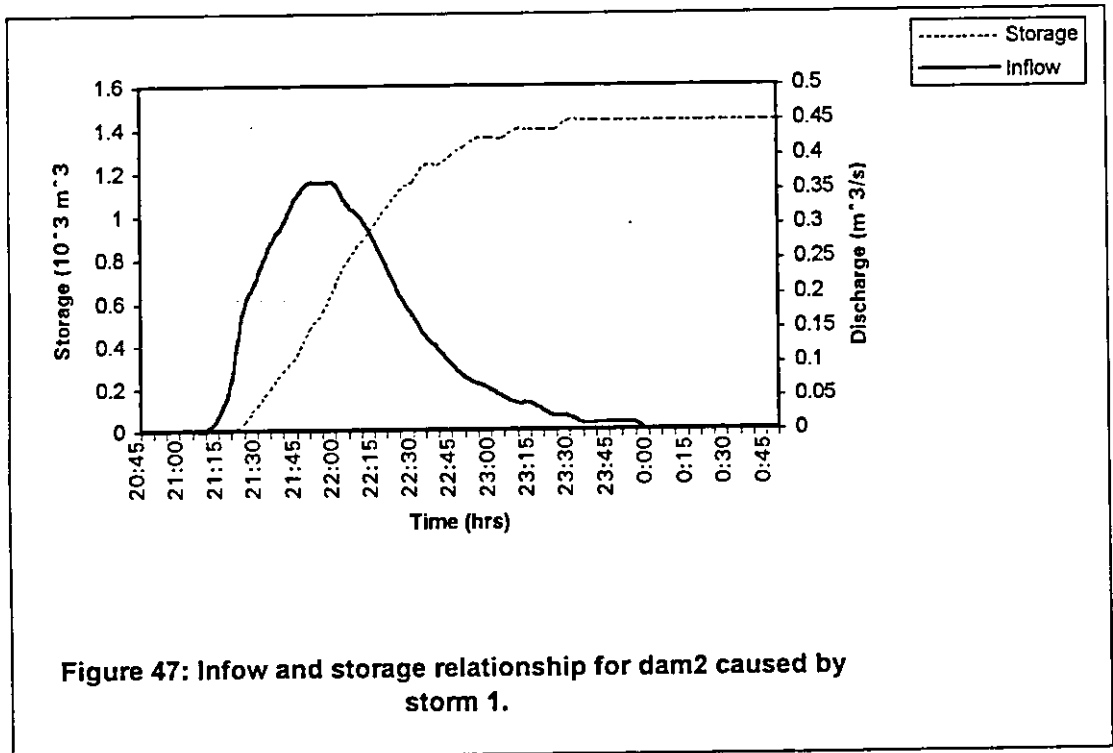
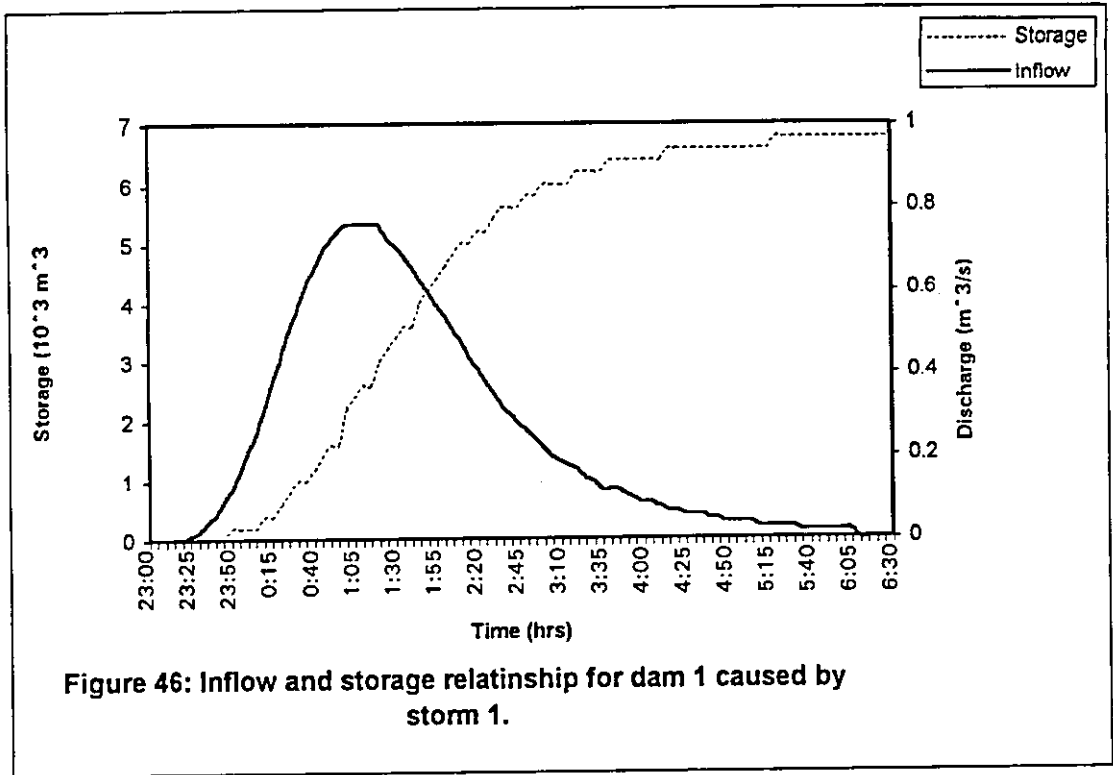
From the table 47, the low maximum water elevation were 800.74 m, 796.82 m, and 794.5 m for dam 1, dam 2, and dam 3 respectively, which means that dam 1 and dam 2 did not reach the full capacity, and the dam 3 was empty. The large maximum stages for all dams caused by storm 3, because the dams were full, and the excess rainfall of storm 3 was higher than other storms.

5.6.3 Simulated Runoff Hydrograph:

The weighted average of the initial loss, and the uniform loss parameters were calculated from the tables 40,10, and 11 for each storm, and presented in table 6. The average initial loss and uniform loss for the basin area were 2.4 mm, and 1.7 mm/hr, respectively. These parameters can be used to predict the runoff hydrograph for Al-Muwaqqar basin or similar basins. The lag time of the subbasins was calculated from the time of concentration for each subbasin (Table 48). The lag time is a function of the time of concentration (Tc), which is a function of channel slope and the channel length. As the channel gets steeper the speed of the flood wave will be faster and the time of concentration will get shorter. The longer the channel the longer time of concentration would be and so the lag time will be large.

From the table 49, the peak flow varied from 0.06 m³/s to 18 m³/s according to the rainfall amount and intensity, and soil surface characteristics. The higher peak flow occurred at storm 3 which has the largest volume. The total volume of runoff caused by all the storms during

1994/1995 season was equal to 745267 m^3 in addition to 45800 m^3 (the total dams capacity). The dams capacity is only 5.8% from the total runoff volume. For example, runoff resulting from storm 4 was enough to fill all the dams.



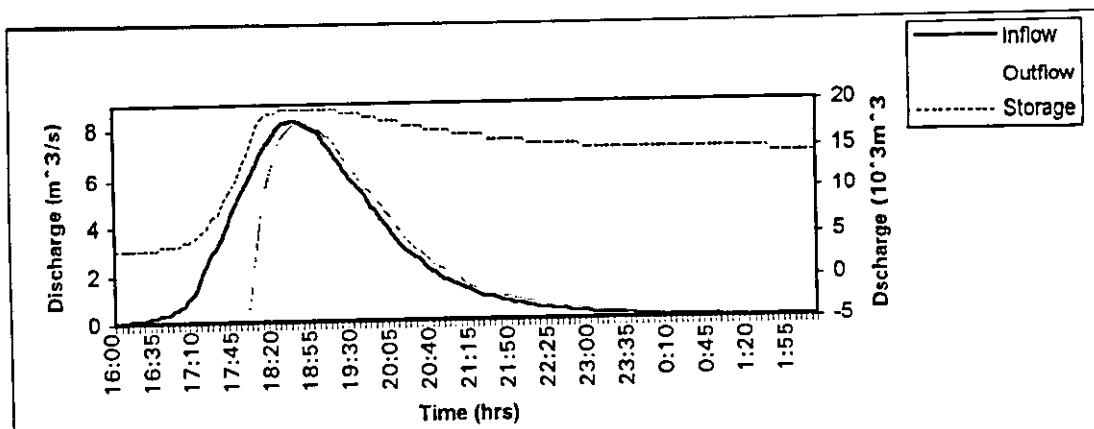


Figure 48: Inflow, outflow, and storage relationship for dam 1 caused by storm 2.

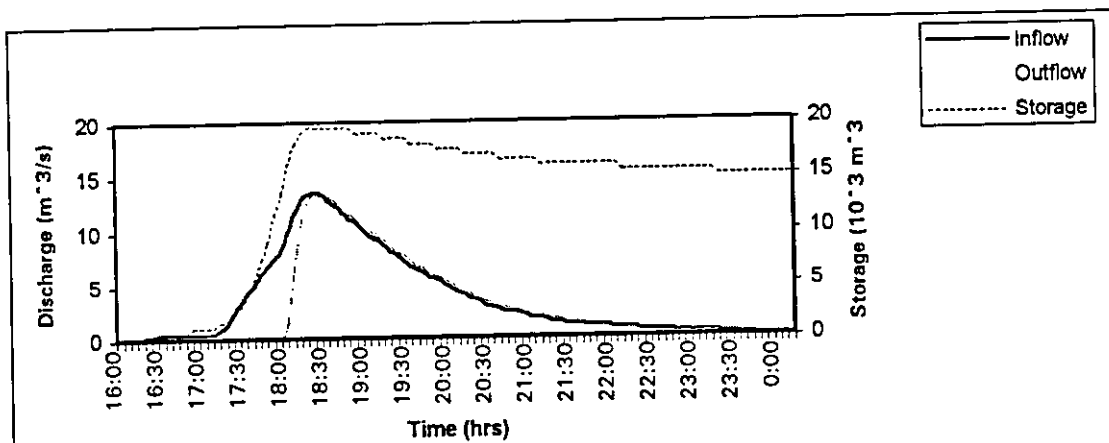


Figure 49: Inflow, outflow, and storage relationship for Dam 2 by storm 2.

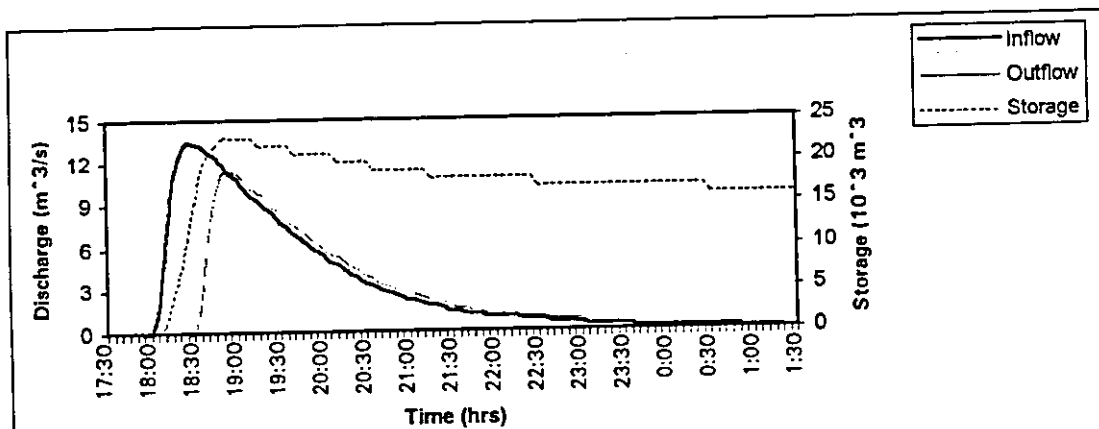


Figure 50: Inflow, outflow, and storage relationship for Dam 3 caused by storm 2.

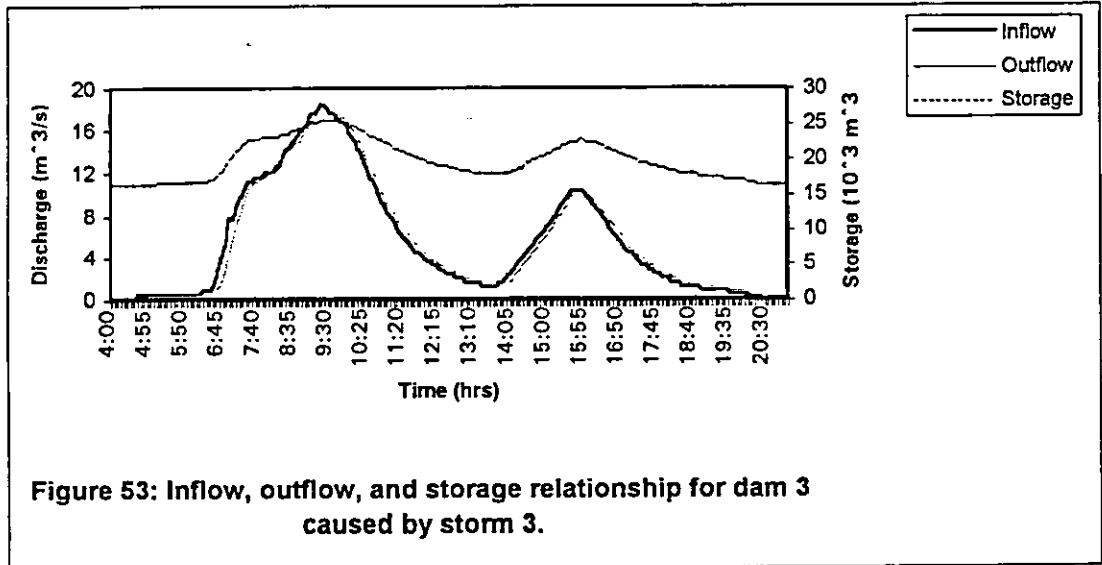
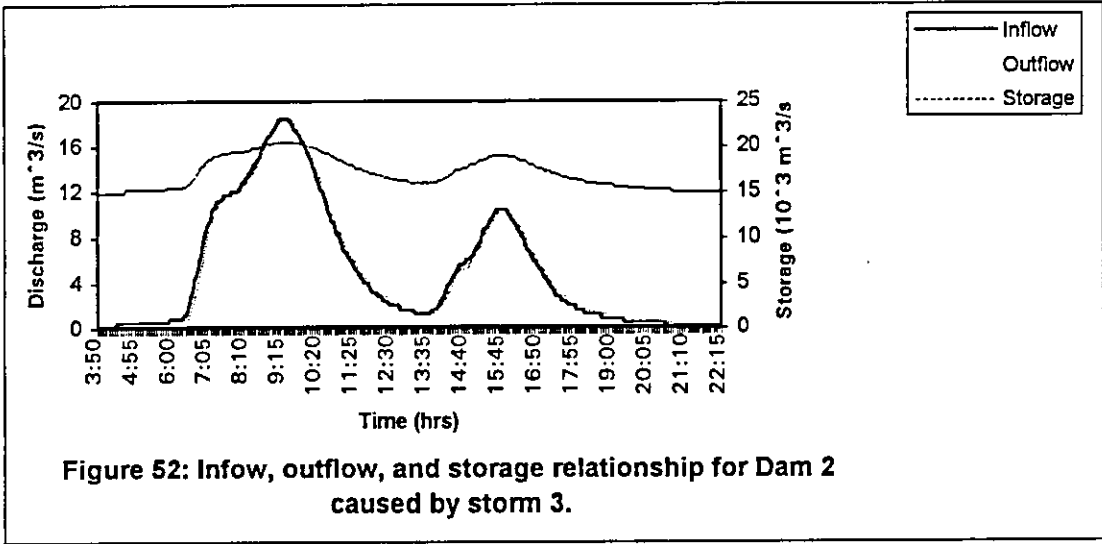
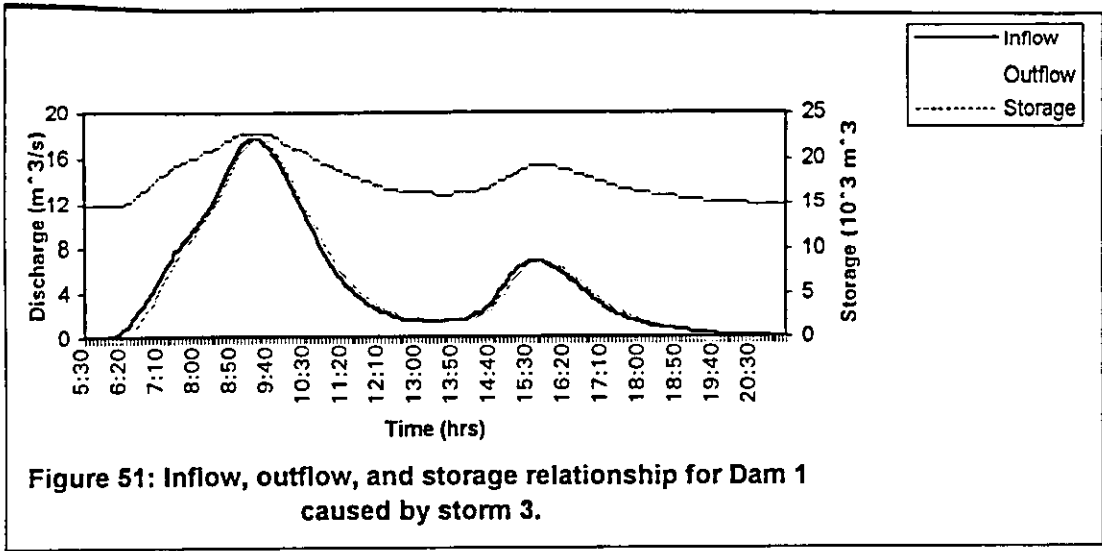


Table 47: The maximum stages of the dams during the 1994/1995 season.

Storm	Date	Dam1 Max. st.	Dam2 Max. st.	Dam3 Max. st.
1	15/11/94	800.74	796.82	794.5
2	23/11/94	801.87	799.5	797.45
3	23/11/94	802.1	799.61	797.61
4	24/11/94	801.77	799.28	797.27
5	2/12/94	801.64	799.14	797.14
6	3/12/94	801.78	799.3	797.29
7	3/12/94	801.51	799.05	797.04
8	19/12/94	801.84	799.38	797.37

Max st.: Maximum stage (m).

Table 48: The lag time for all the subbasins.

Site No	L (Km)	H (m)	Tc (min.)	tp (min.)
S10	15.437	150	193	116
S20	11.389	120	148	89
S30	14.475	146	181	109
S40	0.65	6	17	10.2
S50	1.08	9	27	16.2
S60	4.818	55	74	44.4
S70	1.308	4	45	27

Table 49: The surface runoff volume and the peak flow during the 1994/1995 season.

Storm	Date	Rain. ex. (mm)	Volume (m ³)	Pf (m ³ /s)	Tp (hr)
1	15/11/94	0.003	210.3	0.1	0.9
2	23/11/94	1.11	78010.2	12.0	5.6
3	23/11/94	4.96	347646.4	18.0	6.5
4	24/11/94	0.75	52217.1	5.4	3.1
5	2/12/94	0.66	45979.0	1.9	21.7
6	3/12/94	1.28	89364.8	6.0	6.8
7	3/12/94	0.06	4205.4	0.5	7.3
8	19/12/94	1.82	127633.9	8.3	8.7
Total		10.633	745267		

5. Summary and Conclusions.

Al-Muwaqqar sub-basin is a part of the Azraq basin located at the upstream end of the basin. The sub-basin has an area of 70.1 km² and fall in the 100-200 mm rainfall zone.

Three watersheds were selected with areas of 7.3, 0.5, and 5.8 for site 1, site 2, and site 3, respectively in order to study the relationship between rainfall and runoff. A model developed by U. S. army corps of engineers, 1981, (HEC-1) was used to optimize unit hydrograph and loss rate parameters for the selected site. Verification of the HEC-1 model in the two sites was carried. By using the optimization technique and regionalizing the results, rainfall runoff parameters for ungauged areas can be used to simulate the runoff hydrograph for the basin.

Based on the results and analysis, the following conclusions can be drawn:

1. The basic infiltration rate of the soil is very low, so a significant surface runoff occur even with very low rainfall intensity. This is attributed to crust formation which is characteristics of desert soil.
2. The runoff coefficient for three sites was relatively high, it ranges from 0.23 to 0.40.
3. The verification of HEC-1 model in two watersheds in Muwaqqar

indicated the possibility of streamflow simulation for ungauged catchment or catchments similar to Muwaqqar sub-basin.

4. From the calibration period, the initial and uniform loss with SCS dimensionless unit hydrograph is more accurate than other methods in estimating the runoff for Muwaqqar sub-basin. Therefore this method was used to simulate the runoff hydrograph for the total sub-basin.
5. Most of the total rainfalls that falls over the Muwaqqar sub-basin flows to the desert depressions, where it is lost by evaporation. In Muwaqqar, for example, if these lands where properly managed with water harvesting schemes to produce about 0.79 million cubic meters, about 1200 dunum can be cultivated an irrigated. If this harvested water was stored In appropriate reservoirs with special treatments, it could be used not only for agriculture but even for domestic use or industrial purposes. The storage capacity of the existing Dams is 45800 m^3 which means that only 5.8% of the total sub-basin runoff volume have been stored presently.

6. References

- 1- Shatanawi, M. R., Abu-Awwad, A. M.: "Potential for Water Harvesting Jordan: Present Situation and Futur Needs, "International Conference on Land and Water Resources Management in the Mediterranean Region, Vol. 3, Italy, 1994, PP. 783-792.
- 2- Shatanawi, M., Sarraf, S. and Oweis, T.: "Water Harvesting Project Summary, "Water and Environmeent Research and Study Center, Amman, Jordan, 1994, PP. 1-39.
- 3- Ismail, J. A. K.: "Modeling Rainfall-Runoff Relationship and Reservoir Capacity and Operation for Wadi Waleh watershed," M.Sc. Thesis, University of Jordan, Amman, Jordan, 1986, PP. 95.
- 4- U. S. Army Corps of engineers, HEC-1 Flood Hydrograp User Manual, California, 1981, PP. 330.
- 5- Seshappa, R., G. N., Joseph, R. A. and Jim, F. H.: "Estimating Peak Rates of Runoff and Design Hydrographs from Rainfall in the State of Oklahoma," J. Hydrol., Vol. 4, 1966, PP. 141-170.
- 6- Sumner, M. E. and Stewart, B. A.: Soil Crusting: Chemical and Physical Processes. Lewis Publishers, Boca Raton, Florida, 1992, PP. 33-120.
- 7- Baver, L. D., Gardner, W. H. and Gardner, W. R.: Soil physics, 4th. Edition, John Wiley an Sons, New York, 1972, PP. 365- 377.
- 8- Ben-Hur, M., Shainberg, I. and Morin, J.: "Variability of Infiltration in a Field with surface seal soil," Soil Sci. Soc. Am. J., Vol. 51, 1987, PP. 1299-1302.

- 9- Agassi, M., Morin, J. and Shainberg, I.: "Effect of raindrop impact energy and water salinity on infiltration rates of sodic soils," Soil Sci. Soc. Am. J., Vol. 14, 1985, PP. 186-190.
- 10- Bardford, J. M., Ferris, J. E. and Remley, P. A.: "Interrill Soil Erosion Processes: I. Effect of Surface Sealing on Infiltration, Runoff, and Soil Splash Detachment," Soil Sci. Soc. Am. J., Vol. 51, 1987, PP. 1566-1571.
- 11- Keren, R.: "Water-Drop Kinetic Energy Effect on Infiltration Sodium-Calcium-Magnesium Soils," Soil Sci. Soc. Am. J., Vol. 54, 1990, PP. 983-987.
- 12- Karniel, A., Ben-Asher, J.: "Adaily Runoff Simulation in Semi-arid Watersheds Based on Soil Water Deficit Calculations," J. Hydrol., Vol. 149, 1993, PP. 9-25.
- 13- Chow, V. T., Maidment, D. R., and Mays, W.: "Applied hydrology". McGraw-Hill, New York, U.S.A, 1988, PP. 127-263.
- 14- Boers, Th. M. and Ben-Asher, J.: "A review of Rainwater Harvesting," Agric. Water Manage., Vol. 5, 1982, PP. 145-158.
- 15- Karniel, A., Ben-Asher, J., Dodi, A., Issar, A. and Oron, G.: "An Empirical Approach for Predicting Runoff Yield under Desert Conditions," Agric. Water Manage., Vol. 14, 1988, PP. 243-252.
- 16- Casenave, A. and Valentin, C.: "Runoff Capability Classification System Based on Surface Features Criteria in Semi-arid Areas of West Africa," J. Hydrol., Vol. 130, 1992, PP. 231-249.
- 17- Osborn, H. B., and Lane, L.: "Precipitation-Runoff Relations for Very Small Semiarid Rangeland Watersheds," Water Resources Research, Vol. 5, 1966, PP. 419-426.

- 18- Mikhail, w.: "Rainfall-Runoff Relationship from a Semi-arid Rangeland Watershed in the Edwards Plateau of Taxes," PP. 103- 112.
- 19- Plate, E. J., Ihringer, J. and Lutz, W.: "Operational Models for Flood Calculations," J. Hydrol., Vol. 100, 1988, PP. 489-506.
- 20- Wang, G. T., Singh, V. P. and Yu, F. X.: "A Rainfall-Runoff Model for Small Watersheds," J. Hyd., Vol. 138, 1992, PP. 97-117
- 21- Taff T.: "Simulation of Streamflows for Ungauged Catchments," J. Hydrol., Vol. 129, 1991, PP. 3-17.
- 22- Burn, D. H., and Boorman, D. B.: "Estimation of Hydrological Parameters at ungauged catchment," J. Hydrol., Vol. 143, 1993, PP. 429-454.
- 23- Laurenson, E. M.: "A Catchment Storage Model for Runoff Routing," J. Hydrol., Vol. 2, 1964, PP. 141-163.
- 24- Perumal, M.: "Multilinear Muskingum Flood Routing Method," J. Hydrol., Vol. 133, 1992, PP. 259-272.
- 25- Department of Civil Engineering, Concordia University, Canada, Icarda-Syria, Faculty of Agriculture, The University of Jordan, Draft, development of an optimal arid lands, A joint collaborative Research Proposal , Amman, Jordan, 1991, PP. 1-39.
- 26- Bouwer, H.: "Intake Rate: Single, and Double-Ring Infiltrimeters," Method of Soil Analysis. Part 1. Physical and Mineralogical Properties. 2nd.Edition, Amer. Soc. of Agron. and Soil Sci. Soc. of American, Madison, Wisconsin USA, PP. 835-838.
- 27- University of Jordan, Annual Report of the Water Harvesting Project (No.92-1502-02), Amman, Jordan, 1992, PP. 1-100.
- 28- Chadwick, A. J., Morfett, J. C.: "Hydraulics in Civil Engineering." Allen and Unwin, London, PP. 369-379.

- 29- Hwang, N. H. C.: Fundamentals of Hydraulic Engineering System.
Prentice-Hall, I., C. N. J. Englewood, USA, 1981, PP. 148
- 30- Awwad, M., Shatanawi, M., and Rimawi, O., "Harvested Water as
a Source of Artificial Recharge," Water and Environment Research
and Study Center, University of Jordan, Amman, Jordan, 1993.

الملخص

العلاقة بين كمية الأمطار والجريان السطحي لمساقط مائية ممثلة لحوض الموقر المائي

إعداد

محمود الأخرس

إشراف

الدكتور محمد شطناوي

يعاني الأردن من النقص المتزايد في المياه بسبب تدني معدل سقوط الأمطار، حيث أن حوالي 85% من مجمل مساحة الأردن يصلها من الأمطار ما يقل عن 200 ملم سنويا. ولأن هذه الأمطار تتساقط على شكل زخات رعدية وبشدة مطر عالية وبسبب انخفاض معدل الرشح المائي للتربة بسبب تكون القشرة السطحية، فإن الجريان السطحي يحدث من أمطار ذات شدة منخفضة نسبيا. ومن هنا تظهر أهمية دراسة العلاقة بين كمية الأمطار المتساقطة والجريان السطحي في هذه المناطق. وقد أجريت دراسة العلاقة بين الأمطار والجريان السطحي لحوض الموقر المائي حيث تم اختيار ثلاثة مواقع بمساحة 7.3، 0.5، 5.8 كم². لدراسة تأثير خصائص الأمطار، وخصائص التربة السطحية على الجريان السطحي.

وقد أظهرت النتائج الميدانية أن معامل الجريان السطحي كان مرتفعا، حيث كان 0.25، 0.40، 0.23 للمواقع التي تم دراستها.

تم استخدام نموذج رياضي (HEC-1) للتنبؤ بمنحنى الجريان السطحي، وتم تطبيقه على حوض الموقر المائي. ويقوم هذا النموذج بعمل معايرة لمعاملات الرشح المائي ومعاملات وحدة منحني الجريان السطحي، حيث يحتوي النموذج على أربع طرق لحساب معاملات الرشح المائي ووحدة منحني الجريان السطحي، وقد تم اختبار هذه الطرق وقد أظهرت النتائج أن الطريقة الرابعة هي أدق هذه الطرق، ولذلك تم استخدامها للتنبؤ بالجريان السطحي لحوض الموقر المائي.

كما ويقوم هذا النموذج الرياضي بإجراء مقارنة بين منحني الجريان السطحي الحقيقي ومنحني الجريان السطحي الذي يتنبأ به، وقد تم إجراء هذه المقارنة على موقعين وكانت النتائج جيدة . وبناء على استخدام الطريقة الرابعة في هذا النموذج ، أظهرت النتائج أن كمية الجريان السطحي خلال موسم 95/94 بلغت 0.79 مليون متر مكعب، وهذا يعني أنه فقط 5.8% من كمية الجريان السطحي قد تم تخزينها في السدود التي تبلغ قدرتها التخزينية الحالية 50 ألف متر مكعب .